CoCO2

Prototype system for a Copernicus CO_2 service

Third synthesis of CO_2 and CH_4 observation-based emission estimates

WP8

coco2-project.eu

Co-ordinated by ECMWF

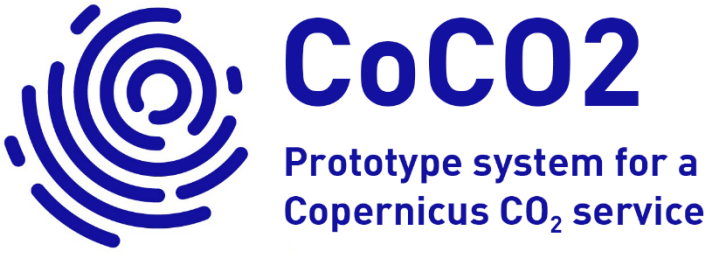

D8.3: Third synthesis of CO_2 and CH_4 observation-based emission estimates

Dissemination Level:	Public
Author(s):	Glen P. Peters, A. M. Roxana Petrescu, Robbie M. Andrew, Kjetil Aas, Gregoire Broquet, Dominik Brunner, Ragnhild Børke, Frédéric Chevallier, Hugo Denier van der Gon, Audrey Fortems-Cheiney, Matthew McGrath, Arjo Segers, Espen Sollum, Aki Tsuruta, Richard Engelen
Date:	21/12/2023
Version:	v1
Contractual Delivery Date:	31/12/2023
Work Package/ Task:	WP8 / T8.3
Document Owner:	Vrije Universiteit Amsterdam
Contributors:	CICERO
Status:	Final

CoCO2: Prototype system for a Copernicus CO_2 service

Coordination and Support Action (CSA)
H2020-IBA-SPACE-CHE2-2019 Copernicus evolution – Research activities in support of a European operational monitoring support capacity for fossil CO_2 emissions

Project Coordinator: Dr Richard Engelen (ECMWF)
Project Start Date: 01/01/2021
Project Duration: 36 months

Published by the CoCO$_2$ Consortium

Contact:
ECMWF, Shinfield Park, Reading, RG2 9AX,
richard.engelen@ecmwf.int

The CoCO2 project has received funding from the European Union's Horizon 2020 research and innovation programme under grant agreement No 958927.

Table of Contents

List of Figures

List of Tables

List of Acronyms

Acronyms used throughout the report are listed here, except for the names of models or datasets:

AD: Activity Data

BU: Bottom-Up

BUR: UNFCCC Biennial Update Reports

CO2MVS: CO_2 Monitoring and Verification Support

CoCO2: Protype system for a Copernicus CO_2 service (EU Horizon 2020 project)

CRF: UNFCCC Common Report Format

DGVM: Dynamic Global Vegetation Model

FCO_2: Fossil CO_2 emissions

$FFCO_2$: Fossil fuel CO_2 emissions

EF: Emission Factor

GHG: Greenhouse Gas

GST: Global Stocktake

IPCC: Intergovernmental Panel on Climate Change

LULUCF: Land Use, Land-Use Change, and Forestry

NGHGI: National Greenhouse Gas Inventory

TD: Top-Down

UNFCCC: United Nations Framework Convention on Climate Change

VERIFY: Observation-based system for monitoring and verification of greenhouse gases (EU Horizon 2020 project)

Executive Summary

This third and final version of this deliverable. The first version was in December 2021, the second version January 2023, and this final version December 2023. In this version, the section on net land CO_2 fluxes has been rewritten, the section on CH_4 has had extensive updates, and the section on fossil CO_2 emissions has been updated and revised with the latest data available.

The aim of the deliverable is to identify, quantify and explain divergences between global inventories, atmospheric inversions, process models, and national inventories submitted to the UNFCCC. We present consistent comparisons of CO_2 and CH_4 emission estimates for various countries to highlight interesting and relevant aspects. We cover fossil CO_2 emissions, net land CO_2 fluxes, and anthropogenic CH_4 emissions. Most of the data products are from the VERIFY project, with a gradual inclusion of CoCO$_2$ products as the project evolves, and some independent datasets.

Progress has been made on making comparisons across datasets, but significant gaps remaining in harmonising system boundaries, providing relevant information on uncertainty, and explaining why data products differ.

- For fossil CO_2 emissions, the importance of adjusting for harmonised system boundaries was demonstrated and that describing differences requires detailed comparison of components (e.g., fossil fuel category or sectors). The fossil CO_2 inversions show proof of concept, but so far lack uncertainty information for a full analysis.
- For net land CO_2 fluxes, comparisons were made with inventories in three groups: 1) bookkeeping models, 2) process-based models, and 3) inversions. System boundary issues remain highly problematic in the land-sector, even when comparing similar models together, and this is an area that requires significantly more research. Lack of data availability and comparability hinders comparisons (particularly for bookkeeping models, process-based models, and inventories), as does knowledge of how well some data products are constrained by observations (particularly inversions).
- For CH_4 emissions, divergences between inventories can be linked back to differences in activity data or emission factors, but this data can be difficult to obtain. For the inversions, the general magnitudes and trends agree, but uncertainties remain large. More effort is needed on providing relevant uncertainty information, particularly more detail on the priors, and the extent to which observations are constraining results leading to statistically significant differences with inventories.

A consistent conclusion across all components analysed is the difficulty of harmonising datasets into a comparable format. The tradition of comparing totals of datasets as published is easy, but problematic. Dataset providers should consider this issue, and data should be presented in a way that (i) makes the system boundary very clear, and (ii) provides breakdowns of the total into components, where possible. To reconcile differences between alternative datasets requires a much deeper understanding of each dataset, such as the methods and input data sources, detailed output of models that go beyond aggregated totals, and providing considerably more information on uncertainties to help understand when differences are statistically significant. Often the necessary data is not easily accessible or is time consuming to access or negotiate access. A systematic reconciliation and comparison will likely require a close dialogue between data providers and inventory experts, together with the analyst. There remain considerable barriers to facilitate robust comparisons, but these barriers can be dealt with through community efforts.

1 Introduction

Background

Emissions and removals of greenhouse gases (GHGs), including both anthropogenic and natural fluxes, require reliable quantification, including estimates of uncertainties, to support credible mitigation action under the Paris Agreement. Reported inventory-based emissions and removals are generally estimated using 'bottom-up' inventory estimates. 'Top-down', observation-based estimates can provide complimentary monitoring and verification of the bottom-up emission estimates. These independent estimates can be performed at multiple scales and for a variety of applications: the global and continental scale for science purposes, country scale for reporting to the UNFCCC, sub-country scale for urban planning, and point sources like large power plants for verification (Pinty et al., 2019), to name just a few examples.

Bottom-up inventory estimates have generally assumed to follow the IPCC reporting guidelines. In general, bottom-up inventory estimates are a combination of activity data (e.g., fuel use) and associated emission factors (e.g., emissions per fuel use). However, in many cases, bottom-up inventory estimates can be a complex combination of different approaches, including the use of actual continuous gas measurements at specific point sources or modelling based on numerous data sources (e.g., transport emissions modelling using traffic data and fleet databases). The development of bottom-up inventory estimates with higher spatial (gridded) and temporal (daily, hourly) resolution may also rely on different observational datasets. Particularly in the land sector, bottom-up estimates may involve a considerable amount of modelling and observation datasets (e.g., forest inventories). The term 'bottom-up' can therefore connote several different things, and we rather refer to datasets by name as opposed to whether they are 'bottom-up'.

Top-down observational estimates combine prior inventory estimates with a variety of observations to provide valuable constraints on the inventories (Deng et al., 2022). The main distinction is that top-down estimates generally use an inversion, or some other sort of model, together with a variety of observations, to provide estimates of emissions that can then be compared with the bottom-up inventory estimates. Since atmospheric concentrations respond to the sum of all emissions and removals, inversion-based estimates are less suited to provide information on individual sectors (unless they are geographically separated), though due to high resolution, observation-based approaches are particularly suited to identify point sources or small geographical areas like cities.

Bottom-up inventories and top-down observational estimates are complementary and should be used together to improve and build trust in National Greenhouse Gas Inventories (NGHGIs) reported to the UNFCCC. With dense observation networks and measurements of auxiliary parameters such as isotopic composition of GHG or concentrations of co-emitted gases, additional source-specific information can be gained to support the validation of national emission inventories at smaller spatial scales. Observation-based estimates can be particularly valuable for trace gases with large uncertainties in their emissions (Maksyutov et al., 2019).

In the context of providing recommendations for the implementation of an observation-based operational anthropogenic CO_2 emissions Monitoring and Verification Support (CO2MVS) capacity within the Copernicus programme, one objective of CoCO2 is to provide inputs to the Global Stocktake (GST) process, in the form of anthropogenic CO_2 and CH_4 emission products for the first GST (2023), at a spatial scale consistent with GST requirements. CoCO2 identified the relevant needs for the periodic GST through the development of a User Requirement Document (URD). The work described in this document represents the starting point for future syntheses to serve future GSTs.

This document is an extension of reconciliation reports and country analysis produced under the VERIFY project (Andrew, 2020; Petrescu et al., 2020; Petrescu et al., 2021a; Petrescu et

al., 2021b; McGrath et al., 2023; Petrescu et al., 2023b), but this document has a more global focus. We identify and analyse CO_2 and CH_4 emissions from a selection of countries to identify differences with UNFCCC National GHG Inventories (NGHGI), and thereby identify countries or sectors where observation-based estimates can complement NGHGIs. We choose countries that show interesting or relevant differences. This document is the third and final in a series of three, due at the end of each year of the project (December 2021, December 2022, December 2023). This report is structured as follows: Chapter 1 presents the background, scope and objectives of this work, Chapter 2 the methodologies, Chapter 3 focuses on the fossil and net land CO_2 fluxes, Chapter 4 presents the CH_4 results both total and sectoral, and the report ends with discussions, conclusions and outlines future needs for research in Chapter 5.

Scope of this deliverable

The scope of this deliverable is to compare annual observation-, inventory-, and model-based emissions (CO_2 and CH_4) and removals (CO_2) estimates against UNFCCC NGHGIs for a selection of countries, generally the largest emitters. We use data products from VERIFY, CoCO2, and other independent datasets. We focus on fossil CO_2 emissions, net land CO_2 fluxes, and anthropogenic and natural CH_4 emissions.

Changes for this third and final version of the deliverable include:

- Fossil CO_2 emissions
  - Update to most recent data
  - Include uncertainty bounds on UNFCCC and EDGAR
  - Updated inversions
- Land CO_2 fluxes
  - Update to most recent data
  - Apply managed land masks and lateral fluxes, where possible
  - Provide deeper explanation of differences between datasets
- Anthropogenic and natural CH_4 emissions
  - Update to most recent data and include new datasets
  - Compare priors between all datasets (activity data and emission factors)
  - Plot anthropogenic and natural CH_4 emissions for eight global emitters and reconcile inventory- and observation-based estimates
- Recommendations for future reconciliation procedures

2 Methodologies

UNFCCC National Greenhouse Gas Inventories (NGHGI, 2023) emissions (CO_2 and CH_4) and removals (CO_2) are compiled by individual countries, with Annex I Parties to the UNFCCC required to report emissions inventories annually using the Common Reporting Format (CRF). The reported data is generally for the period 1990 to N-2 (two years before the current year), but some countries provide data for earlier or later periods. The non-Annex I Parties report their estimates in Biennial Update Reports (BURs) submissions to the UNFCCC, but since these reports are in irregular formats they require manual compilation to obtain a cross-country dataset. For CH_4 we use the original BURs, while for net CO_2 land fluxes we used Grassi et al. (2023).

Fossil CO_2 emissions

The different fossil CO_2 emission data and methods are summarised in Table 1.

The bottom-up inventory-based fossil CO_2 estimates are presented and split per fuel type and reported for the last year when all data products are available, an update to Andrew (2020).

The top-down atmospheric inversions for fossil CO_2 emissions are based on co-emitted species. To overcome the current lack of CO_2 observation networks suitable for the monitoring of fossil fuel CO_2 emissions at national scale, this inversion is based on atmospheric

concentrations of co-emitted species: CO and NO_2. While the spatial and temporal coverage of these CO and NO_2 observations is large, the conversion of the information on these co-emitted species into fossil fuel CO_2 emission estimates is complex and carries large uncertainties. We have not been able to fully characterise the uncertainty in the inversions, therefore limiting our ability to compare to inventories.

Net land CO_2 flux

The net land CO_2 fluxes include CO_2 emissions and removals from LULUCF activities, based on inventories, bookkeeping models, process models, and inversion estimates (Table 2). We considerably rewrote the net land CO_2 flux section in this version of the deliverable. We split the figures into three sets, based on bookkeeping models, land-surface models, and inversions.

We consider inventories from the UNFCCC (Annex I), the FAO, and a compilation of UNFCCC inventories for Annex I countries (CRFs) and non-Annex I countries (BURs) (Grassi et al., 2023). We consider three bookkeeping models (BLUE, H&C, OSCAR) based on the Global Carbon Budget (Friedlingstein et al., 2022b). For the land-surface models, we use an ensemble of dynamic global vegetation models (DGVMs) TRENDYv10 from GCP2021 (Friedlingstein et al., 2022a). For the top-down observational-based estimates, we use inverse model results from GCP2021 (Friedlingstein et al., 2022a) and an improved CAMS inversion including lateral fluxes and managed land masks (Chevallier et al., 2005; Chevallier, 2021).

Anthropogenic and natural CH_4 emissions

The bottom-up inventory-based estimates for CH_4 anthropogenic emissions come from the UNFCCC NGHGIs (2023), three global inventories: EDGAR v7.0, FAOSTAT (with PRIMAP) and GAINS (Table 3) and one CoCO2 product, TNO_PED18-21. These estimates are not completely independent from NGHGIs (see Figure 4 in Petrescu et al. (2020)) as they integrate their own sectorial modelling with the UNFCCC data (e.g. common activity data (AD) and IPCC emission factors (EFs)) when no other source of information is available.

In this version of the report, we also present data for natural CH_4 emissions, for both EU and the top emitters. They include emissions from the geological sources, inland waters (lakes, rivers, and reservoirs), biomass burning, wetlands and mineral soils.

The top-down observation-based estimates from atmospheric inversions combine atmospheric observations, transport and chemistry models and estimates of GHG sources with their uncertainties, to estimate emissions. Emission estimates from inversions depend on the data set of atmospheric measurements and the choice of the atmospheric model, as well as on other settings (e.g., prior emissions and their uncertainties). For CH_4, we use data from both regional (EU) and global inversions developed in the VERIFY and CoCO2 projects as following: the CIF intercomparison (Berchet et al., 2021), CoCO2 CH_4 results from CAMS v21r1 (2 runs) and TM5-4DVAR (TROPOMI), and from third parties such as MIROC4-ACTM (2 runs), CEOS (GOSAT) and CEOS-Chem (TROPOMI) for USA only (Saunois et al., 2020). Inversion priors are summarized here: Priors - Google Sheets.

Table 1: Data sources for the fossil CO_2 emissions included in this study

CO_2 anthropogenic				
	Data/model name	**Contact / lab**	**Species / Period**	**Reference/Metadata**
	UNFCCC NGHGI (2023)	UNFCCC	Anthropogenic fossil CO_2 1990-2021	IPCC Guidelines for National Greenhouse Gas Inventories (IPCC, 2006) UNFCCC NIRs/CRFs (UNFCCC, 2022)
BU	Compilation of multiple CO_2 fossil emission data sources (Andrew, 2020): EDGAR, BP, EIA, CDIAC, IEA, GCP, CEDS, PRIMAP	CICERO	CO_2 fossil country totals and split by fuel type 1990-2022 (or last available year)	EDGAR v7.0_GHG (Crippa et al., 2022) Energy Institute, 2023: https://www.energyinst.org/statistical-review US Energy Information Agency (EIA), https://www.eia.gov/international/data/world CDIAC, https://energy.appstate.edu/research/work-areas/cdiac-appstate International Energy Agency (IEA), https://www.iea.org/data-and-statistics/data-product/greenhouse-gas-emissions-from-energy CEDS (O'Rourke et al., 2021) Global Carbon Product (GCP) (Friedlingstein et al., 2023) PRIMAP-hist (Gütschow and Pflüger, 2022) Regional Emission inventory in ASia (REAS) (Kurokawa and Ohara, 2020) Multi-resolution Emission Inventory model for Climate and air pollution research (MEIC), http://meicmodel.org.cn
TD	Fossil fuel CO_2 inversions	LSCE	Inverse fossil fuel CO_2 emissions 2005-2020	VERIFY Deliverable D2.12 (Fortems-Cheiney and Broquet, 2021a), update of Deliverable D2.11 (Fortems-Cheiney and Broquet, 2021b)

Table 2: Data sources for the land CO_2 emissions included in this study

Product Type / file or directory name	Contact / lab	Variables / Period	References
Inventories			
UNFCCC NGHGI (2023)	UNFCCC	LULUCF Net CO_2 emissions/removals	Based on IPCC Reporting Guidelines (IPCC, 2006) UNFCCC Annex 1 CRFs https://unfccc.int/ghg-inventories-annex-i-parties/2022
Grassi et al (2023)	Giacomo Grassi	LULUCF Net CO_2 emissions/removals	Based on compilation of UNFCCC (2022) inventories and UNFCCC BURs: https://unfccc.int/BURs (Grassi et al., 2023)
FAO	FAOSTAT	CO_2 emissions/removal from LULUCF sectors	(Federici et al., 2015; Tubiello et al., 2021)
Bookkeeping models			
BLUE	LMU Munich	Net C flux from land use change, split into the contributions of different types of land use (cropland vs pasture expansion, afforestation, wood harvest)	Hansis et al. (2015) as updated in Friedlingstein et al. (2023)
H&C	Woodwell Climate Research Center	Net C flux from land use change, split into the contributions of different types of land use (cropland vs pasture expansion, afforestation, wood harvest)	Houghton and Castanho (2023) as updated in Friedlingstein et al. (2023)
OSCAR	IIASA	Net C flux from land use change, split into the contributions of different types of land use (cropland vs pasture expansion, afforestation, wood harvest)	Gasser et al. (2020) as updated in Friedlingstein et al. (2023)
Process-based models			
TRENDY v10 (2020)	MetOffice UK	Land related C emissions (NBP)	Friedlingstein et al. (2022a) and references therein.
Inversion models			
GCP 2021	GCP	Total CO_2 inverse flux (NBP) 6 global inversions (CTE, CAMS, CarboScope, UoE, CMS-Flux, NISMON-CO2)	Friedlingstein et al. (2022a) and references therein.
CAMS via CoCO$_2$	LSCE	CO_2 fluxes, includes lateral fluxes and a managed-land mask	Chevallier (2021)
Lateral flux adjustments (v4.1)	LSCE	Lateral fluxes for all components	Chevallier and Ciais (personal communication, December 2023)

Table 3: Data sources for the CH_4 emissions included in this study

Name	Domain	Description	Contact / lab	References details in Petrescu et al. (2023a)	Status compared to Petrescu et al., 2023 and D8.2
CH_4 Bottom-up anthropogenic					
UNFCCC NGHGI (2023) CRFs and BURs	EU	CH_4 emissions 1990-2021	MS inventory agencies Yearly uncertainties provided by the EU GHG inventory team	UNFCCC CRFs, https://unfccc.int/ghg-inventories-annex-i-parties/2023 UNFCCC BURs, https://unfccc.int/BURs	Updated
EDGAR v7.0	EU and global	Total and sectoral global CH_4 emissions 1990-2021	EC-JRC	Crippa et al., 2020 Crippa et al., 2019 JRC report Janssens-Maenhout et al., 2019 Solazzo et al., 2021	Updated
GAINS	EU and global	Total and sectoral global CH_4 emissions 1990-2020	IIASA	Höglund-Isaksson, L. 2017 Höglund-Isaksson, L. et al., 2020	Updated
FAOSTAT	EU and global	Global CH_4 agriculture and land use emissions, as well as for other sectors (based on PRIMAP) 1990-2020	FAO	Tubiello et al. 2013 Tubiello, 2019, 2022 FAO, 2015, 2023	Updated
TNO_CoCO2_PED 18-21	Global	Prior emissions dataset for 2018 and 2021 developed by TNO	TNO	CoCO2 D2.1 and D2.2 https://www.coco2-project.eu/	
CH_4 bottom-up natural					
LPJ-GUESS	Global	Global CH4 emissions from wetlands, 1990-2021	U Lund	Wania et al., 2009 Wania et al., 2010 Spahni et al., 2011 Zhang et al., 2021	New
JSBACH-HIMMELI	EU	European CH4 emissions from peatlands and mineral soils, 2005-2020	FMI	Raivonen et al., 2017 Susiluoto et al., 2018	Not updated
DAAC ORNL	Global	Global CH4 emissions from lakes (2003-2015) and dam-reservoirs (2002-2015)	NASA	Johnson et al. 2021 and 2022	New
Geological emissions	Global	Global grid geological CH_4 emission model (2019)	Istituto Nazionale di Geofisica e Vulcanologia (INGV)	Etiope et al., 2019 and current work (updated activity data)	Updated

GFED4.1s	Global	Biomass burning global CH_4 emissions, 2000-2020	VU Amsterdam	van der Werf et al., 2017	not updated
CH_4 top-down natural and anthropogenic					
FLExKF-v2023	EU	Regional total CH_4 emissions from inversions with uncertainty, 2005-2021	EMPA	Brunner et al., 2012 Brunner et al., 2017 Segers et al., 2020	Updated
CAMS v21r1	Global	Total and source split partitions for global CH_4 emissions NOAA (1979-2021) NOAA_GOSAT (2009-2021)	TNO	Huijnen et al., 2010 Pandey et al., 2022 Segers et al., 2022	New
CTE-GCP2021	Global	Total global CH_4 emissions with source split partitions and posterior flux uncertainty 2000-2020	FMI	Bruhwiler et al., 2014 Houweling et al., 2014 Giglio et al., 2013 Ito et al., 2012 Janssens-Maenhout et al., 2013 Krol et al., 2005 Peters et al., 2005 Saunois et al., 2020 Stocker et al., 2014 Tsuruta et al., 2017	New
CIF-CHIMERE and CIF-FLEXPARTv10.4	EU	Total regional CH_4 emissions from inversions CHIMERE: 2005-2022 FLEXPART: 2005-2020	LSCE, NILU	Berchet et al., 2021 Fortems-Cheiney et al., 2021	New and updated
MIROC4-ACTM (control and OH varying runs)	Global	Total and source split partitions for global CH_4 emissions (2 runs: control and variable OH), 2001-2021	JAMSTEC	Patra et al., 2021 Chandra et al., 2021	New
TM5-4DVAR (TROPOMI)	Global	Total and source split partitions for global CH_4 emissions, 5/2018-2020	VUA	Huijnen et al., 2010 Lorente et al., 2023	New
GEOS-Chem CTM (TROPOMI for USA)	USA	Total CH_4 emissions for USA, 2019	Harvard University	Nesser et al., 2023	New
CEOS (GOSAT)	Global	Total and source split partitions for global CH4 emissions, 2019	NASA/JPL	Worden et al., 2019	New

Other common methodological issues

In the figures presented in this report, we essentially plot the various inversions and inventory methods on the same figure, to allow a visual comparison. There has not been a full uncertainty analysis, that would for example, quantify if one dataset has a statistically significant difference to another. Very few datasets provide uncertainty information. Methods to present the results, including uncertainties, need to be improved. Additionally, methods are needed to assess the statistical significance of any differences, given reported uncertainties.

System boundary issues are a challenge for all comparisons made here. Independent estimates often have different system boundaries. These can sometimes be minor, but at other times (e.g., land) be significant. Relevant system boundary issues are discussed in each section below, but here we discuss some key issues.

A general system boundary issue is masking of gridded results to the country level, where it is important that it is known how modelling groups have defined emissions in each grid cell and to ensure the mask correctly captures country and economic zone effects, in line with how official NGHGIs are reported. Give the coarse grid in many datasets, results for small countries may be less reliable.

In a UNFCCC context, the net uptake on land (LULUCF) is defined based on a 'managed land proxy'. This proxy was originally intended to represent anthropogenic activities, and is defined to cover land "where human interventions and practices have been applied to perform production, ecological or social functions" (IPCC, 2006). Countries do not report spatial grids of their manged land definitions, but "intact" and "non-intact" forest area has been found to be a good proxy for unmanaged and managed land (Grassi et al., 2021). Applying a non-intact forest area mask to the net land CO_2 flux in an inversion model or DGVM is one way to approximate the system boundary of LULUCF in NGHGIs. Another issue is that BMs only include direct human-induced effects, while NGHGIs also include environmental factors (such as CO_2 fertilisation). We discuss various issues with this approach in the section on net land CO_2 fluxes.

International transport is not included in country totals in NGHGIs, but it is reported as a "memo" based on the sale of bunker fuels in each country (not the use of bunker fuels). A flight starting in France and landing in Poland would be classed as international, even though all the emissions occurred over EU territory. An inversion using satellite information, might see the emissions over each country in the flight path, but that would not appear in the NGHGI. The same problem applies to flights with a landing or take-off in the EU but landing a country outside of the EU. International shipping has the same issues, whether a shipping leaving Europe to cross the Atlantic or a ship along the Rhine crossing country borders.

Despite the potential system boundary issue with international transport, it is unclear whether it is important yet. Inversions currently relying on in-situ observations would not be affected by this, as the observations would not detect the emissions emitted at cruising altitude. For this reason, the TNO emission inventories (from CoCO2 WP2), include landing and take-off of all flights, domestic and international, but not the emissions at cruising altitude. This could nevertheless be an issue for shipping, but the size of the source is probably below the detection limit of current inversion methodologies. As methods improve, and as satellite data are increasingly used, these second-order effects will need a more detailed assessment.

3 Fossil CO_2 emissions

In this section we focus on fossil CO_2 emissions (FCO_2). These can be separated into emissions from the oxidation of fossil fuels ($FFCO_2$) and chemical transformation of fossil carbonates into CO_2, with different datasets having different coverage. While datasets often ultimately draw on the same energy data, methods to prepare the data and assumptions used to estimate CO_2 emissions can differ. Thus, even though fossil CO_2 emissions are thought to have relatively low uncertainty, care is still required to ensure consistency in comparisons.

Inventory-based estimates

Figures 1, 2, 3, and 4 show fossil CO_2 emissions (FCO_2) from global datasets, both globally and for the EU27. 'Raw' totals from these datasets have differing system boundaries, meaning they don't all include the same set of emissions sources. Harmonising is an attempt to remove these differences in coverage to provide more comparable estimates, partly to prevent the false inference of uncertainty relating to the spread of raw estimates. Further details are provided by Andrew (2020). Figures 1 and 3 show unharmonized inventories, while Figures 2 and 4 show harmonised inventories. Importantly, our harmonization process is constrained by the level of detail published in individual datasets, and the harmonization is necessarily partial, not ending up exactly with apples-for-apples comparisons, but generally closer than comparing unharmonized data.

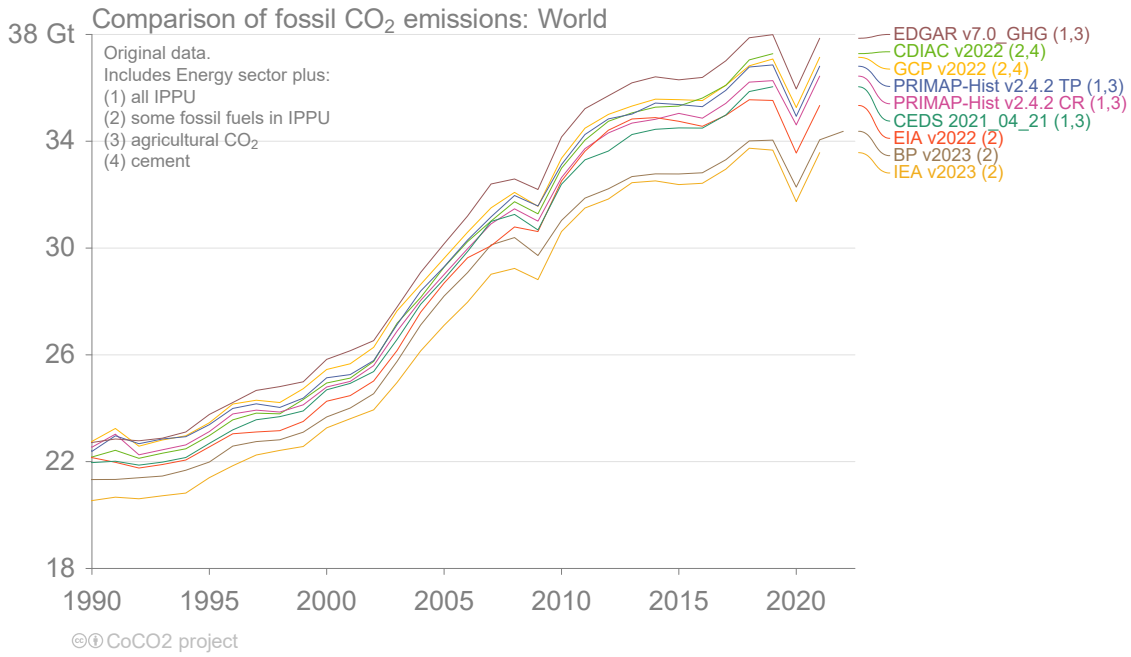

Figure 1: Comparison of unharmonized global fossil CO_2 emissions from multiple inventory datasets.

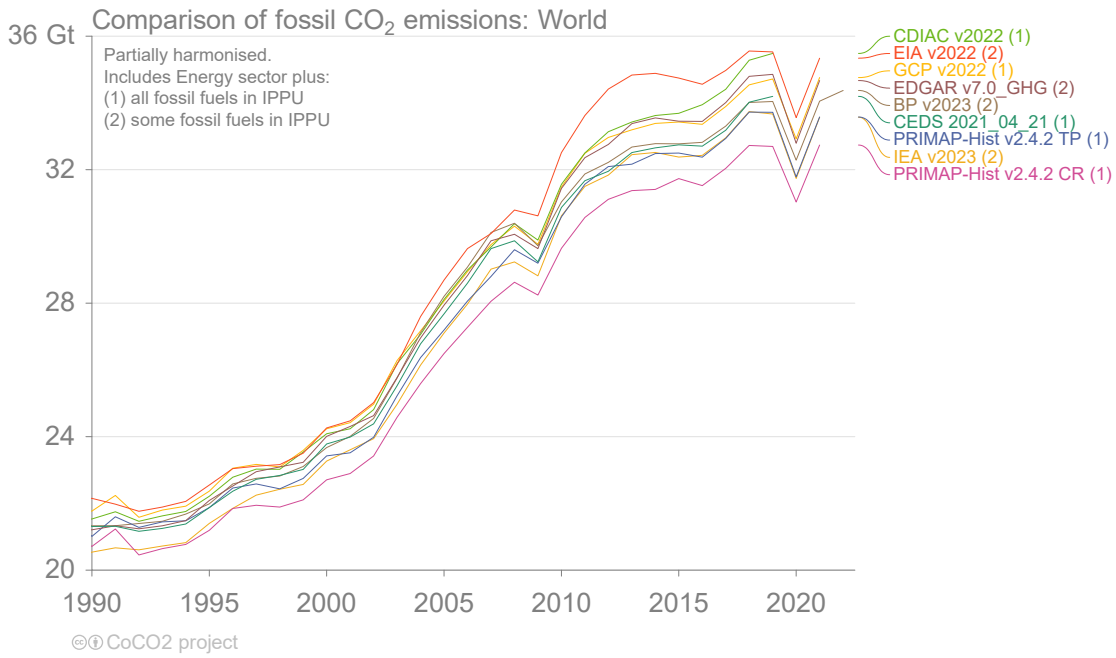

Figure 2: Comparison of global fossil CO_2 emissions from multiple inventory datasets with system boundaries harmonised as much as possible. Harmonisation is limited by the disaggregated information presented by each dataset.

Most datasets agree well within expected system boundary differences (Andrew, 2020). As reported in the previous version of this report (December 2021), we discovered that EIA's estimates were high, and investigation showed that the emissions estimates had grown twice despite the underlying energy data remaining virtually unchanged. Contact with the EIA revealed they had introduced two separate errors leading to double-counting, and their correction led to a drop in EIA's estimates of global fossil CO_2 emissions by about 1 Gt CO_2.

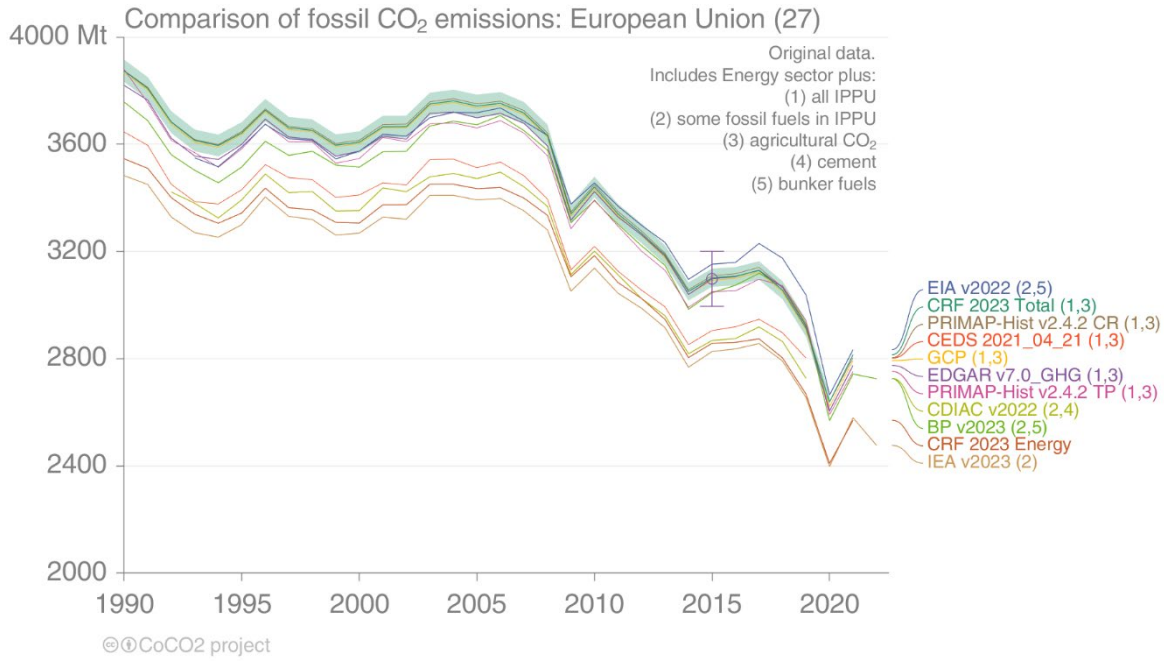

Figure 3: Comparison of EU fossil CO_2 emissions from multiple inventory datasets. CDIAC does not report emissions for countries that did not exist prior to 1992. The uncertainty whiskers at 2015 indicate the uncertainty for EDGAR, while the uncertainty for CRF (UNFCCC reports) is shown as the shaded area.

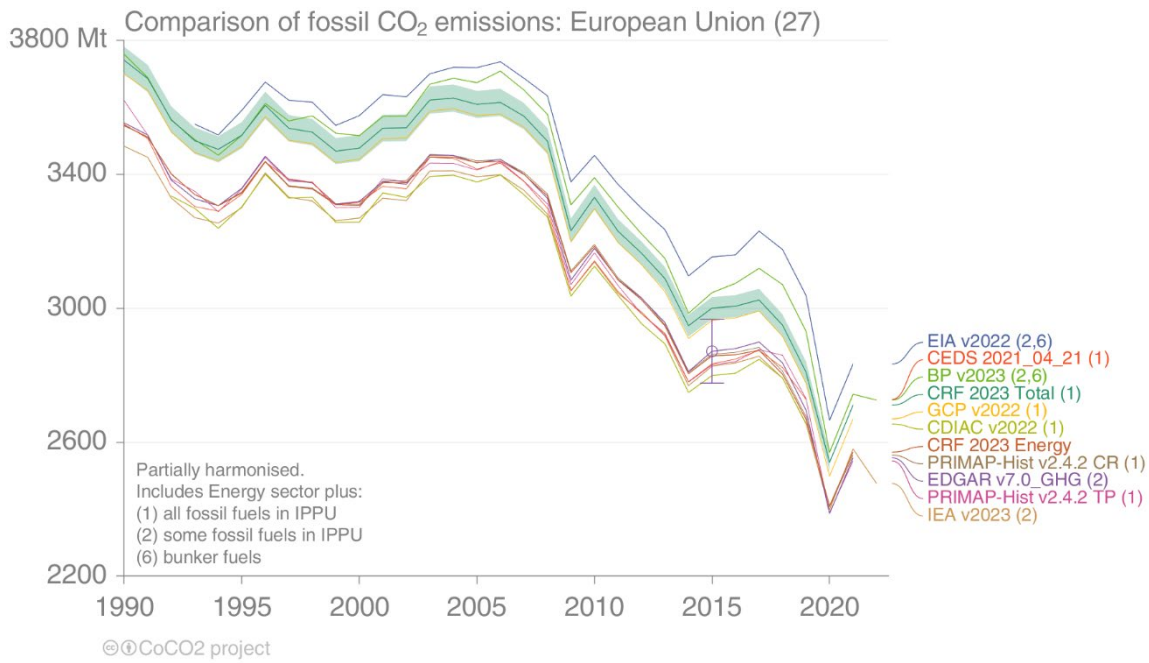

Figure 4: Comparison of EU fossil CO_2 emissions from multiple inventory datasets with system boundaries harmonised as much as possible. Harmonisation is limited by the disaggregated information presented by each dataset. CDIAC does not report emissions for countries that did not exist prior to 1992. The uncertainty whiskers at 2015 indicate the uncertainty for EDGAR, while the uncertainty for CRF (UNFCCC reports) is shown as the shaded area.

For the bottom-up inventory-based estimates, it is possible to produce the figures for all countries. Figure 5 repeats the figures for the two largest emitters, China and USA, and figures for the next-largest emitters can be found in the Annex: India, Russia, Japan, Iran, Germany, Saudi Arabia, South Korea, and Indonesia. For China, the EIA estimates are significantly higher than others, and Andrew (2020) offers some explanation for this. Otherwise, the datasets are similar in most instances, but further work is ongoing to uncover the reasons for remaining divergences between these datasets.

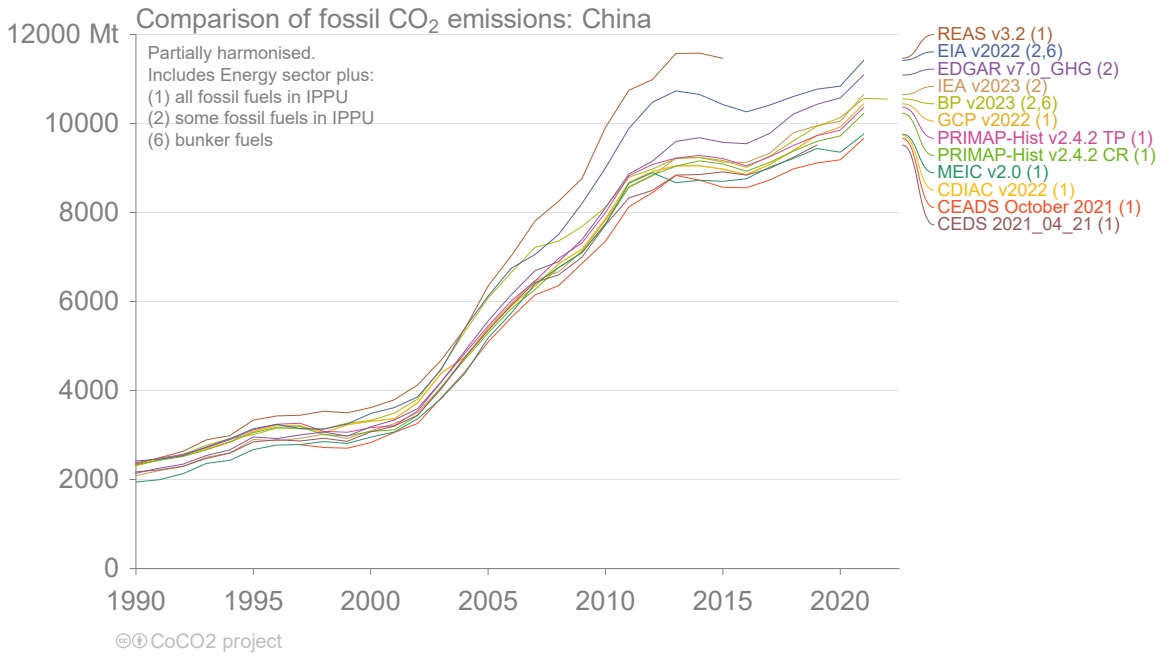

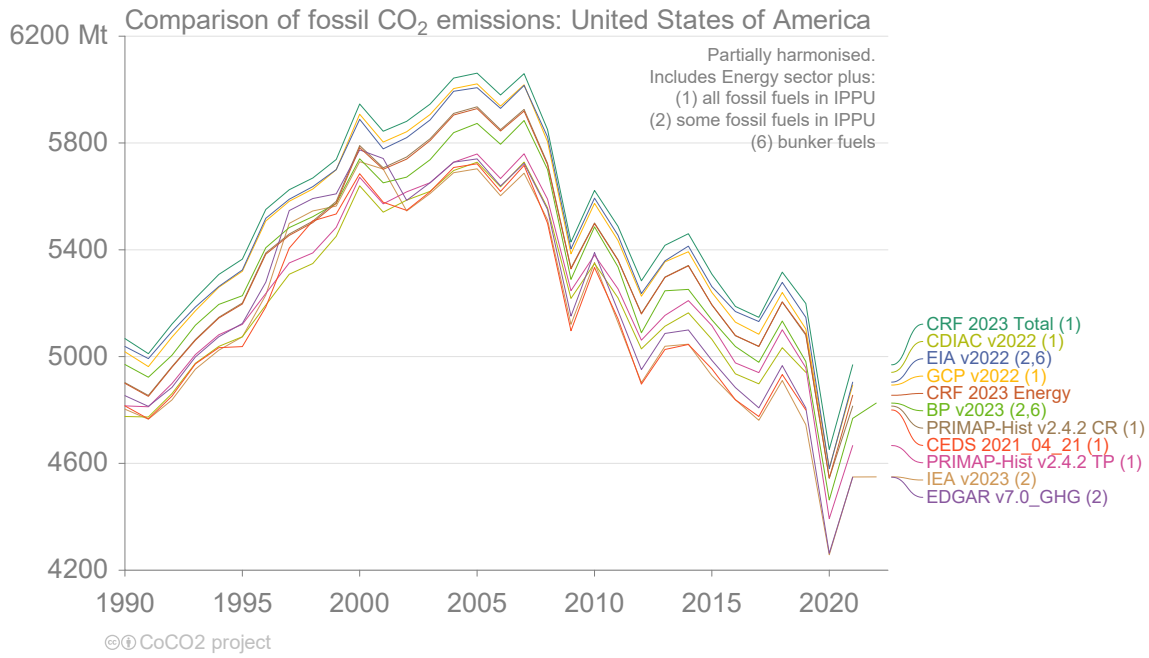

Figure 5: Comparison of China (top) and USA (bottom) fossil CO_2 emissions from multiple inventory datasets with system boundaries harmonised as much as published data detail allows.

Atmospheric inversions

The best top-down observation-based constraint on national scale estimates of anthropogenic CO_2 emissions in Europe over more than the past decade are satellite measurements of NO_2 and CO, which are "proxy" species co-emitted with CO_2 by fossil fuel combustion ($FFCO_2$). These co-emitted species are used because detection of CO_2 itself is currently hindered by the difficulty in distinguishing anthropogenic emissions of fossil CO_2 from background concentrations, both natural and anthropogenic. Results from the first atmospheric inversions of the European $FFCO_2$ emissions in VERIFY (Konovalov and Lvova, 2018); Petrescu et al. (2021a), indicated that there were much larger uncertainties associated with the assimilation of CO data than to that of NO_2 data for such a purpose.

In the first (D8.1) and second (D8.2) versions of this report we presented selected results from outputs from the VERIFY project (deliverable D2.11 and deliverable D2.12), which developed an atmospheric inversion workflow quantifying monthly and annual budgets of the national emissions of $FFCO_2$ in Europe (Fortems-Cheiney and Broquet, 2021b; Fortems-Cheiney et al., 2021). In this version of the report, we present results from deliverable D6.5 of CoCO2, which include results using data streams from three different satellites, and both CO and NOx.

This workflow, implemented in the Community Inversion Framework (CIF; Berchet et al., 2021), estimates the co-emissions (i.e. CO or NOx) that when fed into a regional chemical transport model (CHIMERE; Menut et al., 2013) best match satellite-measured concentrations of that species, while simultaneously minimising the difference between these estimated emissions and those from the prior inventory dataset, TNO-GHGco-v2 or TNO-GHGco-v3 (Denier van der Gon et al., 2020). This is a minimisation of least-squares optimisation process, solved iteratively (Rodgers, 2000; Chevallier et al., 2005). This workflow is applied over the period 2005-2022, depending on the satellite's availability, on a 0.5°×0.5° grid. Ratios of $FFCO_2$ emissions to CO or NO_x emissions directly derived from TNO-GHGco-v3 for five sectors (energy, industry, residential, road transport and the rest of the sectors), for each country and each month are then used to estimate fossil CO_2 emissions from the CO or NO_x estimates produced by the inversion modelling. Several critical aspects of this workflow need to be highlighted: (i) we do not have reported estimates of the uncertainty in the final $FFCO_2$

emissions yet (ii) the $FFCO_2$ emission budgets provided by the TNO-GHGco-v3 inventory are based on the emissions reported by countries to UNFCCC, which are assumed to be accurate in Europe, therefore the inversion prior estimate (which is also its initial estimate in the variational inversion framework) is consistent with the inventory estimates.

The prior fossil emissions estimates provided by TNO include non-combustion emissions (prior estimates were FCO_2, and not $FFCO_2$), the effect of which has not yet been determined. However, given that the use of co-emitted species relies on the assumption that these are emitted during combustion, the inclusion of non-combustion emissions (e.g., process emissions in cement production) will introduce some error.

Figure 6 shows the annual posterior fossil-CO_2 estimates (CoCO2 Deliverable 6.5) compared with the prior estimates for the EU27 provided by TNO (GHGco v3). There are three separate inversion results, derived from three separate satellites. As discussed above, the similarity of the inversion estimates with the inventory estimates here does not indicate a verification of the inventory estimates, but rather suggests that the workflow functions well and that the inversion was not pulled away from its prior estimate by major lack of fit to the satellite CO/NO_2 data. Further work will be needed to make the inversion outputs more independent and less reliant on (prior) inventory estimates before they can be used for verification, and to derive robust estimates of the posterior uncertainties. Despite the agreement with the inventory estimates, Fortems-Cheiney and Broquet (2021b) indicate that the relative uncertainty in their estimates is likely very high (probably similar to that reported by Konovalov and Lvova (2018)) due to high uncertainties in both the NO_x inversions and the conversion into $FFCO_2$ emission estimates. This work is continuing.

It appears that the extrapolation of the prior past 2019 was poor and has introduced divergence that the inversion model results follow, possibly because the uncertainty assigned to the extrapolation was too low. The official territorial estimates submitted the UNFCCC show a sharp decline in 2020 that the extrapolation did not capture. The reason that the UNFCCC emissions estimates lie below the prior in all years is largely because the prior includes emissions that would be categorised as international transport (particularly aviation, landing and take-off emissions) and therefore not included in territorial inventories.

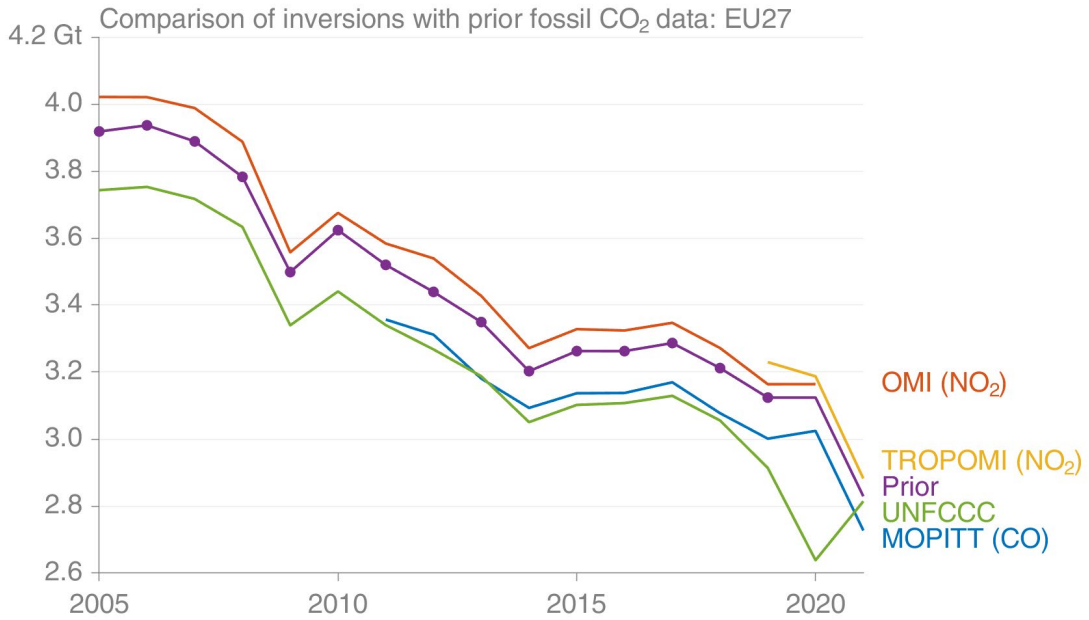

Figure 6: Comparison of inversion results for the EU27 with prior $FFCO_2$ emissions estimated by the TNO-GHGco-v3 inventory (D6.5). The final two points of the prior have been extrapolated. The official EU submission to the UNFCCC is added for reference. Note that the proximity of the inversion results to the prior estimates is not a direct indicator of verification, without additional

information on the prior and posterior uncertainty and supporting statistical analysis (see discussion in the text).

While we still lack quantified posterior uncertainty estimates, they are currently thought to be high. Therefore, the agreement of the inversion result with inventory estimates is encouraging but is insufficient to confirm either of the estimates. The close agreement tells us that the inversion approach has not found sufficient evidence that the inventories are incorrect. Some reasons for this are lack of spatial coverage, sensitivity to the surface in the data, and the relatively high level of observation uncertainties. Country-level results show in some cases near-perfect agreement between the inversion modelling output and inventory estimates. However, this generally results from insufficient satellite data (because of cloud cover) for these countries, and/or that emissions of NO_2 are low (e.g., rural areas), such that minimal 'correction' is obtained to adjust the prior (inventories). Thus far the work involved has been aimed at proving the concepts and building the required modelling infrastructure and workflow. One of the main constraints to reducing uncertainty in this approach is the current lack of observation networks dedicated to the monitoring of $FFCO_2$ emissions, such as the planned constellations of satellite CO_2 spectro-imagers (Fortems-Cheiney and Broquet, 2021b): "the uncertainties in the $FFCO_2$ inversions presented here are still too high to attempt at using these inversions to improve the current knowledge on the $FFCO_2$ national scale emission budgets in Europe, although further progresses are expected".

4 Net land CO_2 fluxes

Net land CO_2 fluxes consistent of both emissions and removals, and due to lack of observations and high uncertainty, differences between datasets are hard to reconcile. There are also major challenges aligning system boundaries of different approaches. In this section we compare UNFCCC NGHGHIs with bookkeeping models, Dynamic Global Vegetation Models (DGVMs), and atmospheric inversions.

The challenges in making comparisons in the land sector

System boundary issues plague comparisons of net land CO_2 fluxes. The question of how to define whether these carbon fluxes are anthropogenic is at the core of this issue (Grassi et al., 2018). The carbon cycle and land surface modelling communities (e.g., IPCC assessment reports) define anthropogenic carbon fluxes on land differently to the inventory community (e.g., IPCC guidelines), though methods have been developed to bridge the differences (Grassi et al., 2021; Grassi et al., 2023).

There are two dimensions to this complex problem (Figure 7): 1) what land areas have anthropogenic changes, and 2) are environmental factors (CO_2 fertilisation, climate, etc) and disturbances anthropogenic? The IPCC Guidelines (used in UNFCCC NGHGI) have defined a self-determined 'managed land' proxy as anthropogenic and include direct factors (e.g., land-use change), indirect factors (e.g., CO_2 fertilisation), and natural factors (e.g., disturbance). 'Managed land' is land where human interventions and practices have been applied to perform production, ecological, or social functions (IPCC, 2006).

Bookkeeping Models (BMs) were the first class of models to estimate net land CO_2 fluxes. They report direct effects on land reported as having a land use change. They exclude indirect effects (CO_2 fertilisation) and disturbances. For land-use changes, BMs consider processes such as deforestation, afforestation, reforestation, and depending on the model, shifting cultivation. They also consider wood harvest and forestry, where the land use does not change (it remains forest), but the forest grows back after harvest. Since BMs exclude indirect effects, the maximum carbon density in each land type remains constant even if environmental factors are changing (e.g., temperature, precipitation, CO_2 concentration, etc). BMs are expected to differ to UNFCCC NGHGIs because of these system boundary issues (Grassi et al., 2023).

Land surface models (LSMs) or Dynamics Global Vegetation Models (DGVMs) consider all land and all effects, but therefore results need to be disaggregated to the appropriate level to

facilitate comparisons with other datasets. The level of disaggregation provided in most analyses requires additional assumptions to do a comparison, in particular, a forest mask to consider only the managed land areas used in NGHGIs (Schwingshackl et al., 2022; Grassi et al., 2023). DGVMs consider interannual variability, through particularly temperature, precipitation, and CO_2 concentration, which hinders comparisons with NGHGIs that generally have methods that average out interannual variability (e.g., National Forest Inventories). Previous comparisons have shown that differences between DGVMs and NGHGIs can be large (Grassi et al., 2018; Petrescu et al., 2020; Schwingshackl et al., 2022; Grassi et al., 2023; McGrath et al., 2023), but it is possible to bridge them by combining BMs and DGVMs (Schwingshackl et al., 2022; Grassi et al., 2023).

Atmospheric inversions consider all land and all effects but require a managed land mask and adjustments for lateral fluxes (Chevallier, 2021; Deng et al., 2022). Inversions are considered the most 'independent' method to compare with NGHGIs, but they require prior estimates of fluxes and a robust observation network to constrain results. If a managed land proxy is needed, then additional uncertainties arise. Robust comparisons also require lateral flux adjustments, such as land-to-sea fluxes and carbon transported by agricultural and forestry trade, to make them consistent with NGHGIs and other methods.

A key question is what land areas and processes dominate emission estimates. Figure 7a shows a schematic of the different land areas and effects, and which aspects are covered by which methods. A weakness of earlier figures is that they do not give a general sense for which effects are dominant. This will vary by country, but generally, the uptake on 'managed land' where there is no land use change (e.g., particularly forest remaining forest) is argued to be the dominant effect (Grassi et al., 2023). Figure 7b gives some more realistic distributions and identifies key processes, though remaining hypothetical.

The most problematic issue is how to allocate emissions or removals from forestland, particularly what we have labelled 'other managed land' and the magnitude of indirect effects (e.g., CO_2 fertilisation). CO_2 uptake in these areas could be due to recovery from previous disturbance, age-class effects in forestry activities, indirect effects like CO_2 fertilisation, in addition to a range of other effects. Different methods and models will apportion different shares to these processes and this is also a key uncertainty understanding the future evolution of CO_2 uptake in forestlands.

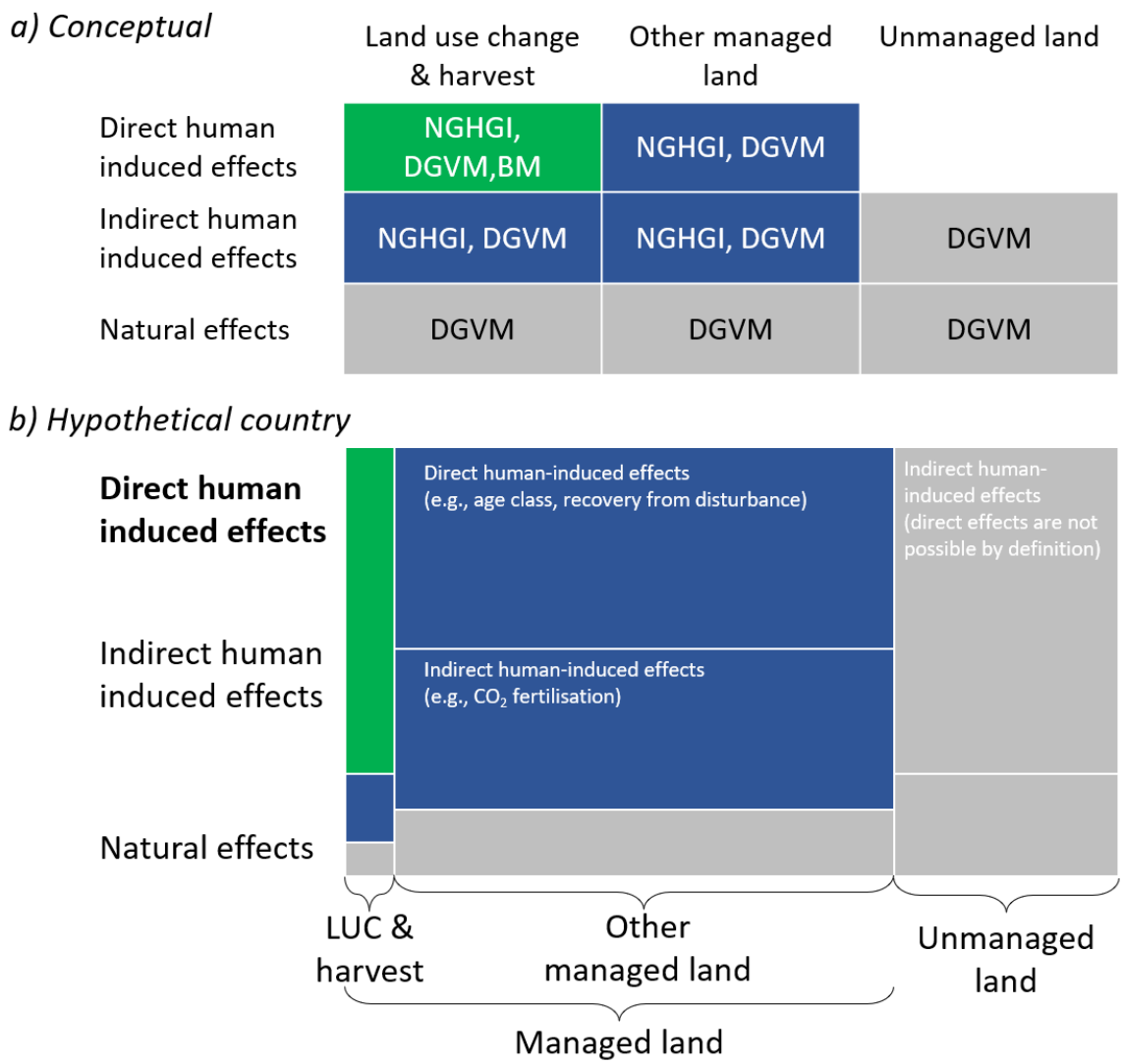

Figure 7: Land can be classified in different ways, and here it is classified on whether it is managed or unmanaged. The managed area can be classified involving a long-term (>20 year) area change (e.g., deforestation or afforestation), a temporary area change (e.g., wood harvest and regrowth), or no area change (e.g., forest remaining forest). Shifting cultivation is not included here. For a given area, the uptake can be from direct effects (e.g., uptake of carbon following a growth curve), indirect (e.g., enhanced uptake due to CO_2 fertilisation), & natural effects (e.g., pest disturbance or wildfire). a) Different models cover different aspects, but it can be hard to decompose the effects across methods. b) In a hypothetical country, the relative size of the effects will depend on the area, and the area could vary considerably across model type. The vertical extent is the proportion of uptake by land type. The colours represent model and method groupings that cover the same processes and areas.

Managed and unmanaged land

The definition and identification of managed land is a crucial factor when comparing estimates. Countries self-determine the lands they define as managed, with most Annex I countries defining all land as managed (Figure 8). There is no agreed upon method to define managed land, and given the definition includes “production, ecological or social functions”, it is potential almost any land could be defined as managed. Indeed, Annex I countries seem to define most land as managed, with the biggest exceptions Canada and Russia. Grassi et al. (2023) develop a ‘managed forests’ mask using a database of intact (unmanaged) and non-intact (managed) forests. This mask is not necessary in countries where all land is managed, and so we focus particularly on some of those countries below to avoid masking issues. In

countries with unmanaged land, where a mask is needed, several additional issues arise. These are discussed in more detail in the relevant sections below.

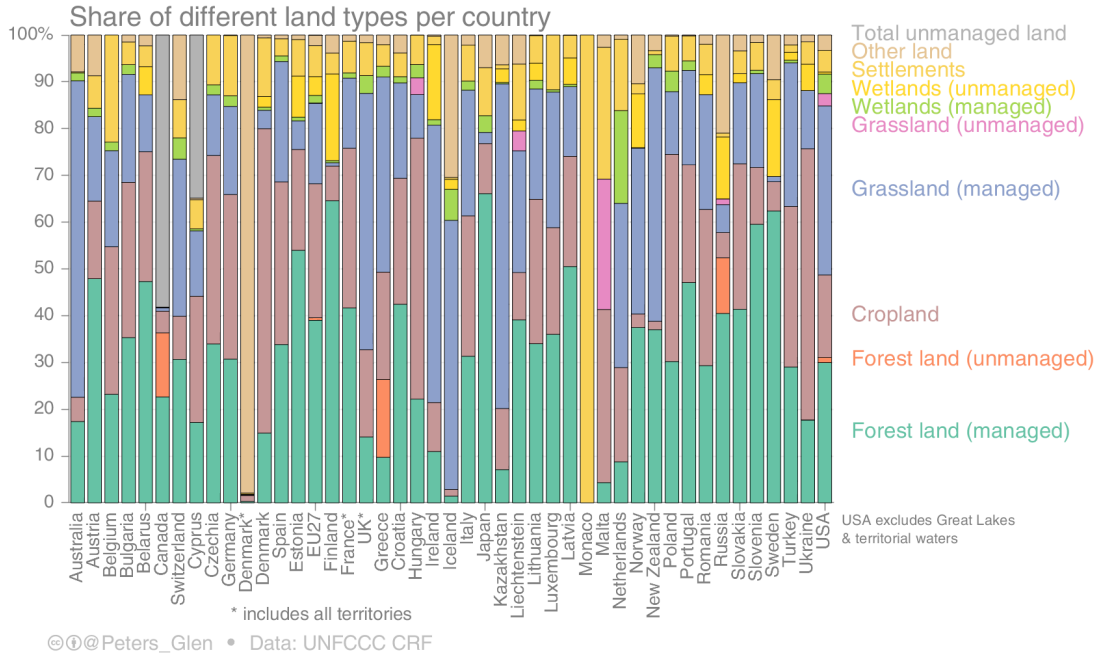

Figure 8: The share of different land types reported in UNFCCC Common Reporting Format for Annex I countries. Very little land is defined as unmanaged.

From concepts to equations

The conceptual framework (Figure 7) invites a more formal definition of the flux:

$DGVM(S3) = A_{M,LUC} (F_{dir}+F_{ind}+F_{dis}) + A_{M,harvest} (F_{dir}+F_{ind}+F_{dis}) + A_{M,other} (F_{dir}+F_{ind}+F_{dis}) + A_{UM} (F_{dir}+F_{ind}+F_{dis})$

where $A_{M,LUC}$ is the managed land where there is land-use change, $A_{M,harvest}$ is the area for harvest shown separately here, $A_{M,other}$ is other managed land, and A_{UM} is unmanaged land. Though, to make this distinction requires appropriate area masks, that in practice, would have to be highly resolve and a function of time. The carbon densities (tCO_2/ha) are for F_{dir} direct effects, F_{ind} indirect effects, and F_{dis} disturbances. These could be defined so that F_{dir} has a steady-state carbon flux based on pre-industrial conditions, $F_{dir} + F_{ind}$ is the steady-state for present conditions, and F_{dis} are the fluxes for disturbances (under some circumstances they could be assumed to average to zero).

The different model types are expressed as

$NGHGI = A_{M,LUC} (F_{dir}+F_{ind}+F_{dis}) + A_{M,harvest} (F_{dir}+F_{ind}+F_{dis}) + A_{M,other} (F_{dir}+F_{ind}+F_{dis})$

$BM = A_{M,LUC} F_{dir} + A_{M,harvest} F_{dir}$

Using these equations, the difference between the DGVMs and the NGHGI should just be a matter of careful mapping of land areas, using the correct carbon densities. The difference between BMs and NGHGIs would be

$NGHGI – BM = A_{M,LUC} (F_{ind}+F_{dis}) + A_{M,harvest} (F_{ind}+F_{dis}) + A_{M,other} (F_{dir}+F_{ind}+F_{dis})$

Grassi et al. (2023) argued that this gap can be bridged using DGVMs, though the TRENDY S2 experiment, which uses pre-industrial land areas and carbon densities:

$DGVM(S2) = A_M^{PI} F_{dir} + A_{UM}^{PI} * F_{dir}$

To combined with inventories requires removing the A_{UM}^{PI} through a land mask (Grassi et al., 2023), leading to an estimate of the NGHGI using BMs and TRENDY S2:

$NGHGI^{BM+S2} = BM + A_{M,other}^{PI} F_{dir} = A_{M,LUC} F_{dir} + A_{M,harvest} F_{dir} + A_{M,other}^{PI} F_{dir}$

The difference between this approach and the actual NGHGI is the 'Loss of Additional Sink Capacity' (Friedlingstein et al., 2023), as there is an inconsistency in the areas and carbon densities used. TheNGHGI and TRENDY S3 use transient carbon densities and areas, while S2 uses preindustrial areas and carbon densities, with a modern-day mask to correct for the relevant areas.

Formulating the problem this way helps clarify several issues. Understanding areas is one important aspect, particularly how they differ between methods ($A_{M,LUC}$, $A_{M,harvest}$, $A_{M,other}$) and the clarifying the carbon densities and how they are effected by environmental factors (like CO_2 fertilisation). The land areas may also be defined differently in different methods. UNFCCC requires land to stay in a fixed category for 20 years (default). Afforestation (from grassland) would be GL-FL for 20 years and then transfer to FL-FL, even if it is still growing. While in a BM the land would forever remain CL-FL. For this reason, it may not be possible to compare afforestation and reforestation between NGHGIs and BMs.

The construction of the TRENDY S2 and S3 simulations also create challenges. TRENDY S2 assumes preindustrial land, while TRENDY S3 has dynamic land from preindustrial to current land. To correct for these land areas, various masks or additional adjustments are required (Ciais et al., 2022).

Previous versions of this deliverable

The net land CO_2 fluxes are based on inventories, process models, and atmospheric inversions estimates from VERIFY, extended to include a $CoCO_2$ inversion (using CAMS). In the first version of this report (D8.1), the bookkeeping models (BLUE, OSCAR, Houghton & Nassikas), inventory datasets (UNFCCC, FAO), the TRENDYv10 ensemble (min, median, max), the atmospheric inversions (min, mean, max), plus a CAMS inversion including lateral fluxes and a managed land mask (Chevallier, 2021) were all included on the same figure (Figure 9). The problem with this figure is that it mixes too many datasets with many different system boundaries, making comparisons difficult.

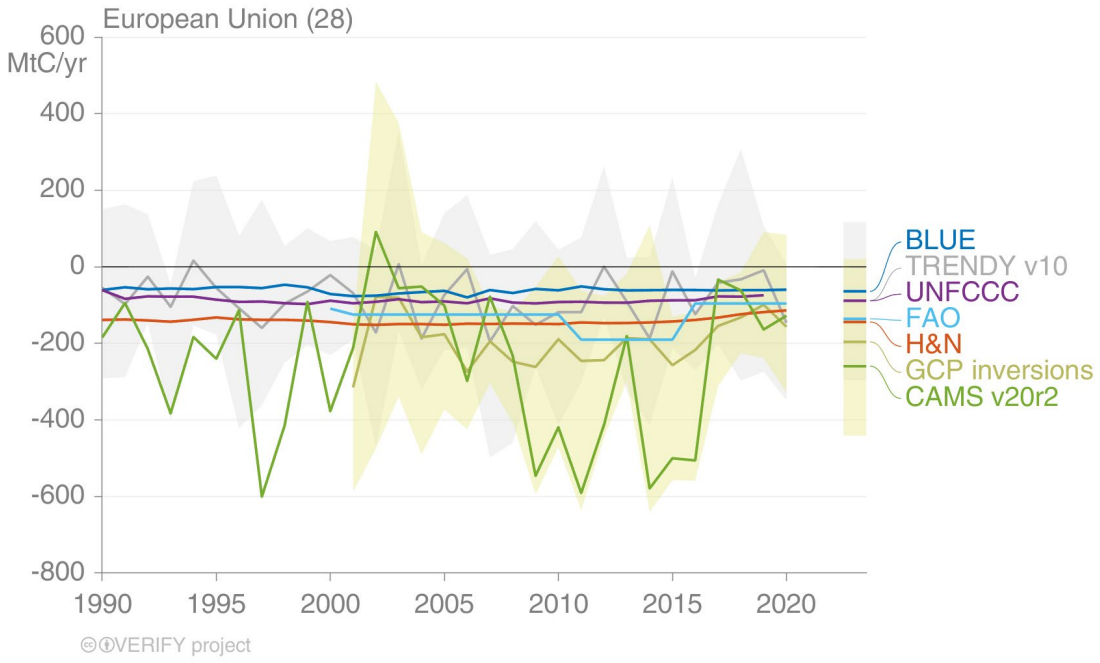

Figure 9: A comparison of inventories and inversions land CO_2 fluxes for the EU28 (EU27+UK). Shaded areas show maxima and minima of the TRENDY (grey) and GCP inversions (yellow). The figure is from the first version of this deliverable (D8.1).

In the second version of this deliverable (D8.2), the comparisons were separated by the type of model: 1) bookkeeping models, 2) land-surface models, and 3) inversion-based estimates. In each of these figures, the comparisons are made relative to the UNFCCC NGHGI estimates (Annex I countries) or the estimates of Grassi et al. (2022) (non-Annex I countries).

This version of the deliverable (D8.3) continues the separation by type of model, but additionally performs a deeper analysis by 1) comparing components of the bookkeeping models, 2) using country masks for TRENDY and making comparisons using both S2 and S3, and 3) using country masks and lateral flux adjustments for the inversions. Attempts are made to describe the country comparisons in more detail, with explanations for the differences.

Several articles were published in the last 12 months that help further this version of the deliverable. Two articles were published that apply the TRENDY S2 adjustments to the BMs to map better to NGHGIs, allowing us to now use those methods (Schwingshackl et al., 2022; Grassi et al., 2023). An article comparing observation-, inventory-, and model-based estimates of CO_2 emissions was published (McGrath et al., 2023), with Deng et al. (2022) doing a similar analysis for other countries. The Houghton and Nassikas BM has been updated (Houghton and Castanho, 2023). The BMs are all updated based on the latest Global Carbon Budget (Friedlingstein et al., 2023), but TRENDYv10 DGVMs and GCP2021 inversions are still used.

Bookkeeping and inventory-based estimates

Direct comparisons of BMs and NGHGIs do not make sense (section 4.1), without adjusting for 'managed land' (Grassi et al., 2023). Figure 10 shows the BM estimates and their average (Friedlingstein et al., 2023), together with an estimate of the NGHGIs at the global level (Grassi et al., 2023) and the average of the BMs added to the non-intact ('managed') forest estimate based on the median of the TRENDY S2 simulations with the non-intact forest mask (Grassi et al., 2023). The adjustment clearly brings the BMs and NGHGHIs in line. Adjusting the BMs for 'managed land' seems to be therefore highly important. The agreement at the global level is remarkably good, though, we further discuss regional results below.

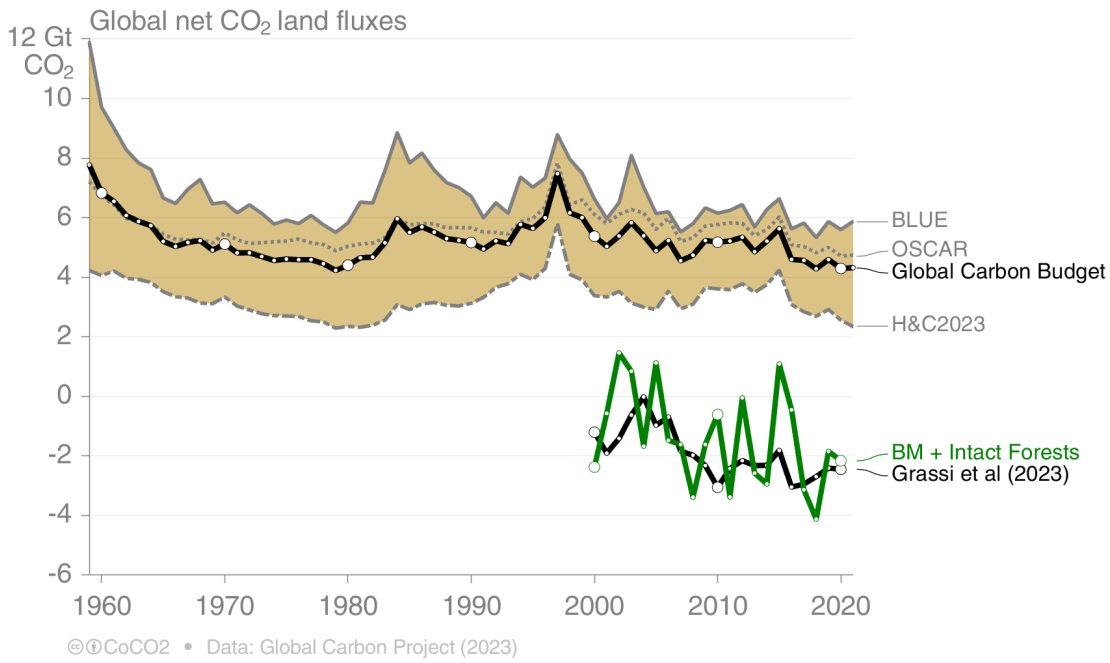

Figure 10: The net CO_2 land flux as estimated in the Global Carbon Budget (from three BMs), as estimated using inventories (Grassi et al 2023), and as the sum of BMs (mean) and the TRENDY S2 mask to give non-intact ('managed') forests.

Despite the importance of the 'managed land' adjustment, it remains relevant to compare components of BMs with components of NGHGIs. Comparisons with BMs may help

understand why the 'managed land' adjustment is needed and why it performs better in some regions than others (Schwingshackl et al., 2022). Figure 11 shows the results of the BMs for the global total, disaggregated into comparable components:

- **Total deforestation** is relatively flat at the global level. Nearly 60% of total deforestation is "permanent deforestation" and the remainder is 'shifting cultivation' (not separated in the figure). *Shifting cultivation* is an agricultural practice where there is a cycle of cutting forest for agriculture and then abandoning, which is not uncommon in the tropics. There is a slight downward trend in permanent deforestation.
- **Total regrowth** is composed of a flux due to af/reforestation (40%) and shifting cultivation (60%). Regrowth and deforestation in areas of shifting cultivation nearly cancel. Globally, the BMs collectively show a slight strengthening of the af/reforestation flux, particularly OSCAR, but af/reforestation is more than twice compensated by permanent deforestation.
- **Wood harvest and management** is dominated by wood harvest, with management including only fire suppression. The wood harvest includes products that flow into a Harvested Wood Product (HWP) pool and decay over time, in addition to the regrowth of the harvest area (if not deforestation). Globally, this is a small net source.
- **Other transitions** include transitions and fluxes on cropland, grassland, wetland, settlements, and similar. Globally, this is a small net source.

The addition of the four components in Figure 11 and organic soils (not shown) gives the total E_{LUC} flux from the BMs, as reported in the Global Carbon Budget (Friedlingstein et al., 2023).

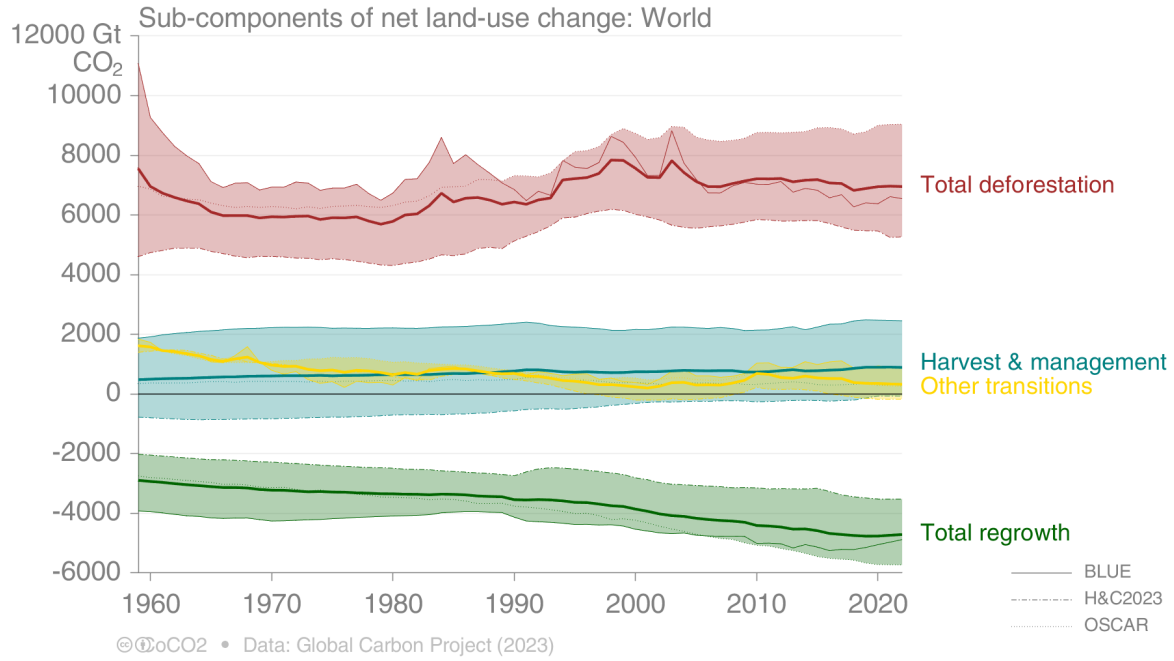

Figure 11: Components of the BMs by component, with the median of the three BMs shown as a solid line. Based on Friedlingstein et al (2023).

These categories are commonly used in BMs and aid comparisons with NGHGIs, though the definitions are not always consistent. NGHGIs are based on land types, not processes, such as forestland, grassland, and cropland. Fluxes are allocated based on the land type. In a NGHGI, af/reforestation is allocated to forestland, but it is in a subcategory 'conversion' for 20-years (default) and then 'remaining' forestland. In a BM, af/reforestation remain in the "total regrowth" category. Thus, the NGHGI 'managed land' uptake, may include significant uptake from earlier (>20 year) af/reforestation activities. This is one area where there may be double counting in the 'managed land' adjustment made to BMs. Likewise, in a NGHGI, deforestation is allocated to final land type. Thus, if a forest is deforested and becomes cropland, then it is

allocated to cropland (as a conversation for 20 years, then as remaining). The shifting cultivation flux included in BMs probably does not represent a land use change, and therefore may not appear in the NGHGI, as it likely happens within the 20-year transition period required for a land use transition. These differences between allocating to processes (BMs) and allocating land types (NGHGIs) make comparisons more difficult, but achievable.

Figure 12 (EU27) shows the components of BMs mapped to the equivalent NGHGI land type, and estimates from Grassi et al. (2023) for the NGHGI (covering non-Annex I countries) and the TRENDY S2 non-intact forest estimates used as a proxy for 'managed land'. It is possible to also disaggregate afforestation, but that is not done here for reasons of comparability (explained below). The NGHGI and Grassi et al estimates don't agree exactly as Grassi et al (2023) have allocated organic soils on forestland, cropland, and grassland, to a separate component ('organic soils'). The net-LULUCF fluxes do agree between the datasets as the total includes all components. The difference between NGHGIs and Grassi et al (2023) in the components therefore give an indication of the emissions attributed to organic soils.

The **forest flux** (top-left) includes both the "wood harvest and other management" and "total regrowth". The "wood harvest and management" uptake is small in the BMs for the EU27, with "total regrowth" dominating. The two components are combined for consistency with the NGHGI (forestland), though, comparisons can be made with regrowth as well. The IPCC Guidelines require a 20-year (default) transition period for a land use type to change. Thus, if grassland is converted to forest, it will remain in a forest "conversion" category for 20-years in the NGHGI and then be transferred to the 'forest remaining forest' category. If the forest continues to take up carbon after 20 years, this will continue in the NGHGI forest category. This is allocated differently in BMs, where the afforestation flux remains as regrowth and is not reallocated to another category. This would imply that the BM "total regrowth" category could be much larger than the NGHGI, which is true for the EU27 (not shown explicitly), but it is not known if this is the only reason.

The non-intact (managed) forest adjustment (green) is of similar magnitude to the uptake in BLUE and H&C. In the Grassi et al. (2023) approach, this flux is *added* to the BMs, but in the case of the EU27, the corresponding adjusted BM estimates are too large (Figure 16), particularly if applied to BLUE and H&C and not the BM average. This is also the case for the USA (not shown). This warrants further investigation, on why the 'managed land' adjustment is too large in the EU27 and the USA. The EU27 has had intensive forest activities over the decades, and if these are represented in the historical data driving the BMs, then it could be expected that the BMs should have reasonable estimates of uptake on 'managed land'. The problem is that this uptake occurs as 'managed land' in the NGHGI, as the af/reforestation activities that occurred more than 20 years ago are transfer to forestland.

The **total deforestation** agrees well between NGHGIs, H&C, and OSCAR, but not BLUE, while the **other transitions** are higher in the NGHGIs. These differences may also relate to the 20-year accounting period used in the NGHGIs. If a forest is converted to grassland (deforestation), the flux will appear in the NGHGI 'grassland conversion' category (deforestation) and then after 20 years be placed in 'grassland remaining grassland' category (other transitions). In the BMs, all deforestation related fluxes will be allocated to deforestation. Thus, it may be necessary to compare after combining deforestation and other transitions. These differences still require further investigation.

When comparing the BMs and the NGHGI with the **net LULUCF flux**, the issues with allocation and the 20-year transition period will partially cancel. In the EU27, the BMs are not that far from the reported NGHGI for the EU27, which means including the TRENDY S2 'managed land' adjustment would overestimate the uptake (see also McGrath et al., 2023). This contrasts most other countries (Schwingshackl et al., 2022). For the EU27, the H&C BM maps very closely to the NGHGI, which is a point for further discussion, as it may be that the H&C input data sufficiently captures the land-use history in the EU27 and can therefore reproduce the current uptake. OSCAR on the other hand, barely gives any uptake in the EU27.

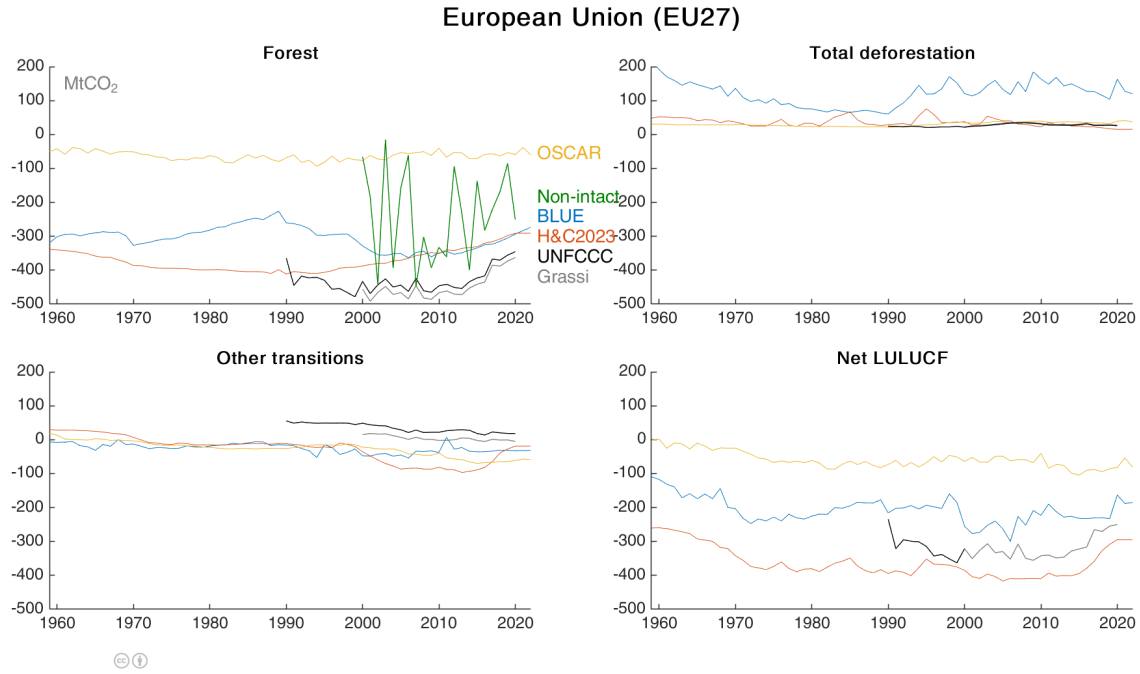

Figure 12: Net land CO_2 flux for BMs by component for the EU27, with estimates also shown for Grassi et al (2023) with alternative NGHGI estimates and TRENDY S2 estimates of non-intact (managed) forests. The 'non-intact' uptake estimate is not added to the BMs here.

The top three largest emitters for E_{LUC} are Brazil, Indonesia, and the Democratic Republic of the Congo. For these countries, there is a relatively reasonable agreement between the BMs and NGHGIs (Schwingshackl et al., 2022; Grassi et al., 2023), particularly given the expected uncertainties for these countries. This is interesting, but likely represents shared input assumptions across the different BMs. We therefore do not make comparisons between BMs and the NGHGIs for those countries here. Another way to think about which countries to compare are the countries with the largest differences between the BM and the NGHGIs, thus, where the 'managed land' adjustment is most important. The countries with the biggest differences are, depending on BM, China, USA, Brazil (driven by OSCAR), Russia, and Congo (which may be more reflective of a poor NGHGI estimate). Interestingly, two of the regions are Annex I countries (EU27, USA), where one would assume better reporting and data availability. We focus next on China.

China accounts for around 20% of the global gap between NGHGIs and BMs, and Figure 13 compares BM and NGHGI components. The NGHGI includes large-scale afforestation, but this is not captured in the BMs or DGVMs (top left) (Schwingshackl et al., 2022). The NGHGI also reports zero deforestation, in contrast to the BMs. This raises the question whether the difference between the NGHGI and BMs is really driven by 'managed forests' or other factors, such as poor land-use transition data used as input into the BMs. Similar findings are found looking at other countries with big differences: are differences due to lack of sufficient input data for the BMs, incorrect NGHGIs, or the 'managed land' adjustment?

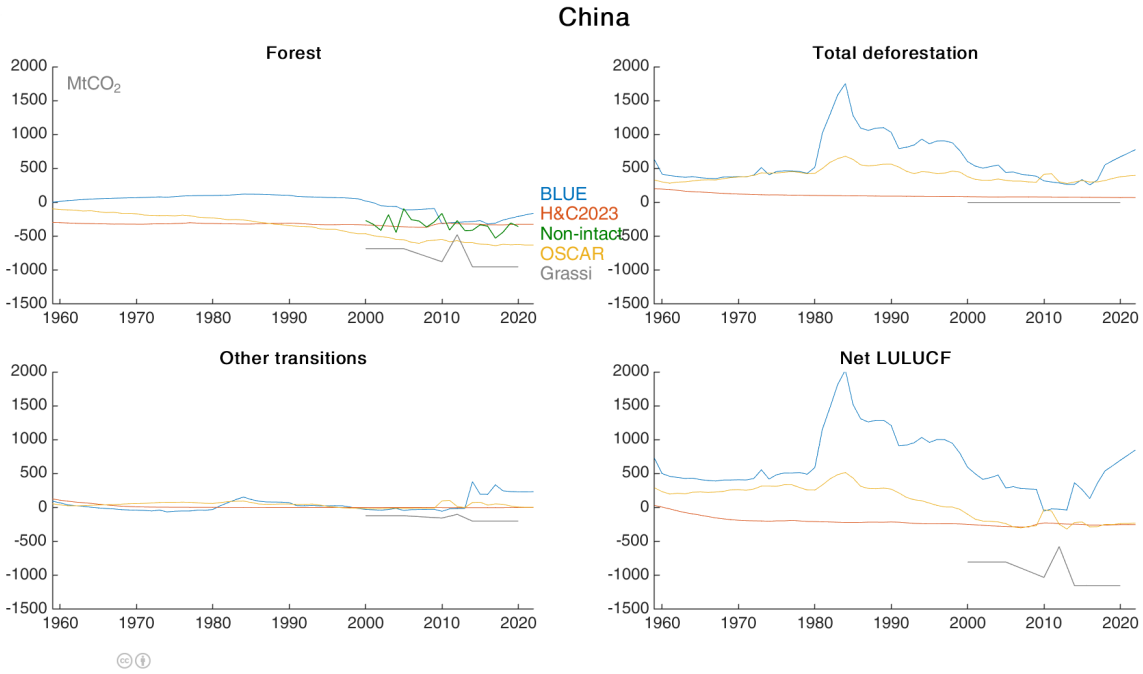

Figure 13: Net land CO_2 flux for BMs by component for China, with estimates also shown for Grassi et al (2023) with alternative NGHGI estimates and TRENDY S2 estimates of non-intact (managed) forests. The 'non-intact' uptake estimate is not added to the BMs here.

These comparisons, while only demonstrative, do not rule out the BMs as being useful for comparisons of NGHGIs. While the use of 'managed land' may, in general, help shift the BMs closer to NGHGIs (Schwingshackl et al., 2022; Grassi et al., 2023), this is not always the case at the regional level. It may be that for various data and reporting reasons, the BMs do reasonably well in some Annex I countries (e.g., the approach by H&C may be more consistent with NGHGIs). Alignment between BMs and NGHGIs could be coincidental in some instances. However, in other cases, there may be a clear reason for similarities. Since most of the EU land area is managed and the H&C takes a country level approach using FAO data that covers all land, then the similarity in estimates for the EU could imply the indirect effects are relatively small (Petrescu et al., 2020); essentially, H&C may have sufficient historical land use data and carbon densities to 'spin up' to the current land sink. BLUE and OSCAR use an alternative grid-based land-use product (LUH2), ultimately still relying on FAO data, but the data may not be sufficient to 'spin up' to the current land sink. OSCAR weighs various simulations that are partly driven by the H&C forcing (i.e. FAO and FRA) and partly by the LUH2 forcing. The assumed carbon densities in each approach is believed to be important in explaining different between approaches (Bastos et al., 2021). While the main difference between BMs and the NGHGI at the global level remains the 'managed land' uptake, the underlying reason at the country or regional level may be more nuanced (Schwingshackl et al., 2022).

Most analysis so far has focused on comparing the average across BMs and the average across DGVMs (Schwingshackl et al., 2022; Grassi et al., 2023). However, when considering each BM individually, there can often be a BM that performs better than others and matches the NGHGI reasonably well. These individual BM comparisons need more work to understand what is driving the differences, and to what extent a 'managed land' adjustment is needed in all cases. A productive focus would be to see what land areas are driving the results in each region, across the different models and inventories.

Inventory-based land-surface models

As process-based land surface models, the Dynamic Global Vegetation Models (DGVMs), can provide additional details to inventories, and allow modelling of future evolution of the net land CO_2 flux. The process-based models are forced by climate and therefore have interannual

variability, while bookkeeping models and inventories are based on data or methods that essentially smooth out variability. This makes comparisons more complicated.

A total of 17 DGVMs follow a consistent protocol to allow model comparisons (Friedlingstein et al., 2022b). The different simulations in the TRENDY protocol are:

- S0 is a control simulation using fixed pre-industrial (1700) atmospheric CO_2 and a time-invariant pre-industrial land cover distribution,
- S1 applies historical changes in atmospheric CO_2 and Nitrogen inputs,
- S2 applies S1 and climate,
- S3 applies S2 and changing land cover distribution and wood harvest rates.

The 'natural' land sink is given by S2 and the net land CO_2 flux is given by S3, the difference (S3-S2) is comparable to the estimated land use flux from the BMs, after accounting for the 'Loss of Additional Sink Capacity' (Friedlingstein et al., 2022b). There are three main choices on how to compare the TRENDY DGVM results with the UNFCCC NGHGIs:

1. Compare BMs and the TRENDY LUC estimate (S3-S2)
2. Compare NGHGHI with BMs adjusted for 'managed forests' (BM + mask S2)
3. Compare NGHGHI and the TRENDY estimated net CO_2 land flux (mask S3)

Of these, the TRENDY S3 comparisons is most consistent with the UNFCCC NGHGIs system boundary, but a mask is needed to deal with 'managed land'. We consider each of these comparisons in turn.

NGHGIs versus Bookkeeping Models

The difference between TRENDY S3 and TRENDY S2 should be equivalent to the BMs, after accounting for the 'Loss of Additional Sink Capacity' (LASC) (Friedlingstein et al., 2023). Figure 14 shows a comparison of the BMs, DGVMs (S3-S2), and NGHGI (Grassi et al., 2023). The NGHGI is expected to be lower than the BM and DGVM estimates, and this is discussed in the next section. The LASC represents a transient and increasing trend, and in this context, one could argue there is reasonably good agreement between the BMs and DGVMs. However, a more useful comparison is at the regional level.

Figure 15 repeats the comparison for Brazil. The NGHGI is comparable to all other estimates here, suggesting the 'managed land' issue is not so important in Brazil. The advantage of looking at Brazil is that it has a very strong deforestation signal, which appears to peak in adjacent years across the datasets. The DGVMs (S3-S2) do not seem to pick up the deforestation signal, at least not to the strength reported in the BMs and NGHGHI. The choice of land-use data is important for estimating Brazilian LUC emissions (Rosan et al., 2021).

While Brazil only represents one country, it indicates that the TRENDY and BM results in other countries may not pick up the deforestation signal. Conceptually, a direct comparison with NGHGIs and TRENDY S3, with appropriate forest mask, is the most consistent. Thus, a broader point here is whether the TRENDY S3 simulations will be suitable to compare to the NGHGIs. A comparison of the TRENDY S3-S2 simulations with the BMs indicates that TRENDY S3 may not always pick up the deforestation signal, which would imply it is not in the input land-use transition data (Rosan et al., 2021). If the input data is not sufficient, making a comparison of TRENDY S3 and NGHGIs more challenging, even if it makes sense conceptually.

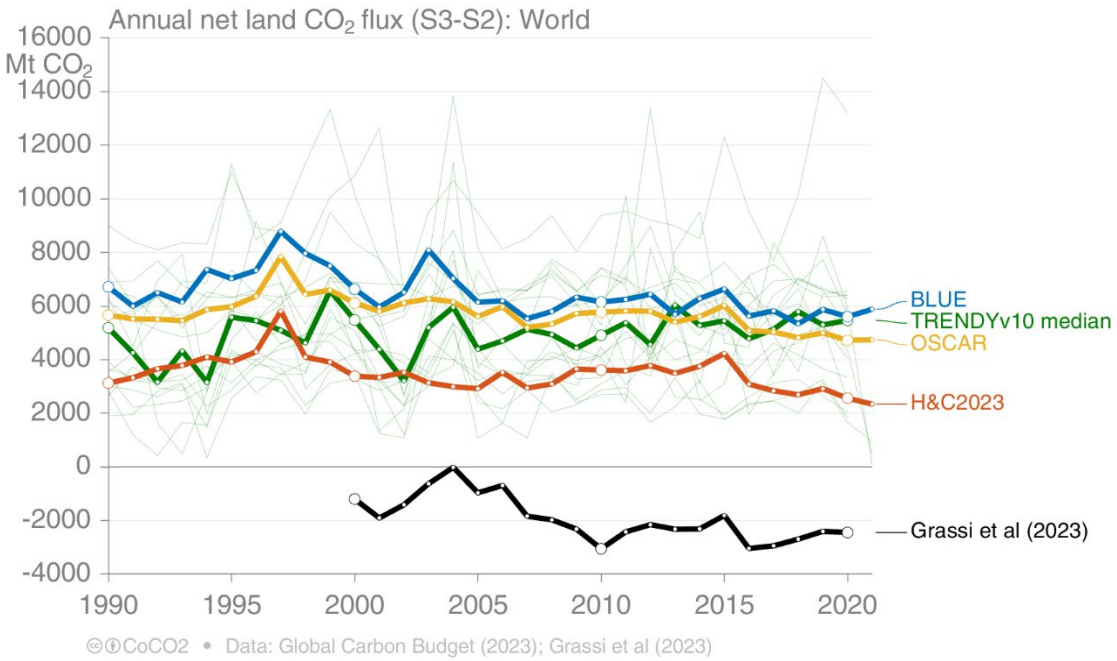

Figure 14: A comparison of the global LUC estimates from BMs, the TRENDY DGVM individual (S3-S2) results and median, and the NGHGI estimated at the global level.

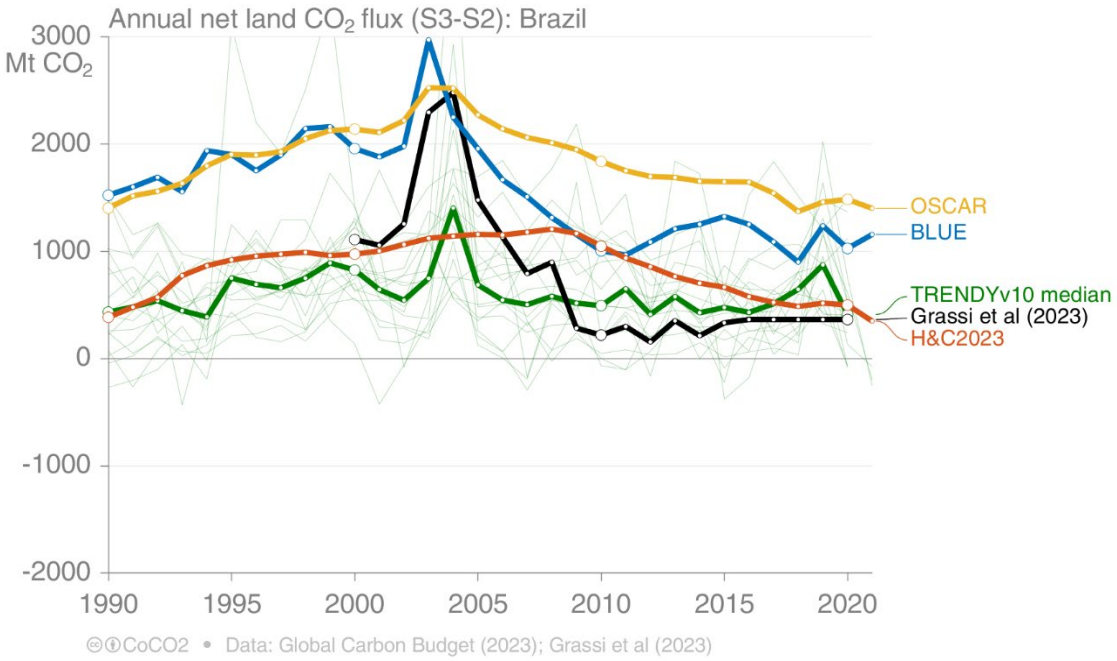

Figure 15: A comparison of the global LUC estimates from BMs, the TRENDY DGVM individual (S3-S2) results and median, and the NGHGI for Brazil.

NGHGIs versus Bookkeeping Models and 'managed land' proxy

Grassi et al. (2023) developed a method to map between BMs and NGHGIs, using the TRENDY S2 simulations together with a mask of 'managed forests' (defined as intact forests). A key point here is that the method is developed as a *mapping* between BMs and NGHGIs, not as a means of verification of NGHGIs. TRENDY S3 may be a more direct means of verification of NGHGIs (next section).

Already in Figure 12 (EU27) and Figure 13 (China) we explored more detailed comparisons of NGHGIs and BMs, also showing the estimate of TRENDY S2 with a 'managed land' (non-intact forest) mask. Figure 16 and Figure 17 perform the adjustment proposed by Grassi et al (2023), for the EU27 and China, to continue the discussion on these two countries previously. Performing the adjustment for the EU27 makes the carbon uptake larger than reported by the NGHGI. Though, interpreting this is difficult given the large spread in the BMs. It may be that the methodology and data used by H&C is able to capture the dynamics of the EU land sink, while OSCAR cannot. Decomposing the reasons behind the differences would require more analysis to understand the diverging results.

The case in China is different, as the 'managed land' adjustment is not large enough to bridge the gap between BMs and NGHGIs. As argued by others (Schwingshackl et al., 2022), it could be that the BMs and DGVMs simply miss the large recent afforestation activities in China, or it could also be that China is overreporting uptake in its forests. The Grassi et al (2023) estimate, based on BURs, reports no deforestation for China despite significant estimates in the BMs (Figure 17).

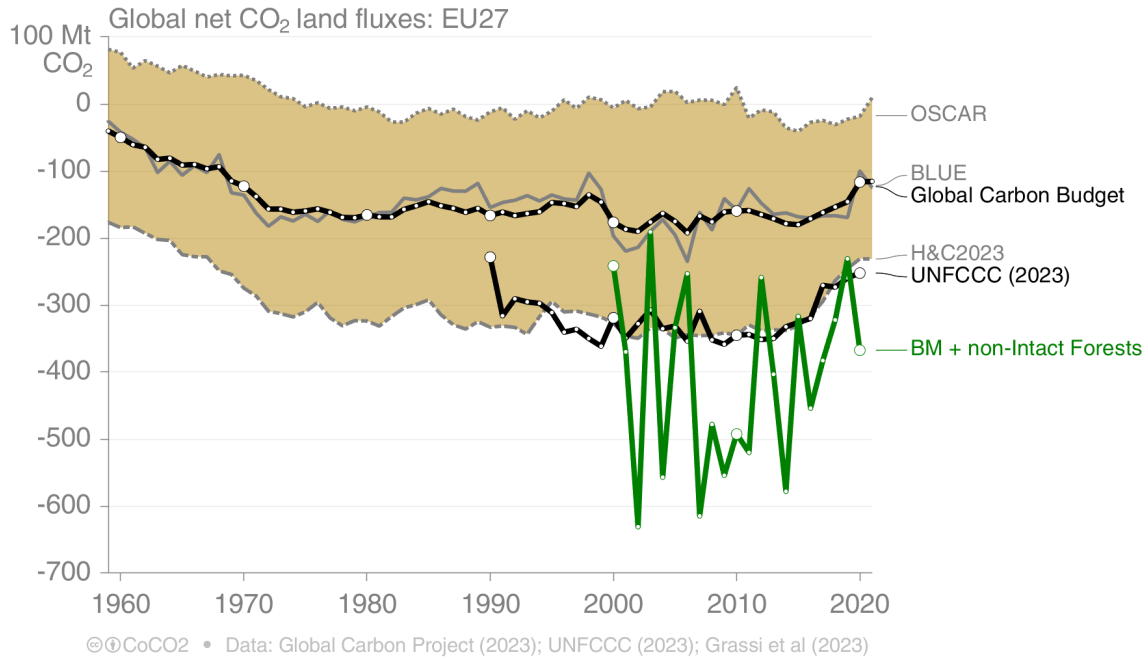

Figure 16: Estimated net land fluxes in the EU27 for the three BMs used in the GCB (Friedlingstein et al 2023) together with the UNFCCC estimated net-LULUCF flux, and the adjustment of the BMs with the TRENDY S2 (masked for non-intact forests).

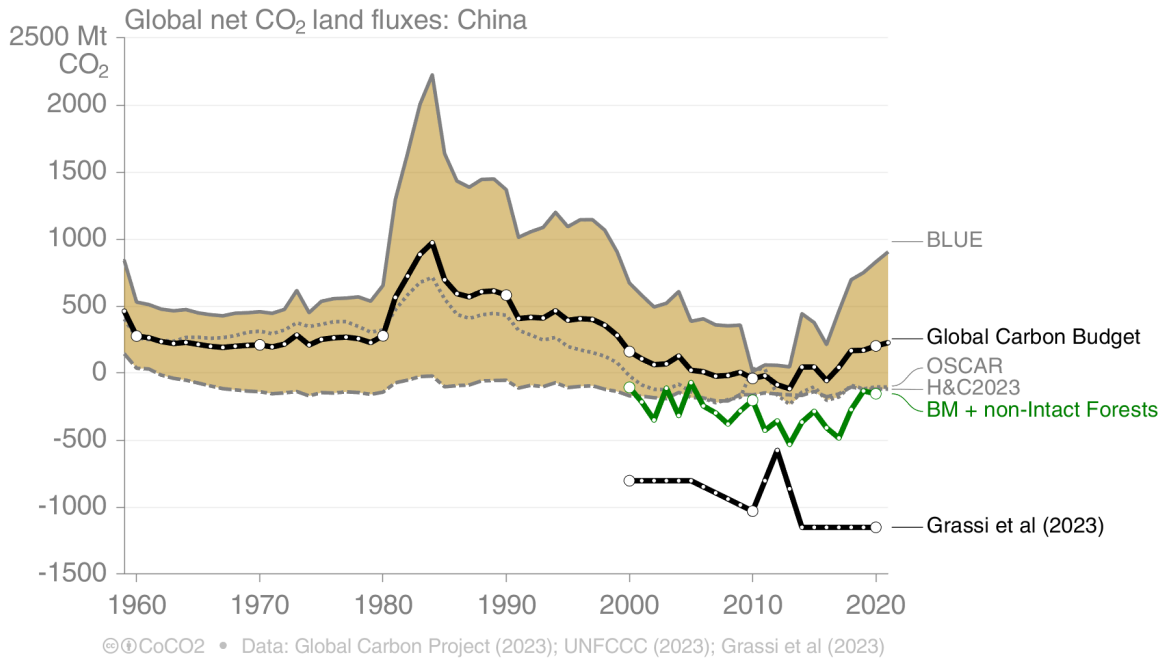

Figure 17: Estimated net land fluxes in China for the three BMs used in the GCB (Friedlingstein et al 2023) together with the UNFCCC estimated net-LULUCF flux, and the adjustment of the BMs with the TRENDY S2 (masked for non-intact forests).

While the adjustments using TRENDY S2 moves the BMs very close to the NGHGIs at the global level (Figure 10), the regional differences tell a different story. The EU27 and China are cases where the adjustment does not work so well. The Indonesia results show close agreement between NGHGIs and BMs (not shown), but this may be because they are dominated by overlapping datasets for organic soils. Brazil also shows generally good agreement (not shown), despite some noise, but again, there is perhaps surprisingly good agreement between BMs and the adjustment is not doing that much to move the estimates. The USA, on the other hand, demonstrates a large variation (not shown). It is perhaps disturbing that the TRENDY S2 adjustment performs poorly in regions like the EU27 and the USA, where one would expect the best quality area and carbon density data. The generally good performance in Indonesia and Brazil may represent that the signal is dominated by deforestation, and the TRENDY S2 adjustment, though large, offers small relative gains. There is clearly a need for more research to understand why the BMs deviate from the NGHGIs and why the TRENDY S2 adjustment works almost perfectly at the global level, despite patchy performance at the regional level.

NGHGIs versus TRENDY S3

We argue here that if the purpose is to compare NGHGIs with independent datasets, then one would best compare NGHGIs with TRENDY S3, which has dynamic land use and changing climate and CO_2 concentrations. This is most consistent with the NGHGI. Though, a 'managed land' proxy is still needed to adjust S3 to be consistent with the NGHGI. Conceptually, this comparison can also be linked back to the adjustments done by Grassi et al (2023), represented here as NGHGI ~ BM + αS2, where α is the non-intact forest share. Since BM=S3-S2 (ignoring the LASC), then the NGHGI ~ (S3-S2) + αS2. Grassi et al (2023) provide estimates of intact and non-intact forests, allowing α to be estimated, but this adjustment may not equally apply to TRENDY S3. A useful corner case is to compare countries where nearly all land is defined as managed (e.g., USA, EU27, China), then α=1 and NGHGI ~ S3, without the need for a mask. The challenges arise when α<1, when a mask is needed, and whether the mask used for S2 is also useable for S3, or whether other approaches are needed.

For countries with close to 100% managed forests (e.g., EU27, USA, China), the match between NGHGIs and S3 does not depend on applying a managed land mask. Figure 18 shows a comparison of TRENDY S3 and NGHGI for the EU27. Despite the variability in individual models and the median, the match is particularly good. Referencing back to the comparison of BM and TRENDY S2 (Figure 16), this may suggest that the BMs are not collectively representative of NGHGI or that the TRENDY S2 adjustment does not work for the EU27. Although not shown here, a similar result is found for the US, though TRENDY S3 does have an overall weaker sink. Perhaps not surprisingly, in China the uptake is too weak in TRENDY S3 (Figure 19), which again may confirm that international datasets have not incorporated sufficient afforestation or that the Chinese NGHGI is overestimating the uptake.

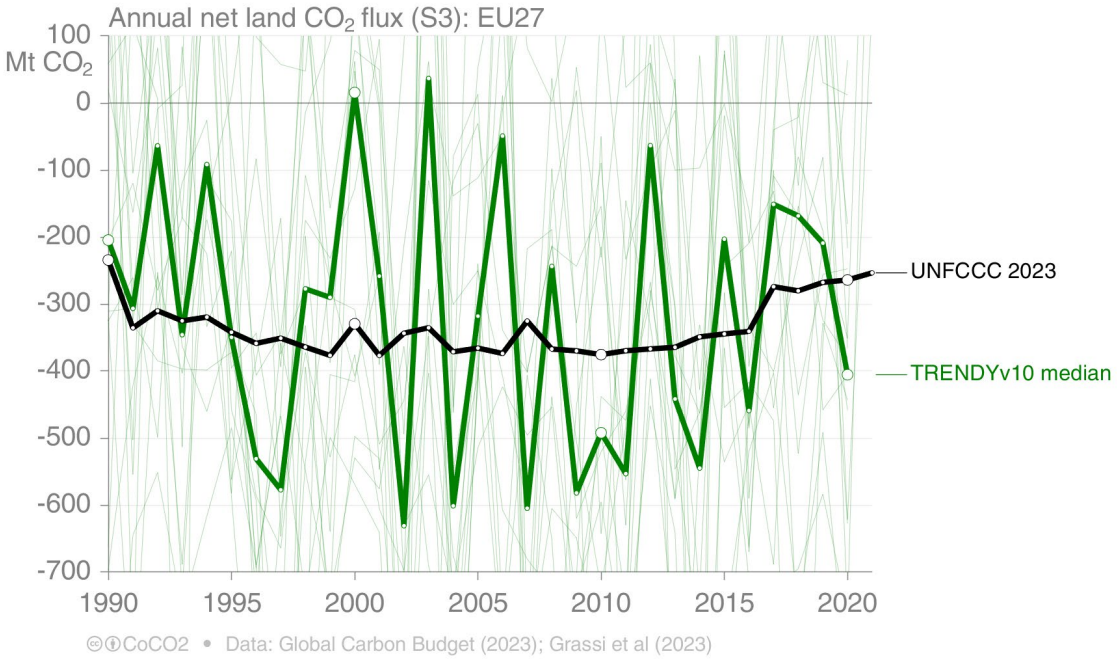

Figure 18: A comparison of UNFCCC NGHGIs for the EU27 and the TRENDY S3 individual results and median.

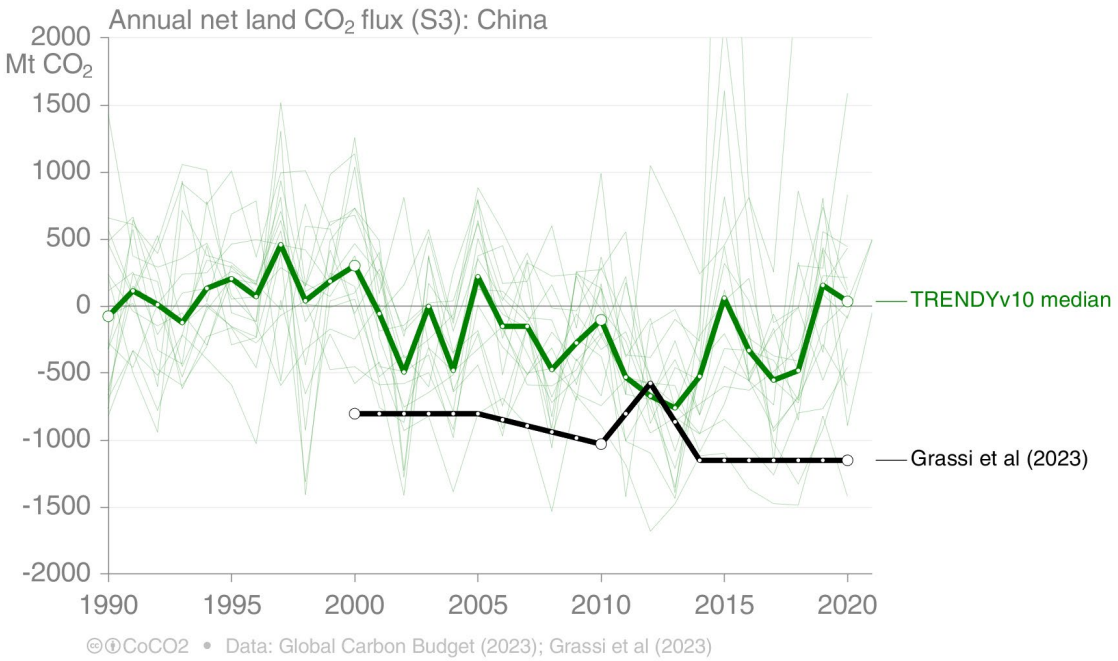

Figure 19: A comparison of UNFCCC NGHGIs for China and the TRENDY S3 individual results and median.

For regions where not all land is managed (α<1), the non-intact forest (managed land) mask is needed, as for TRENDY S2. However, it is unclear how this mask will apply for S3. There are potentially several issues with using the same mask. For TRENDY S2, the mask covers only forest land (20% forest cover), and the mask for 2012 is applied for all years. Theoretically, deforestation that occurred before 2012 would be outside the mask (consistent with NGHGIs), while deforestation after would be inside the mask after 2012. The challenge with a TRENDY S3 simulation, is that land-use change is dynamic, thus the mask needs to be dynamic as well. Additionally, the raw TRENDY results may have too coarse grid resolution to be able to reasonably separate afforestation, deforestation, and managed land. There is a possibility to use the plant function types to help disaggregate within a grid cell, but only a few TRENDY simulations provide this data (two for S3 have all the necessary data, while about five for S2 and another five with sufficient data to make reasonable estimates). Even if a time varying mask was available, it is unlikely that it would be sufficiently accurate, relative to the TRENDY model resolution, to be able to detect or capture deforestation or afforestation appropriately.

Within this deliverable we were not able to apply the mask to TRENDY S3 given insufficient data provided for the TRENDY S3 simulations. Though, we continue to explore workarounds. We envisage two key challenges applying the S3 approach. First, it is necessary to know whether the DGVMs can pick up strong deforestation (or afforestation) signals by comparing S3-S2 and the BMs. Second, it is necessary to know whether the grid resolution of the DGVMs, in addition to the forest mask (static in time) is sufficient to capture the land use dynamics of deforestation: Deforestation starts within a forest mask but ends outside the forest mask. Further work is required to explore the challenges and opportunities of using TRENDY S3.

Inversion-based estimates

Inversions using observation data are a powerful way to independently assess the accuracy of NGHGIs, however they do face some challenges. Figure 20 shows six global inversions, these inversions essentially represent six configurations of the land uptake that is consistent with the observations. A close inspection shows large regional variations, suggesting the regional-level inversion results are insufficiently constrained by current observations. In addition, the inversions are quite coarse, making it difficult to apply a mask to ‘managed land’

for two reasons: 1) Mapping the mask to grid points, 2) disaggregating each grid point into forest (intact and non-intact) and non-forest fluxes.

Inversions also need to adjust for lateral fluxes (Ciais et al., 2021). The inversion sees what the atmosphere sees, which may be different to what NGHGIs estimate. Using cropland as an example, carbon is removed from the biosphere at harvest, but respiration occurs where people reside. While the crop harvest and respiration process may be carbon neutral, an inversion would see a horizontal displacement of the flux (Ciais et al., 2007). In additional ro crops, Ciais et al. (2021) included lateral fluxes for forests and rivers. The river export is biogenic carbon from inland waters to the ocean, which was atmospheric origin as it was fixed by net primary production. There is also a term for outgassing from rivers and lakes. Ciais et al. (2022) provides a detailed description of each term, how it is derived and applied. Deng et al. (2022) performed a comparison of inversions with NGHGIs, showing the magnitude of the forest mask and lateral fluxes. Several other studies have included lateral flux adjustments (e.g., Petrescu et al., 2021a; McGrath et al., 2023). These lateral flux adjustments are important to compare inversions with NGHGIs, but more analysis is needed on the size of the effects and how consistent they are with NGHGIs.

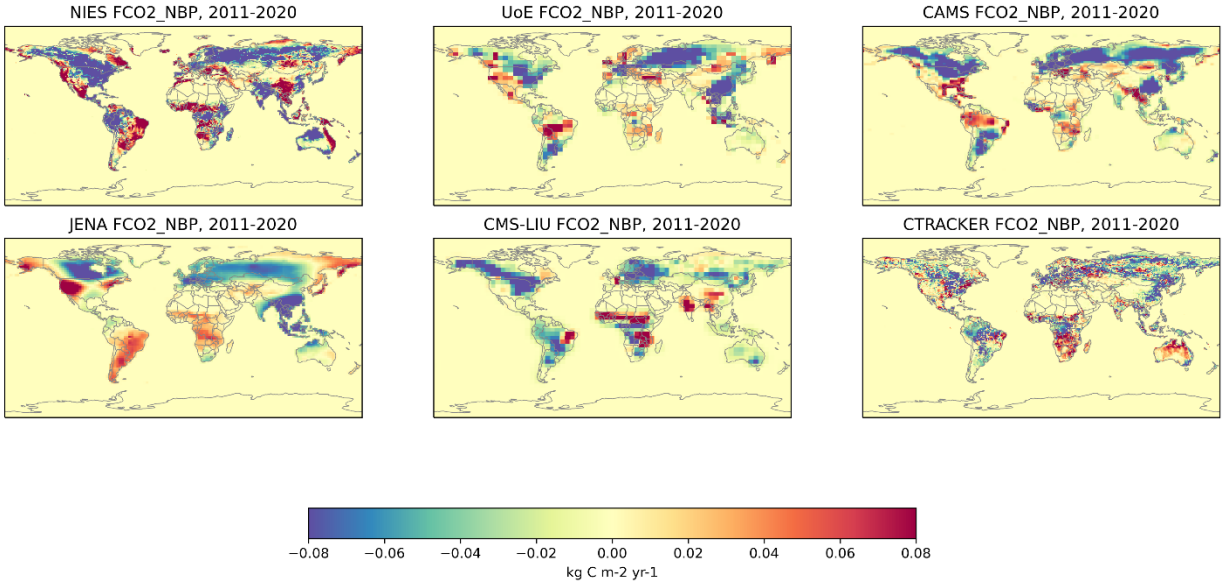

Figure 20: Global inversions from the Global Carbon Budget.

It is possible to do a direct comparison of inversions and NGHGIs, without masking for 'managed land'. There are two justifications for this direct comparison, which will be explored throughout this section. First, in some regions, close to 100% of the land is managed (e.g., USA, EU27, China), meaning that a managed land mask is not needed. Second, each inversion would have the same lateral flux adjustment, given the variability across inversions, the lateral flux adjustment is likely much smaller. Nevertheless, we include inversion results with and without the lateral flux adjustments as a point of reference on their relative importance.

Figure 21 shows the inversion results and their mean compared to inventory estimates for the EU27. The inversions collectively find a much stronger sink in the EU27, compared to all other datasets reported in this deliverable. It is unclear if the inversions are correct, or whether the inversion is inadequately constrained. The lateral flux adjustment is shown to be large here, bringing the inversions closer to the inventory, but with the wrong trend.

Figure 22 shows the same figure for China, indicating strong agreement between the inversion and the NGHGI, with a relatively minor lateral flux adjustment. The agreement between the raw inversion and NGHGI may support the hypothesis mentioned earlier that BMs and DGVMs are not detecting the recent afforestation in China, or the close agreement could just be

coincidental. It is unknown how constrained the inversion results are, requiring more information from the inversion modellers. In the USA (not shown), there is close agreement between the inversion mean and the NGHGI.

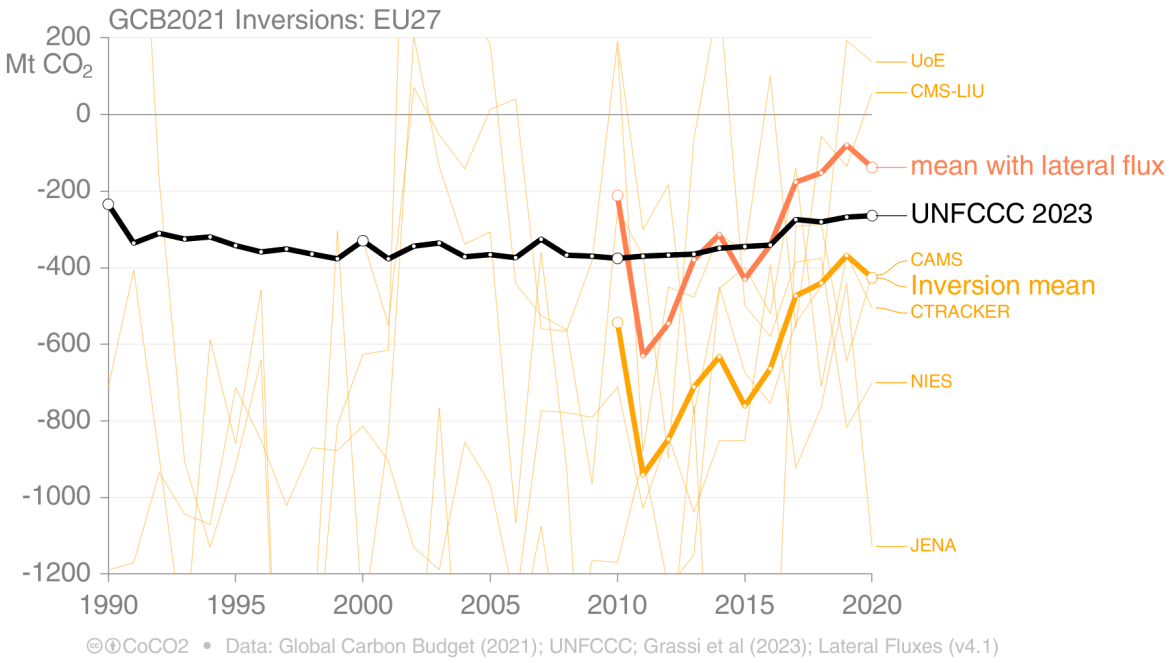

Figure 21: The net land CO_2 flux from six inversions (thin lines) and median and NGHGI for the EU27, with an estimate of the lateral flux adjustment applied to the median only.

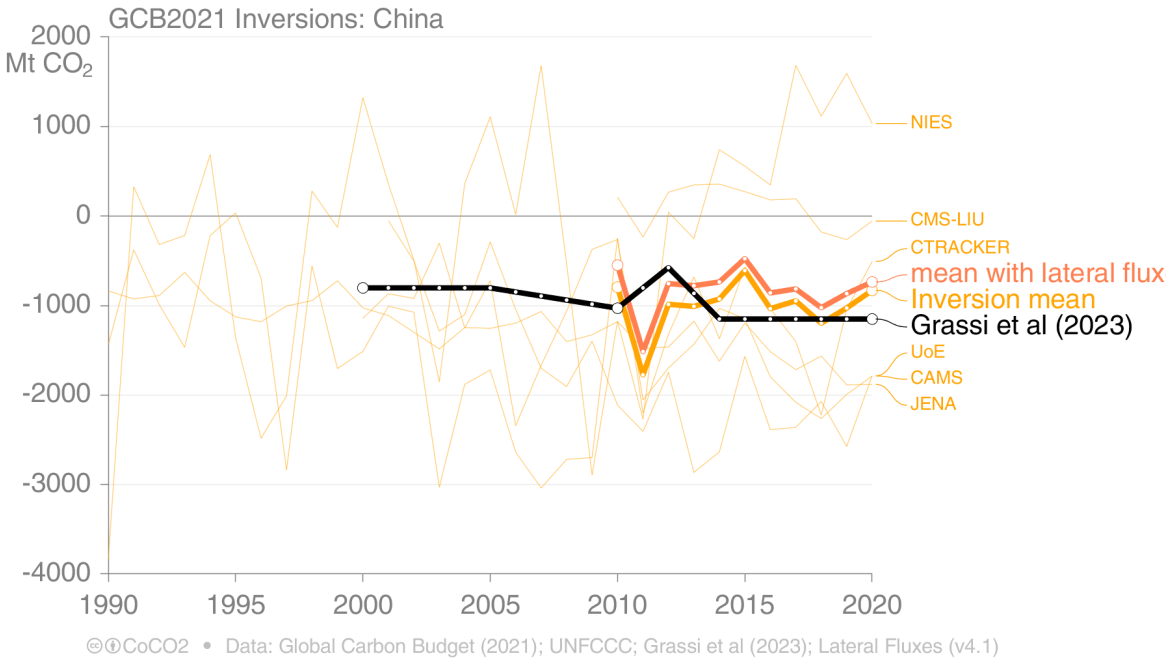

Figure 22: The net land CO_2 flux from six inversions (thin lines) and median and NGHGI for China, with an estimate of the lateral flux adjustment applied to the median only.

In both the EU27 and China, the lateral flux adjustments were found to be important. The lateral flux adjustments used here are made up of several components. Figure 23 (EU27) and Figure 24 (China) show the *net* lateral flux adjustment, for the various components:

- **Crop sink**: The CO_2 uptake when crops are grown (spatially located)

- **Crop source**: Respiration when crops are consumed (either via humans or livestock)
- **Forest sink**: CO_2 removed at forest harvest and put into the HWP (spatially located)
- **Forest source**: Decay and burning of HWP, adjusted for trade (import – export)
- **River sink**: Flow from rivers out of the country or region
- **River emissions**: Outgassing from rivers and lakes

The figures show the net of each of these terms (sink minus source), and when available, the estimate from Deng et al. (2022) is shown. Depending on the region, the lateral flux adjustment is dominated by different components. The net river fluxes are close to constant. There is globally a net uptake in forest harvest (due to storage in HWPs). Given the magnitude of the lateral flux adjustments for some countries, they need careful analysis to make sure they are consistent with the way NGHGI fluxes are defined. It is also possible to do lateral flux adjustments for bioenergy (liquid and solid), but that is not done here.

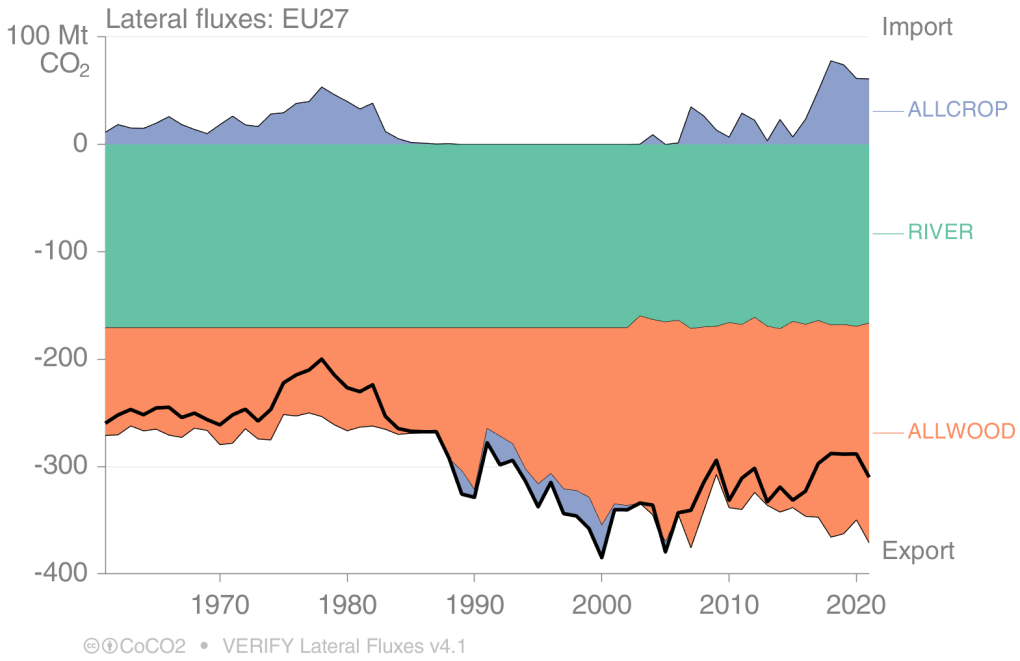

Figure 23: Components of the *net* lateral flux adjustment for the EU27.

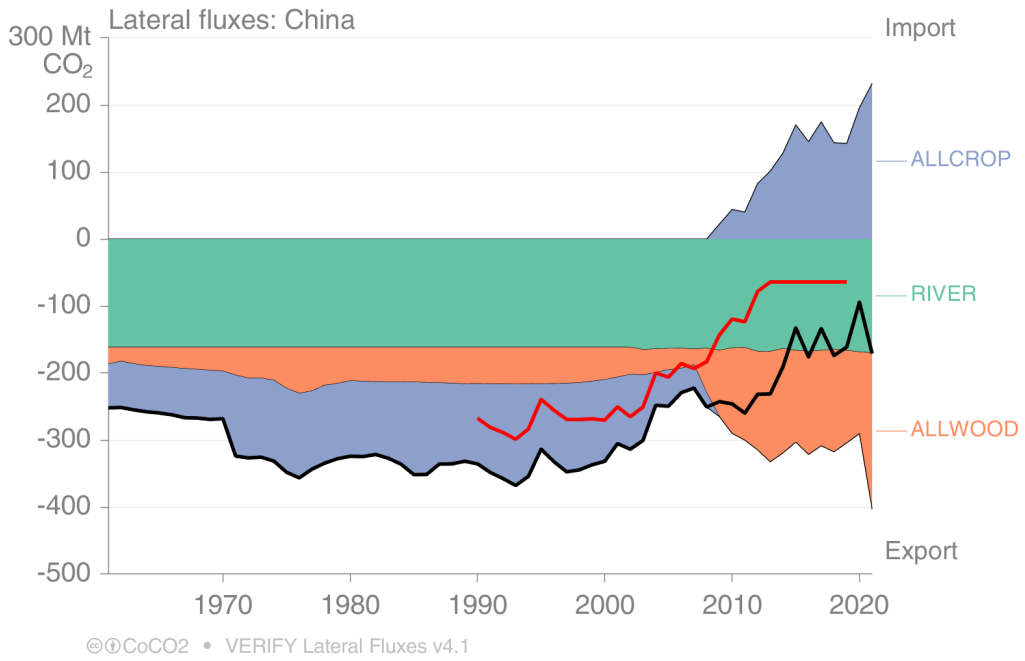

Figure 24: Components of the *net* lateral flux adjustment for the EU27, also showing the Deng et al (2022) results for comparison.

Further analysis is needed in regions where only a part of the land is managed. One challenge here is where to allocate the deforestation flux. Formally, in the NGHGI, deforestation would not occur on forest land but other land such as grassland or cropland (e.g., forest converted to grassland, then after 20 years grassland remaining grassland). For the inversions to map to the NGHGI, it would be necessary that the mask was sufficiently dynamic to correctly mask around deforested land at each time step. This is not possible, as the mask is based on 2012. Because of this, we use visual inspection to determine if the forest mask captures deforestation, and therefore where the NGHGI deforestation flux should be allocated to allow a reasonable comparison. An additional issue is how to disaggregate grid cells when the managed land mask splits a grid cell. Here we distribute the flux proportionally to areas, such that if 30% of the grid cell is non-forest, then 30% of the flux is non-forest. Other methods could be used, such as drawing on the plant function types in the DGVMs, but that is not done.

Indonesia has a strong deforestation flux, and thus is a good candidate to see whether the inversions detect it. Additionally, Indonesia reports 100% of land managed, but the Grassi et al (2023) forest mask assumes 80% is managed, so the land masking is less of an issue for Indonesia than other regions. Figure 25 disaggregates the Indonesian inversion results and NGHGI into intact (unmanaged) forest, non-intact (managed) forest, and non-forest. The net CO_2 fluxes on land are small for unmanaged forests in Indonesia. We have allocated the deforestation flux to non-forest land, therefore the managed land flux terms out to be well represented by the inversions. However, irrespective of where it is allocated, the inversions do not detect the deforestation flux. We find similar results in Brazil, where the inversions have not detected the deforestation flux.

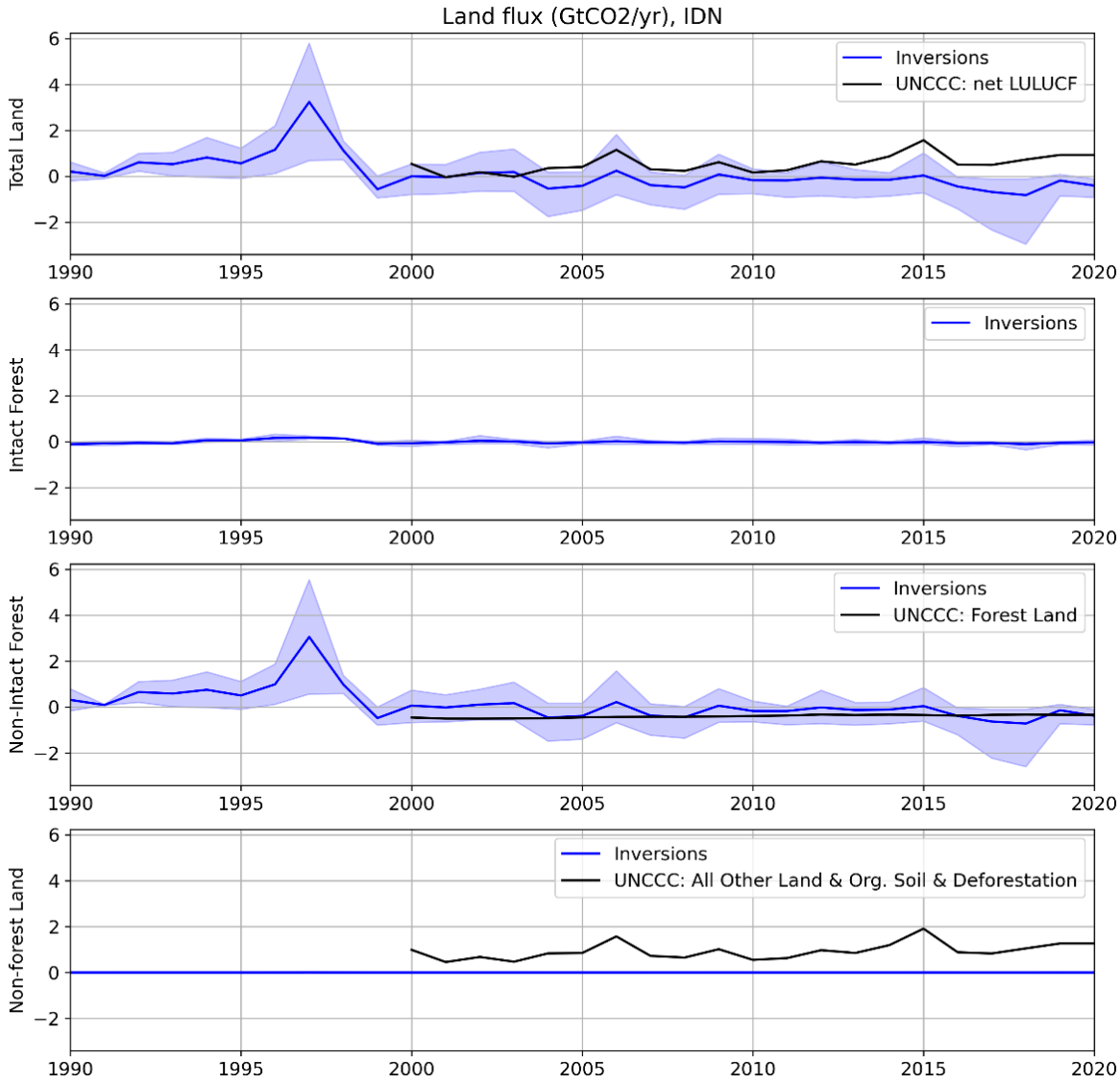

Figure 25: The GCP2021 inversion results with the Grassi et al (2023) land mask used to disaggregate total land (top) into intact (unmanaged) forests, non-intact (managed forests), and other land (bottom).

Canada has been an outlier country where the inversions suggest a considerably stronger sink (Deng et al., 2022). Figure 26 shows the inversions and NGHGI for Canada, demonstrating the significantly stronger uptake suggested by inversions. Canada also has vast areas that are not managed. A part of the uptake, around one quarter ($0.5GtCO_2$), occurs on unmanaged forest land, which is consistent with around one quarter of forest land being unmanaged. Virtually no net uptake occurs on non-forest land. This confirms that the vast difference between inversions and NGHGI occurs in forests, both managed and unmanaged.

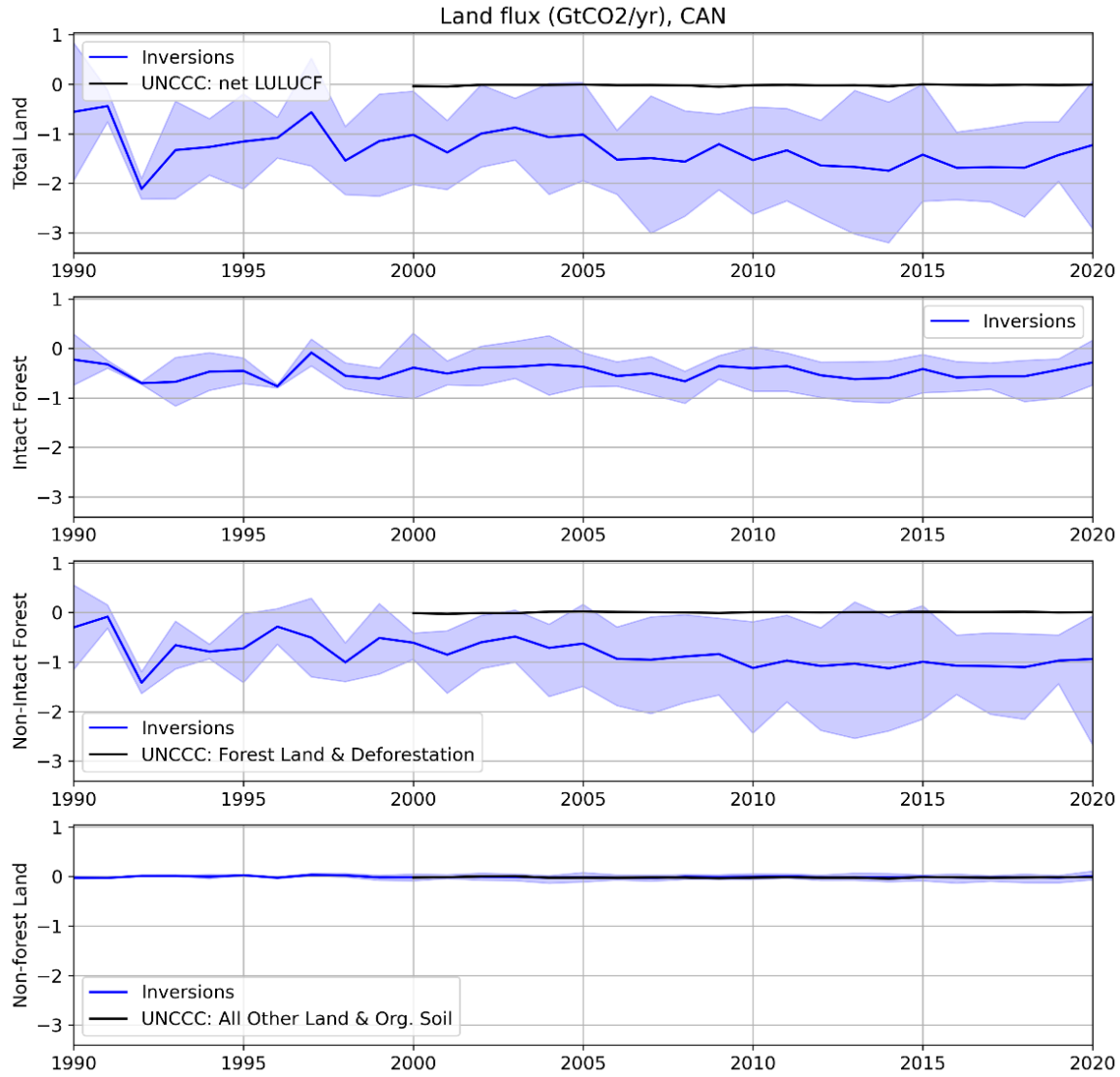

Figure 26: The GCP2021 inversion results with the Grassi et al (2023) land mask used to disaggregate total land (top) into intact (unmanaged) forests, non-intact (managed forests), and other land (bottom).

The CAMS inversion has been repeated to include lateral carbon fluxes and a managed land mask, with one inversion constrained on air samples and another on OCO-2 (satellite). Figure 27 shows the inversions for Canada. While the OCO-2 inversion maps closely to the Canadian NGHGI, the air-sample driven inversion does not. This may indicate that the inversions based on the air-sample data are not sufficiently constrained in Canada. The OCO-2 inversion also matches well the Indonesian flux in the last five years (not shown). In contrast, the inversions do not perform as well in Brazil (Figure 28) or in the USA, Russia, China, or the EU (not shown). For Brazil, the OCO-2 driven inversion has a very different trend to the NGHGI, while the air-sample driven inversion misses the large deforestation signal in the 2000s. Thus, we are in the same position again, not knowing if agreement between inversions and NGHGIs is due to chance or a well constrained inversion or NGHGI. Clearly, further analysis on these topics is needed.

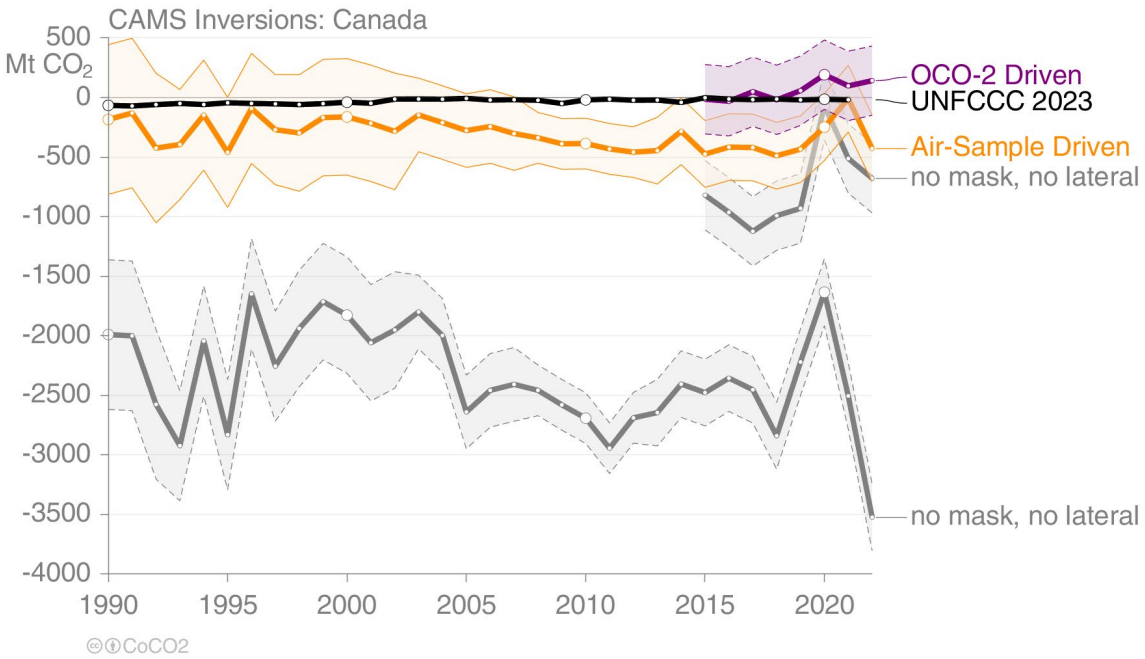

Figure 27: The CAMS inversions without (grey) and with (orange / purple) adjustments for lateral carbon fluxes and a managed land mask for Canada, for an inversion constrained on Air-Samples (orange) and OCO-2 (purple). The uncertainty band for one standard deviation is shown for the adjusted inversion.

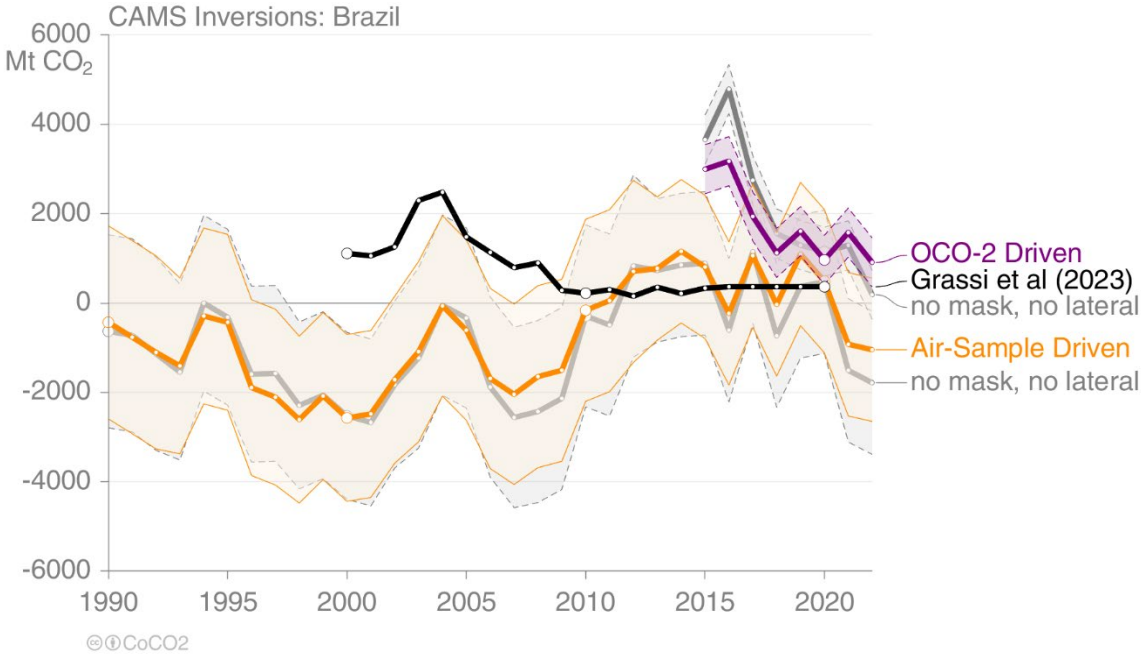

Figure 28: The CAMS inversions without (grey) and with (orange / purple) adjustments for lateral carbon fluxes and a managed land mask for Brazil, for an inversion constrained on Air-Samples (orange) and OCO-2 (purple). The uncertainty band for one standard deviation is shown for the adjusted inversion.

Summary discussion of net land

In this revised section on net land CO_2 fluxes, the issues in comparing estimates on land were highlighted. Without adjusting datasets for consistent system boundaries, one could argue that there is little to be gained in comparing different land use data products. A key driver of the

results is potentially the land areas covered, which are not routinely provided by different datasets. If land areas are available, then back calculation of implied carbon densities and their changes over time can be compared to provide additional interpretation of different data products. A continued issue is how to interpret agreement or differences in results. If an independent approach agrees with the NGHGI, is this by chance or confirmation of consistent datasets? A lot of the comparisons have been done using ensembles, but more focus is likely needed on individual models and data products, at the country level, to really draw out the differences between estimates, and whether we can be confident in agreements or differences. Clearly, more work is required in this area.

5 CH_4 emissions

Methane is the second most important GHG after CO_2 but more potent because of its higher radiative efficiency. CH_4 contributes to ~17% of the total global GHGs emissions using a Global Warming Potential (GWP100, CO_2-eq), but around 50% of current observed warming (IPCC AR6) due to its potent but short-lived nature. Sector wise, the primary sources of anthropogenic CH_4 emissions are agriculture (enteric fermentation), fossil fuel production, and waste management. In this report, we compare and analyse anthropogenic and natural CH_4 emissions for eight global countries, from observation- and inventory-based bottom-up and top-down sources and compare them to national inventories reported to UNFCCC, from the Common Reporting Format tables (CRFs) for Annex I Parties and from the Biannual Updated Reports (BURs) for the non-Annex I Parties.

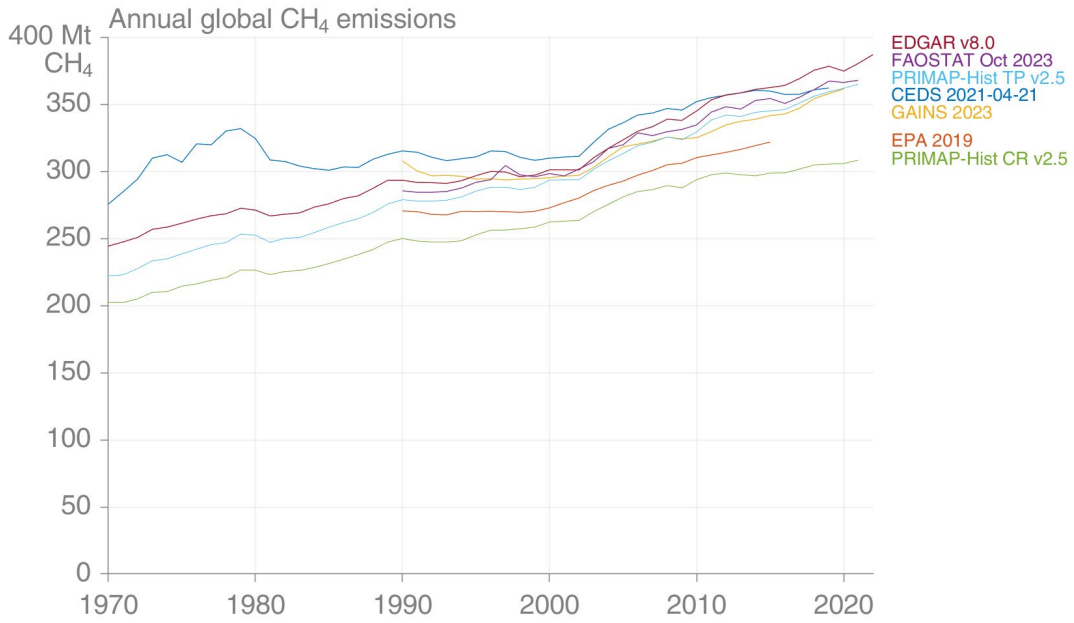

Figure 29: Total global CH_4 anthropogenic emissions from seven inventories, updated from Minx et al., 2021. The FAOSTAT independently estimates CH_4 from AFOLU, but uses PRIMAP-hist v2.4 for the remaining sectors.

Figure 29 presents the total global anthropogenic CH_4 emissions from seven inventories. All the datasets agree in terms of increasing trends during the last two decades, with differences in absolute emissions values. The differences between inventories are mainly caused by methodologies of producing or using AD, EFs or technological abatement (Minx et al., 2021). For example, the EPA inventory uses the reported emissions by the countries to the UNFCCC (often Tier 3) while other inventories produce their own estimates using a consistent approach for all countries and country-specific AD and EFs. FAOSTAT and EDGAR mostly apply a Tier-1 approach to estimate CH_4 emissions, while GAINS uses a Tier-2 approach. CEDS is based

on pre-existing emissions estimates from FAOSTAT and EDGAR, which are then scaled to match country-specific inventories, largely those reported to the UNFCCC (Minx et al., 2021). For EU27 the use of AD and EFs and linkages between data sources has been summarized in Figure 4 in Petrescu et al., 2020.

Inventory-based bottom-up estimates

The anthropogenic CH_4 emissions from inventory data covers emissions time series from 1990 to last available reported year and is presented for the EU and seven other global emitters: USA, Brazil, China, Indonesia, India, Russia and DR Congo. The data belongs to UNFCCC (2023, CRFs/BURs), EDGAR v7.0, GAINS, FAOSTAT completed by PRIMAP-hist v2.4, and the TNO_CoCO2_PED priors emissions datasets for 2018 and 2021. The TNO PED data is based on the UNFCCC reported data in 2020 for PED2018 and 2023 for PED 2021 and is detailed in the CoCO2 deliverables D2.1 and D2.2 (available at https://www.coco2-project.eu).

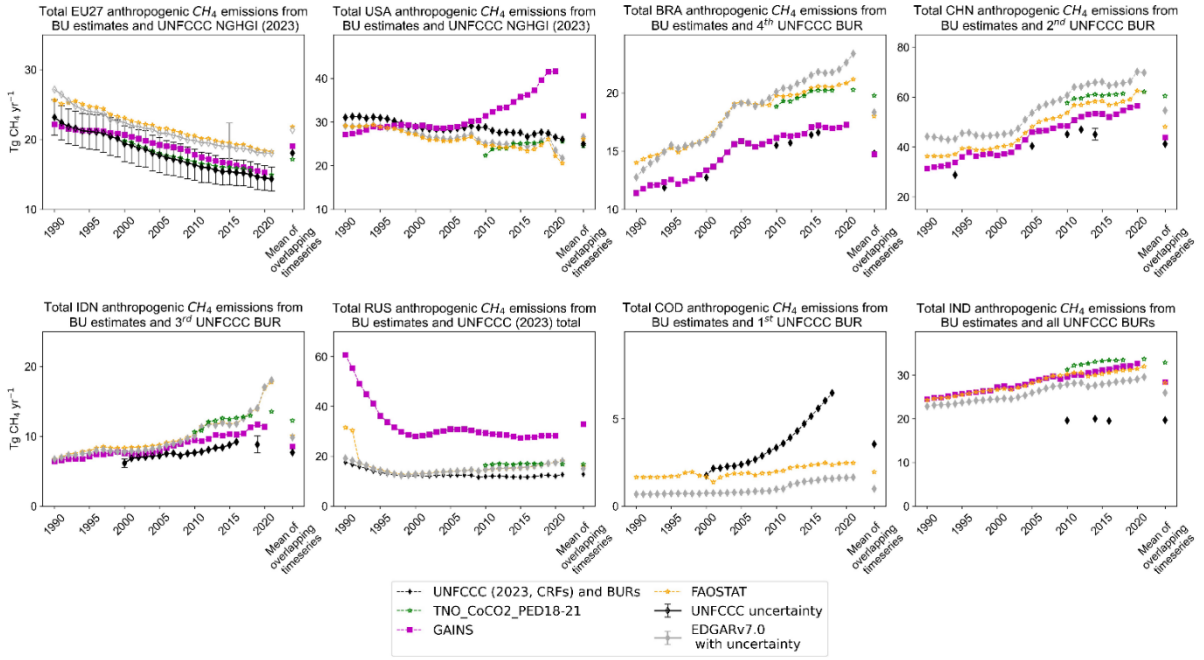

Figure 30: Total anthropogenic CH4 emissions from the UNFCCC CRFs and BURs (excl. LULUCF) and four bottom-up inventories (EDGARv7.0, GAINS (no IPPU), FAOSTAT (PRIMAP - hist v2.4 based, except for AFOLU), TNO_CoCO2_PED18-21) presented for the EU and seven global emitters. The relative error on the UNFCCC value represents the NGHGI (2023) reported uncertainties computed with the error propagation method (95% confidence interval) and gap-filled to provide respective estimates for each year. China and Indonesia report uncertainties, for 2014 and 2000 and 2019 respectively (BUR). Total COD UNFCCC BUR emissions do not include IPPU. The EDGARVv7.0 uncertainty is only for 2015 and was calculated according to Solazzo et al., 2021 for EDGARv5.0.

From Figure 24 we note that, except for the EU and USA which show decreasing trends in emissions from all datasets, all other countries show increasing trends.

In the EU, all inventory-based data sources are consistent with each other for capturing recent CH_4 emission reductions, but they are not independent because they use similar methodology with different versions of the same AD (Petrescu et al., 2020, Figure 4). The total 2018 CH4 emissions in the CoCO2 PED were ~4% higher than reported to UNFCCC in 2023. As CoCO2 PED was based on the national reporting but in the year 2020, these changes are due to changes in the estimations made by the member states.

In the USA, GAINS reports higher emissions after 2010, largely found in the Energy sector, resulting from the EFs used for conventional gas production as well as for unconventional shale gas extraction, which has increased rapidly since 2006. Also in Russia, GAINS

emissions are much higher than NGHGIs and the other two data sets due to the revisions of the assumptions on the average composition of the associated gas generated from oil production based on information provided in Huang et al. (2015). The higher emissions in GAINSv4 might be caused by a greater source from venting of associated gas instead of flaring.

For Brazil, UNFCCC and GAINS report emissions of similar magnitudes and trends. The EDGARv7.0 and FAOSTAT report on average around 23 % more emissions for the 1990-2021 period, but closely follow the NGHGIs trends. The similarity between trends could be explained by the use of the same EFs following Tier-1 IPCC 2006 Guidelines and UNFCCC NIRs (Janssens-Maenhout et al., 2019), while the higher emissions could appear when using different AD information.

For China the inventory estimates agree with the BUR reported data, with EDGARv7.0 showing the highest estimates. According to both GAINS and EDGARv7.0, the primary drivers for growth in Chinese CH_4 emissions are due to a mix of sources, mainly from the IPCC 2006 sector 1.B.1, fugitive emissions from solid fuels activity linked to increased coal mining.

In Indonesia the three global datasets agree well up until 2010. From 2010, the inventories show a continued increase in emissions, while the UNFCCC BUR emissions suggest a decline. EDGARv7.0 reports a large increase in emissions from fugitive emissions from solid fuels (coal mining) (IPCC 2006, sector 1.B.1.) at an increased average rate of 19 % per year and has increased by a factor of 152 until 2021 compared to 1990.

For Russia, GAINS emissions are much higher than NGHGIs and the other two data sets due to the revisions of the assumptions on the average composition of the associated gas generated from oil production based on information provided in Huang et al. (2015). The higher emissions in GAINSv4 might be caused by a greater source from venting of associated gas instead of flaring. FAOSTAT data for the Russian Federation starts in 1992, since the country did not exist before this date. The former USSR statistics were used prior to 1992 without adjustments and this is the cause of the 1990 and 1991 outliers in time series. The slightly increasing trend observed in EDGARv7.0 and FAOSTAT are set by emissions from the Energy sector.

In DR Congo, UNFCCC BUR data reports a strong increase in emissions, which is due to a rapid growth of CH_4 emissions from the Waste sector, by a factor of four until 2018 compared to 2000. This increase happened at an average yearly rate of +8 %, with an initial sharp increase of +30 % between 2000 and 2001, and we believe these needs further investigation.

In India, all global inventories agree on trends and magnitude but differ considerably from the Indian BUR, with EDGARv7.0, GAINS and FAOSTAT reporting 67% (2010), 68 % (2014) and 65 % (2016) higher than the official Indian estimates.

Observation-based atmospheric inversions

Figure 25 presents the total atmospheric inversions CH4 estimates versus UNFCCC official reported emissions for the EU and the seven non-EU emitters. The mean column on the right of each chart represents the mean of the overlapping time series (2009-last available year, except for TROPOMI, which was available only for 2018-2020). For China, the last BUR is available for 2014, and therefore we used that value. The inversions show total CH_4 emissions, including both anthropogenic and natural sources, while UNFCCC includes only total anthropogenic emissions.

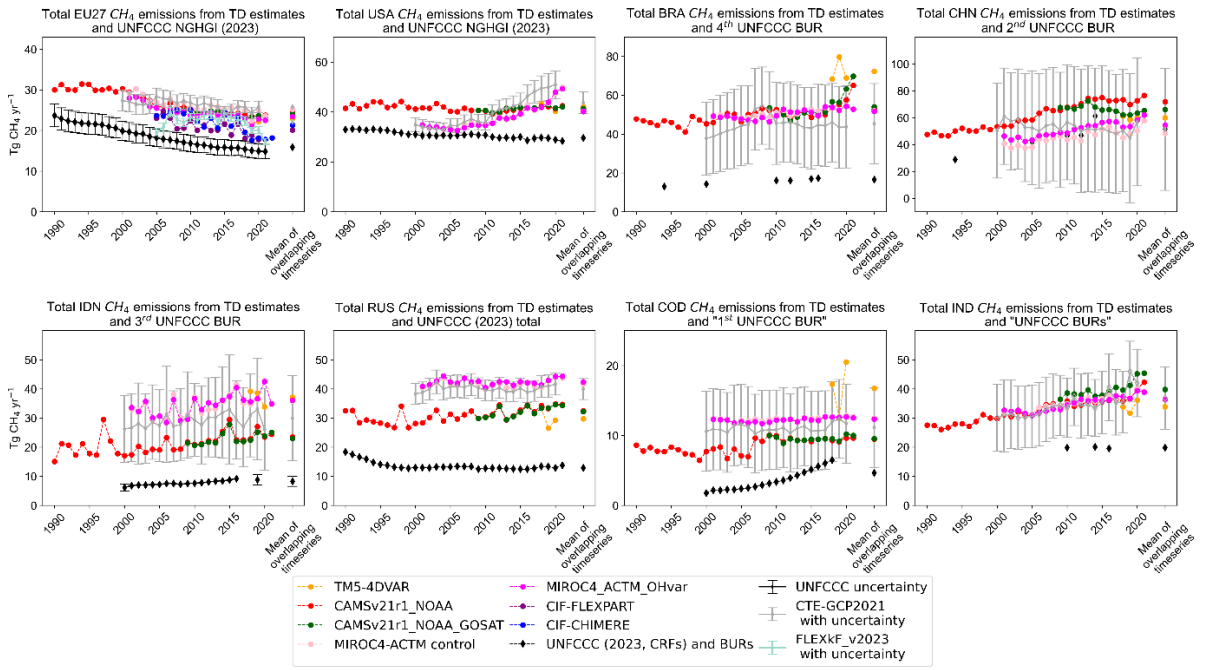

Figure 31: Total anthropogenic CH4 emissions (incl. LULUCF) from UNFCCC NGHGI (2023) CRFs (EU, USA and Russia) and BURs (Brazil (4th in 2021), China (2nd in 2019), Indonesia (3rd in 2021), DR Congo (1st in 2022), India (all three BURs: 2016, 2018 and 2021) and total TD estimates as following: for EU regional inversions (FLEXkF_v2023, CIF-FLEXPART and CIF-CHIMERE) and global inversions (TM5-4DVAR, CAMSv21r1_NOAA, CAMSv21r1_NOAA_GOSAT, CTE-GCP2021 and MIROC4-ACTM runs) products.

In the EU, the averaged 2009-2021 total CH_4 emissions from global inversions are in the range of 23-26 Tg CH_4 yr^{-1}, in line with previous estimates (Petrescu et al., 2023b). As this is the total flux, while the UNFCCC NGHGI (2023) report only anthropogenic emissions (15.8 ± 1.8 Tg CH_4 yr^{-1}), the difference can at least in part be explained by the sum of the natural emissions (~7 Tg CH_4 yr^{-1}).

In the USA, trends observed in the TD products are somehow controversial. The discrepancy between the trends from CAMS and those from MIROC4-ACTM and CTE-GCP2021 are most likely caused by the increasing oil and gas emissions from the Eastern USA (Permian Basin), captured by the latter. The same increasing trend is also captured by GAINS (Figure 24). In their runs, both MIROC4-ACTM and CTE-GCP2021 use oil and gas priors from GAINS, while CAMS uses priors from EDGAR.

For Brazil, inversions yield an average (range) total CH_4 emissions of 55 (42-72) Tg CH_4 yr^{-1}, with TM5-4DVAR reporting the highest estimate. The two CAMS inversions report an increased trend during 2017-2021, with 15 Tg CH_4 higher emissions in 2021 than in 2017. There is also a peak in the TROPOMI observation in 2019, and the TM5-4DVAR model attributed this to biomass burning events, identified in the reported partitions.

In China, the TD estimates mostly agree, except for CAMS inversions which find 10 to 20 Tg CH_4 yr^{-1} higher emission than the other inversions. Both MIROC4-ACTM runs (control and OH inter-annual variability (IAV) varying run; Patra et al., 2021) are in line with the BURs. Trend wise, all inversions agree on increased emissions after 2019.

For Indonesia, most TD results agree on the trend and show a slight increase in emissions. Similar trend is also seen by the BURs. However, the CAMS inversions result in about 10 Tg CH_4 yr^{-1} lower emissions than the other inversions (MIROC4-ACTM and CTE-GCP2021).

In Russia, the slight decreasing trend observed in the NGHGIs is not seen by inversions, and MIROC4-ACTM and CTE-GCP2021 results are about 10 Tg CH_4 yr^{-1} higher than CAMS.

In DR Congo, inversions do not show any trend. The two high values in 2018 and 2020 seen by the TROPOMI satellite are triggered by high emissions from wetlands reported in the TM5-4DVAR partitions.

For India, the TD estimates of total emissions agree well on increased trends and magnitudes. In contrast, UNFCCC reporting does not show a trend, but too little reported data from BURs is available, therefore a plausible conclusion cannot be drawn.

Uncertainties from inverse systems

This section is kept as previously written for D8.2. The main reason was to stress again the importance observation networks have in inversion systems, and how a denser coverage can help lowering uncertainties.

CTE-CH4 inversion system referenced by Tsuruta et al. (2017) provided prior and posterior fluxes and uncertainties (standard deviation) from surface inversions for 2005-2018 (those used by Thompson et al. (2022)). There are two sets of inversions: “VERIFY_inclusive" (or S4 run in VERIFY) which uses as many available stations as possible, and “VERIFY_core" (or S5 run in VERIFY) which only uses stations covering a sufficiently long period. The degrees of freedom in the state vector of the system was low, and therefore, the uncertainty estimates may not differ much between the two. Below we present three examples of uncertainty reduction maps, produced with data from the CTE system and which exemplifies how important the increase in the number of observation stations (2006-2018) is in reducing uncertainties in flux estimates.

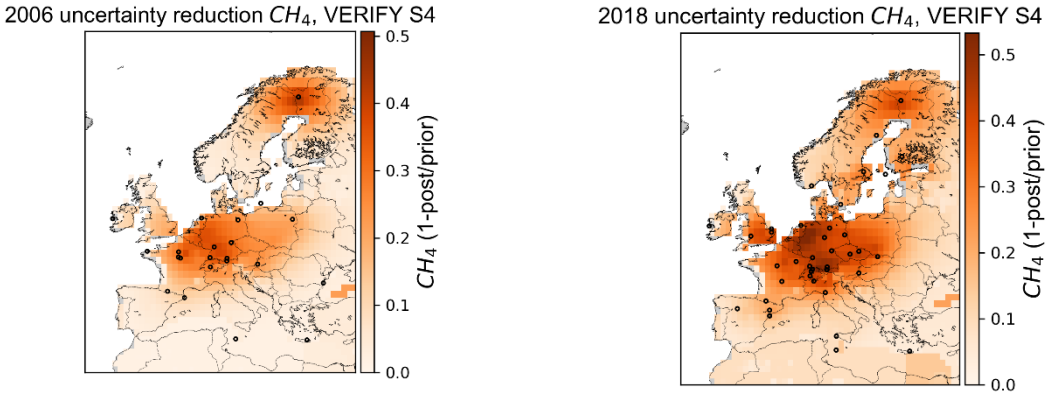

Figure 32: VERIFY_inclusive (S4) inversion run, uncertainty reduction maps computed as (1 − Δpost/Δprior) for 2006 and 2018 with different sets of observation stations.

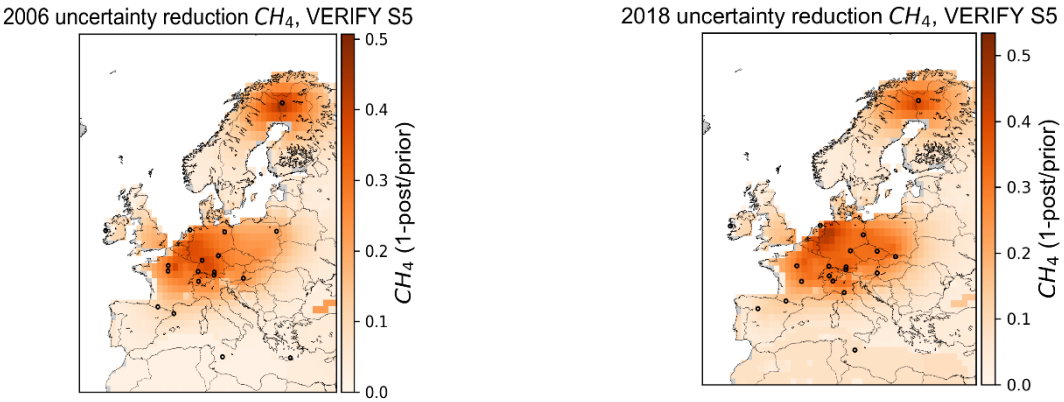

Figure 33: VERIFY_core (S5) inversion run, uncertainty reduction maps computed as (1 − Δpost/Δprior) for 2006 and 2018 with different sets of observation stations.

From the two VERIFY results, the S4 run with all stations (Figure 24) shows higher uncertainty reductions in 2018 compared to 2006 because of more measurements available. Most reductions are observed in Central Europe (the Netherlands, Germany and Switzerland). For S5 with core stations (Figure 25) the reductions are smaller, and observed in E Poland, N Italy and Spain.

The differences between the two years shown in the uncertainty maps are mostly due to the assimilated observation network sites. Some sites show weaker or stronger effects on the reduction of uncertainty. For those showing less effect, the main reasons are i) uncertainty assigned to the observations (i.e. how much weight/trust we put on it), ii) differences between prior/observations are large (i.e. 'wrong' magnitude or distribution of prior emissions, or bad transport modeling), and iii) prior emissions around the sites are simply very small, and therefore the inversion does not change fluxes much (i.e. prior flux uncertainty is small). For the sites that have a higher effect on uncertainty reduction, these reasons are important to be included in the inversion.

CTE-CH4 also provided us with GOSAT assimilated fluxes, for 2010-2017. In Figure 34 we present the uncertainty reduction maps between 2010 and 2017. Because the covariance structure is not the same as the latest surface inversion and Europe is optimized on 1x1 grid, but with long spatial correlation (100 km vs 500 km), it is not possible to examine the effect of the satellite information by comparing to the CTE-CH4 surface inversions presented here. However, it is interesting to note how satellite data assimilation infers changes on a regional scale. Unlike surface stations, satellite data have more power to constrain northern emissions than central Europe.

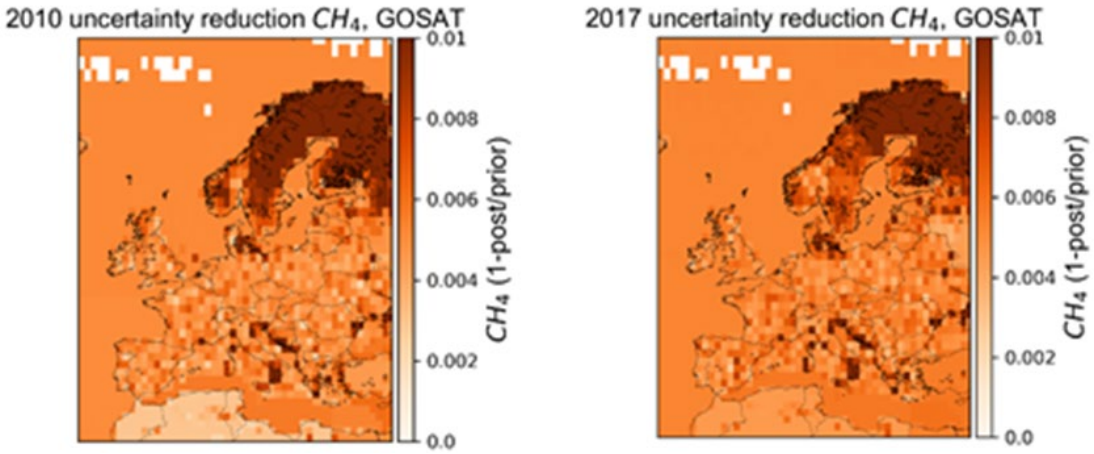

Figure 34: CTE-CH4 GOSAT inversion run, uncertainty reduction maps computed as (1 − Δpost/Δprior) for 2010 and 2017.

Because the covariance structure is not the same as the latest surface inversion and Europe is optimized on 1x1 grid, but with long spatial correlation (100 km vs 500 km), it is almost impossible to examine the effect of the satellite information by comparing to the CTE-CH_4 surface inversions presented here. However, it is interesting to note how satellite data assimilation infers changes on a regional scale. Unlike surface stations, satellite data have more power to constrain northern emissions than central Europe.

Reconciliation and recommendations

Petrescu et al. (2023a) explained how a straightforward, direct comparison of the fluxes between different inversion systems is not possible because of the different ways each inversion allocates and groups the natural and anthropogenic fluxes. Next to this, a robust

estimate of natural fluxes is still needed, to better explain the gap between anthropogenic inventories and total emissions seen by inversions. To summarize our work, Figure 29 shows the total CH_4 fluxes for the EU and the seven global emitters, separating BU anthropogenic sources disaggregated per sectors, BU natural emissions, TD natural emissions from regional and global inversions, and total emissions from global TD estimates.

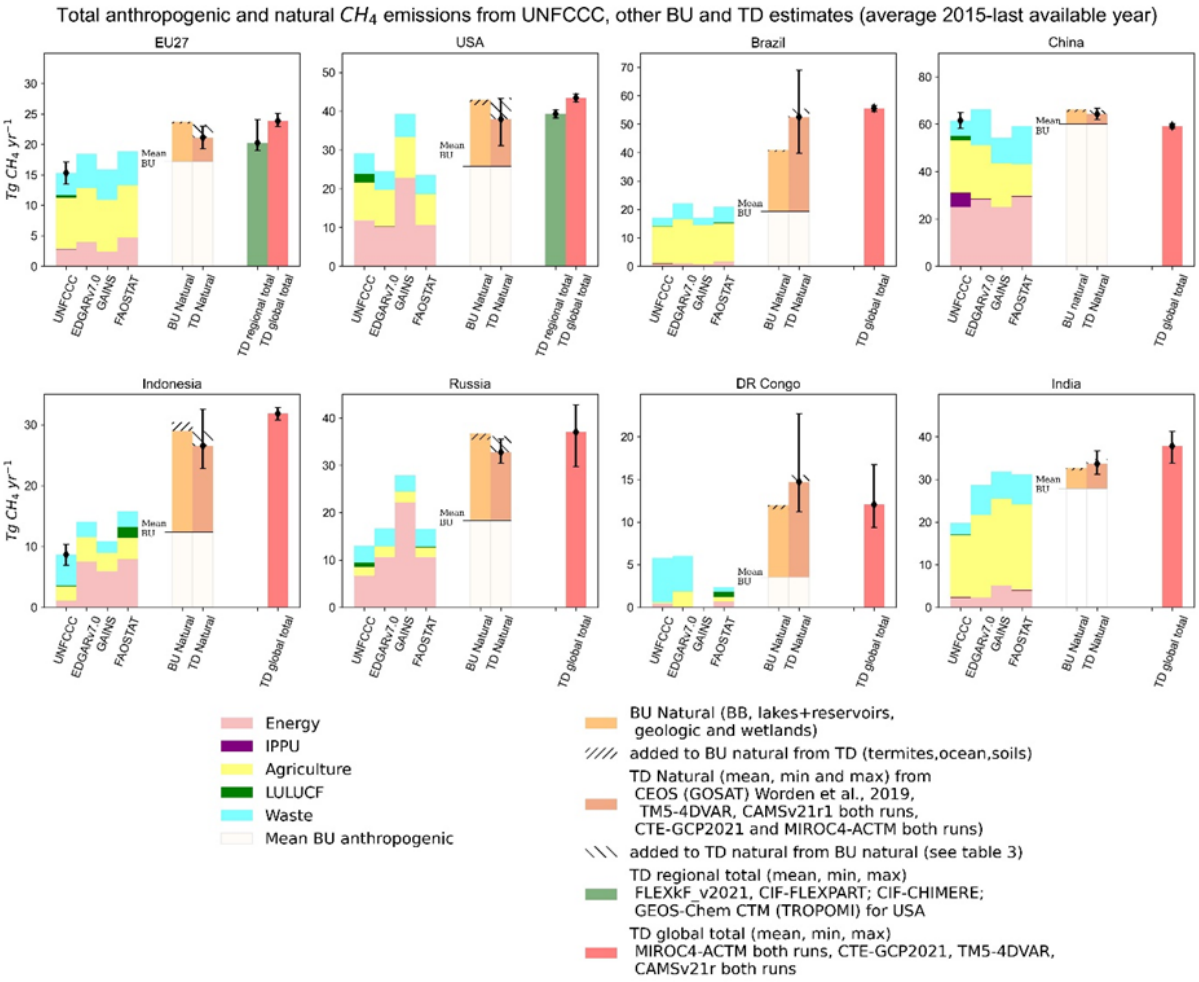

Figure 35: Total anthropogenic and natural CH_4 emissions from BU and TD estimates presented as average of 2015-last available year for EU and seven global emitters. The BU anthropogenic estimates belong to: UNFCCC NGHGI (2023) CRFs and BURs (incl. LULUCF) as totals and sectoral shares, EDGARv7.0, GAINS and FAOSTAT (with PRIMAP). The BU Natural emissions for the EU are the sum of the VERIFY products (biomass burning, inland waters, geological and peatlands plus mineral soils (Petrescu et al., 2021b; Petrescu et al., 2023b). For the seven non-EU emitters, the BU Natural fluxes are the sum of wetland emissions (LPJ-GUESS), lakes and reservoirs fluxes (ORNL DAAC, Johnson et al., 2022), geological (updated activity in SI) and biomass burning emissions (GFED4.1s) (Table 3). The natural emissions have been plotted starting at the mean of the BU anthropogenic estimates, to retain comparability across the natural emission estimates, but also compare with the total TD estimates. The total regional TD estimates (for EU) belong to the mean and min/max of FELXkF_v2023, CIF-FLEXPART and CIF-CHIMERE and for USA GEOS-Chem CTM (TROPOMI) for the year 2019 (Nesser et al., 2023). The total global TD inversions represent the average of the 2015-last available year of the mean and min/max of CTE-GCP2021, MIROC4-ACTM both runs, CAMS v21r both runs and TM5-4DVAR.

Petrescu et al. (2023a) discuss the identified issues of reconciliation. Here are the final reccomendations which may help improve future comparisons between approaches:

1. Generate spatially distributed data of NGHGIs by the respective inventory agencies.

2. A better quantification of uncontrolled spontaneous events of point source estimates to complement NGHGIs (Maasakkers et al., 2016 and 2022 for the EPA in the USA).
3. Denser atmospheric observation networks to feed into inversions and reduce uncertainties at grid-cell levels.
4. Routine provision to quantify uncertainties from inversion models.
5. Develop methods to compare estimates and ensembles with inventory estimates.
6. Increase quality in systematic measurements of fluxes to produce better priors with better uncertainties.
7. More accurate transport models to increase robustness in emission estimates.
8. Clear prescribed inventory methods to estimate and assess uncertainties, particularly statistical significance.
9. Accurate model outputs (EFs) to be used in direct comparisons with inventory data.
10. Accurate estimates of natural emissions with better spatial distribution, to subtract from total inversion estimates and compare with anthropogenic NGHGIs.
11. Develop a common language, terminology and data formats to compare inversions with NGHGI formats.

6 Data availability

If you are interested in figures from different countries or regions, please contact the authors.

7 Conclusion

This deliverable presents comparisons of inventory- and observation-based approaches, building on earlier work in VERIFY and applied here to the largest emitters or countries that can be used to draw out interesting lessons. We highlight the differences and discrepancies between UNFCCC NGHGI, independent inventories, process-based models, and atmospheric inversion estimates. The analysis focused on the fossil CO_2 emissions, net land CO_2 fluxes, and natural and anthropogenic CH_4 emissions.

For fossil CO_2 emissions, the analysis highlighted the differences between datasets and the importance of harmonising datasets for meaningful comparisons. We had limited data on CO_2 inversions but showed and discussed inversion results for Europe. The results show a general consistency between inventories and NO_2 based inversions, but without additional analysis of prior and posterior uncertainties it is not possible to assess the consistency quantitively.

For net land CO_2 fluxes, a variety of datasets are available to provide country-level estimates: bookkeeping models, process-based models, inversions-based estimates, in addition to the NGHGIs. Comparisons were made with inventories in three groups: 1) bookkeeping models, 2) process-based models, 3) inversions. In each case, the issues of system boundaries were discussed. Under some conditions, where key assumptions in different datasets match, it is possible to make meaningful comparisons between datasets. However, in most cases, key assumptions do not align (such as managed land areas, direct versus indirect effects), and this inhibits meaningful comparisons in many cases. Without additional data and analysis, it is not possible to explain differences between alternative datasets. While datasets overlap in some countries, they do not in others, and it is unclear if agreement is coincidence or meaningful consistency between datasets. An active area of research is understanding the differences between datasets, to provide sufficient confidence to disseminate more broadly.

For CH_4 emissions, we make comparisons with a variety of inventory-based estimates and inversions. Anthropogenic emissions have declined in the USA and EU (regulations) and Russia (dissolution of the Soviet Union). For the inventories, divergences between data sets can generally be attributed to different methodology and tiers used by each of the investigated inventories, when data is available to make comparisons (such as activity data and emission factors). For the inversions, the general magnitudes and trends agree, but uncertainties are too large to be more specific. We investigated the priors used by different inversion systems as well as the allocation of emissions (disaggregated partitions) to specific sectors. The use of a variety of priors across different inversion systems inhibit comparability. The robust quantification of natural CH_4 emissions will also play an important role in future reconciliation procedures. Uncertainty reduction maps can be used to identify the importance of specific observations, with the location or the period of observations. There is still a very scarce observation network available in Africa, South America, and Asia. For a more robust analysis, more detail is needed on prior and posterior uncertainties, to help identify statistically significant differences between datasets.

With anticipated improvements in atmospheric modeling and observations, as well as modeling of natural fluxes, future development needs to resolve key knowledge gaps and better quantify uncertainty. Observation- and model-based methods may emerge as a powerful tool for verifying and complementing emission inventories, but more effort is needed on ensuring consistency between datasets. Quite often insufficient data inhibits the ability to compare datasets. Data providers should aim to (i) make the system boundary very clear, and (ii) provide sufficient disaggregation of input and output data to facilitate comparisons. There is also a reliance on using model ensembles, instead of analyzing individual model results. Ultimately, comparisons at the country level between individual models and data products may be the only way to sufficiently understand differences and improve the comparability of estimates.

8 References

Andrew, R., 2020. A comparison of estimates of global carbon dioxide emissions from fossil carbon sources. Earth System Science Data 12, pp 1437–1465.

Bastos, A., Hartung, K., Nützel, T.B., Nabel, J.E.M.S., Houghton, R.A., Pongratz, J., 2021. Comparison of uncertainties in land-use change fluxes from bookkeeping model parameterisation. Earth Syst. Dynam. 12 (2), 745-762.

Berchet, A., Sollum, E., Thompson, R.L., Pison, I., Thanwerdas, J., Broquet, G., Chevallier, F., Aalto, T., Berchet, A., Bergamaschi, P., Brunner, D., Engelen, R., Fortems-Cheiney, A., Gerbig, C., Groot Zwaaftink, C.D., Haussaire, J.M., Henne, S., Houweling, S., Karstens, U., Kutsch, W.L., Luijkx, I.T., Monteil, G., Palmer, P.I., van Peet, J.C.A., Peters, W., Peylin, P., Potier, E., Rödenbeck, C., Saunois, M., Scholze, M., Tsuruta, A., Zhao, Y., 2021. The Community Inversion Framework v1.0: a unified system for atmospheric inversion studies. Geosci. Model Dev. 14 (8), 5331-5354.

Chevallier, F., 2021. Fluxes of Carbon Dioxide From Managed Ecosystems Estimated by National Inventories Compared to Atmospheric Inverse Modeling. Geophysical Research Letters 48 (15), e2021GL093565.

Chevallier, F., Fisher, M., Peylin, P., Serrar, S., Bousquet, P., Bréon, F.-M., Chédin, A., Ciais, P., 2005. Inferring CO2 sources and sinks from satellite observations: Method and application to TOVS data. Journal of Geophysical Research: Atmospheres 110 (D24).

Ciais, P., Bastos, A., Chevallier, F., Lauerwald, R., Poulter, B., Canadell, J.G., Hugelius, G., Jackson, R.B., Jain, A., Jones, M., Kondo, M., Luijkx, I.T., Patra, P.K., Peters, W., Pongratz, J., Petrescu, A.M.R., Piao, S., Qiu, C., Von Randow, C., Regnier, P., Saunois, M., Scholes, R., Shvidenko, A., Tian, H., Yang, H., Wang, X., Zheng, B., 2022. Definitions and methods to estimate regional land carbon fluxes for the second phase of the REgional Carbon Cycle Assessment and Processes Project (RECCAP-2). Geosci. Model Dev. 15 (3), 1289-1316.

Ciais, P., Bousquet, P., Freibauer, A., Naegler, T., 2007. Horizontal displacement of carbon associated with agriculture and its impacts on atmospheric CO2. Global Biogeochemical Cycles 21 (2).

Ciais, P., Yao, Y., Gasser, T., Baccini, A., Wang, Y., Lauerwald, R., Peng, S., Bastos, A., Li, W., Raymond, P.A., Canadell, J.G., Peters, G.P., Andres, R.J., Chang, J., Yue, C., Dolman, A.J., Haverd, V., Hartmann, J., Laruelle, G., Konings, A.G., King, A.W., Liu, Y., Luyssaert, S., Maignan, F., Patra, P.K., Peregon, A., Regnier, P., Pongratz, J., Poulter, B., Shvidenko, A., Valentini, R., Wang, R., Broquet, G., Yin, Y., Zscheischler, J., Guenet, B., Goll, D.S., Ballantyne, A.-P., Yang, H., Qiu, C., Zhu, D., 2021. Empirical estimates of regional carbon budgets imply reduced global soil heterotrophic respiration. National Science Review 8 (2), nwaa145.

Crippa, M., Guizzardi, D., Banja, M., Solazzo, E., Muntean, M., Schaaf, E., Pagani, F., Monforti-Ferrario, F., Olivier, J.G.J., Quadrelli, R., Risquez Martin, A., Taghavi-Moharamli, P., Grassi, G., Rossi, S., Oom, D., Branco, A., San-Miguel, J., Vignati, E., 2022. CO_2 emissions of all world countries. Publications Office of the European Union, Luxembourg ISBN 1831-9424. Available at: https://edgar.jrc.ec.europa.eu/ (accessed 20 September 2022).

Deng, Z., Ciais, P., Tzompa-Sosa, Z.A., Saunois, M., Qiu, C., Tan, C., Sun, T., Ke, P., Cui, Y., Tanaka, K., Lin, X., Thompson, R.L., Tian, H., Yao, Y., Huang, Y., Lauerwald, R., Jain, A.K., Xu, X., Bastos, A., Sitch, S., Palmer, P.I., Lauvaux, T., d'Aspremont, A., Giron, C., Benoit, A., Poulter, B., Chang, J., Petrescu, A.M.R., Davis, S.J., Liu, Z., Grassi, G., Albergel, C., Tubiello, F.N., Perugini, L., Peters, W., Chevallier, F., 2022. Comparing national greenhouse gas budgets reported in UNFCCC inventories against atmospheric inversions. Earth Syst. Sci. Data 14 (4), 1639-1675.

Denier van der Gon, H.A.C., Dellaert, S.N.C., Visschedijk, A.J.H., Kuenen, J., Super, I., 2020. Second High Resolution emission data 2005-2017. VERIFY project (GA 776810) deliverable D2.2. Available at: https://verify.lsce.ipsl.fr/index.php/repository/public-deliverables/wp2-verification-methods-for-fossil-co2-emissions/d2-2-second-high-resolution-emission-data-2005-2017 (accessed 1 February 2022).

Federici, S., Tubiello, F.N., Salvatore, M., Jacobs, H., Schmidhuber, J., 2015. New estimates of CO2 forest emissions and removals: 1990–2015. Forest Ecology and Management 352, 89-98.

Fortems-Cheiney, A., Broquet, G., 2021a. Final re-analysis of the national scale CO_2 anthropogenic emissions over 2005-2015. LSCE/CEA VERIFY project (GA 776810) deliverable D2.12.

Fortems-Cheiney, A., Broquet, G., 2021b. Second re-analysis of the national scale CO_2 anthropogenic emissions over 2005-2015. LSCE/CEA VERIFY project (GA 776810) deliverable D2.11. Available at: https://projectsworkspace.eu/sites/VERIFY/Deliverables/WP2/VERIFY_D2.11_Second%20Re-analysis%20of%20the%20national%20scale%20CO2%20anthropogenic%20emissions%20over%202005-2015_v1.pdf (accessed 11 February 2022).

Fortems-Cheiney, A., Broquet, G., Pison, I., Saunois, M., Potier, E., Berchet, A., Dufour, G., Siour, G., Denier van der Gon, H., Dellaert, S.N.C., Boersma, K.F., 2021. Analysis of the Anthropogenic and Biogenic NOx Emissions Over 2008–2017: Assessment of the Trends in the 30 Most Populated Urban Areas in Europe. Geophysical Research Letters 48 (11), e2020GL092206.

Friedlingstein, P., Jones, M.W., O'Sullivan, M., Andrew, R.M., Bakker, D.C.E., Hauck, J., Le Quéré, C., Peters, G.P., Peters, W., Pongratz, J., Sitch, S., Canadell, J.G., Ciais, P., Jackson, R.B., Alin, S.R., Anthoni, P., Bates, N.R., Becker, M., Bellouin, N., Bopp, L., Chau, T.T.T., Chevallier, F., Chini, L.P., Cronin, M., Currie, K.I., Decharme, B., Djeutchouang, L., Dou, X., Evans, W., Feely, R.A., Feng, L., Gasser, T., Gilfillan, D., Gkritzalis, T., Grassi, G., Gregor, L., Gruber, N., Gürses, Ö., Harris, I., Houghton, R.A., Hurtt, G.C., Iida, Y., Ilyina, T., Luijkx, I.T., Jain, A.K., Jones, S.D., Kato, E., Kennedy, D., Klein Goldewijk, K., Knauer, J., Korsbakken, J.I., Körtzinger, A., Landschützer, P.,

Lauvset, S.K., Lefèvre, N., Lienert, S., Liu, J., Marland, G., McGuire, P.C., Melton, J.R., Munro, D.R., Nabel, J.E.M.S., Nakaoka, S.I., Niwa, Y., Ono, T., Pierrot, D., Poulter, B., Rehder, G., Resplandy, L., Robertson, E., Rödenbeck, C., Rosan, T.M., Schwinger, J., Schwingshackl, C., Séférian, R., Sutton, A.J., Sweeney, C., Tanhua, T., Tans, P.P., Tian, H., Tilbrook, B., Tubiello, F., van der Werf, G., Vuichard, N., Wada, C., Wanninkhof, R., Watson, A., Willis, D., Wiltshire, A.J., Yuan, W., Yue, C., Yue, X., Zaehle, S., Zeng, J., 2022a. Global Carbon Budget 2021. Earth Syst. Sci. Data.

Friedlingstein, P., O'Sullivan, M., Jones, M.W., Andrew, R.M., Bakker, D.C.E., Hauck, J., Landschützer, P., Le Quéré, C., Luijkx, I.T., Peters, G.P., Peters, W., Pongratz, J., Schwingshackl, C., Sitch, S., Canadell, J.G., Ciais, P., Jackson, R.B., Alin, S.R., Anthoni, P., Barbero, L., Bates, N.R., Becker, M., Bellouin, N., Decharme, B., Bopp, L., Brasika, I.B.M., Cadule, P., Chamberlain, M.A., Chandra, N., Chau, T.T.T., Chevallier, F., Chini, L.P., Cronin, M., Dou, X., Enyo, K., Evans, W., Falk, S., Feely, R.A., Feng, L., Ford, D.J., Gasser, T., Ghattas, J., Gkritzalis, T., Grassi, G., Gregor, L., Gruber, N., Gürses, Ö., Harris, I., Hefner, M., Heinke, J., Houghton, R.A., Hurtt, G.C., Iida, Y., Ilyina, T., Jacobson, A.R., Jain, A., Jarníková, T., Jersild, A., Jiang, F., Jin, Z., Joos, F., Kato, E., Keeling, R.F., Kennedy, D., Klein Goldewijk, K., Knauer, J., Korsbakken, J.I., Körtzinger, A., Lan, X., Lefèvre, N., Li, H., Liu, J., Liu, Z., Ma, L., Marland, G., Mayot, N., McGuire, P.C., McKinley, G.A., Meyer, G., Morgan, E.J., Munro, D.R., Nakaoka, S.I., Niwa, Y., O'Brien, K.M., Olsen, A., Omar, A.M., Ono, T., Paulsen, M., Pierrot, D., Pocock, K., Poulter, B., Powis, C.M., Rehder, G., Resplandy, L., Robertson, E., Rödenbeck, C., Rosan, T.M., Schwinger, J., Séférian, R., Smallman, T.L., Smith, S.M., Sospedra-Alfonso, R., Sun, Q., Sutton, A.J., Sweeney, C., Takao, S., Tans, P.P., Tian, H., Tilbrook, B., Tsujino, H., Tubiello, F., van der Werf, G.R., van Ooijen, E., Wanninkhof, R., Watanabe, M., Wimart-Rousseau, C., Yang, D., Yang, X., Yuan, W., Yue, X., Zaehle, S., Zeng, J., Zheng, B., 2023. Global Carbon Budget 2023. Earth Syst. Sci. Data 15 (12), 5301-5369.

Friedlingstein, P., O'Sullivan, M., Jones, M.W., Andrew, R.M., Gregor, L., Hauck, J., Le Quéré, C., Luijkx, I.T., Olsen, A., Peters, G.P., Peters, W., Pongratz, J., Schwingshackl, C., Sitch, S., Canadell, J.G., Ciais, P., Jackson, R.B., Alin, S.R., Alkama, R., Arneth, A., Arora, V.K., Bates, N.R., Becker, M., Bellouin, N., Bittig, H.C., Bopp, L., Chevallier, F., Chini, L.P., Cronin, M., Evans, W., Falk, S., Feely, R.A., Gasser, T., Gehlen, M., Gkritzalis, T., Gloege, L., Grassi, G., Gruber, N., Gürses, Ö., Harris, I., Hefner, M., Houghton, R.A., Hurtt, G.C., Iida, Y., Ilyina, T., Jain, A.K., Jersild, A., Kadono, K., Kato, E., Kennedy, D., Klein Goldewijk, K., Knauer, J., Korsbakken, J.I., Landschützer, P., Lefèvre, N., Lindsay, K., Liu, J., Liu, Z., Marland, G., Mayot, N., McGrath, M.J., Metzl, N., Monacci, N.M., Munro, D.R., Nakaoka, S.I., Niwa, Y., O'Brien, K., Ono, T., Palmer, P.I., Pan, N., Pierrot, D., Pocock, K., Poulter, B., Resplandy, L., Robertson, E., Rödenbeck, C., Rodriguez, C., Rosan, T.M., Schwinger, J., Séférian, R., Shutler, J.D., Skjelvan, I., Steinhoff, T., Sun, Q., Sutton, A.J., Sweeney, C., Takao, S., Tanhua, T., Tans, P.P., Tian, X., Tian, H., Tilbrook, B., Tsujino, H., Tubiello, F., van der Werf, G.R., Walker, A.P., Wanninkhof, R., Whitehead, C., Willstrand Wranne, A., Wright, R., Yuan, W., Yue, C., Yue, X., Zaehle, S., Zeng, J., Zheng, B., 2022b. Global Carbon Budget 2022. Earth System Science Data 14 (11), 4811-4900.

Gasser, T., Crepin, L., Quilcaille, Y., Houghton, R.A., Ciais, P., Obersteiner, M., 2020. Historical CO2 emissions from land use and land cover change and their uncertainty. Biogeosciences 17 (15), 4075-4101.

Grassi, G., Conchedda, G., Federici, S., Abad Viñas, R., Korosuo, A., Melo, J., Rossi, S., Sandker, M., Somogyi, Z., Vizzarri, M., Tubiello, F.N., 2022. Carbon fluxes from land 2000–2020: bringing clarity to countries' reporting. Earth Syst. Sci. Data 14 (10), 4643-4666.

Grassi, G., House, J., Kurz, W.A., Cescatti, A., Houghton, R.A., Peters, G.P., Sanz, M.J., Viñas, R.A., Alkama, R., Arneth, A., Bondeau, A., Dentener, F., Fader, M., Federici, S., Friedlingstein, P., Jain, A.K., Kato, E., Koven, C.D., Lee, D., Nabel, J.E.M.S., Nassikas, A.A., Perugini, L., Rossi, S., Sitch, S., Viovy, N., Wiltshire, A., Zaehle, S.,

2018. Reconciling global-model estimates and country reporting of anthropogenic forest CO2 sinks. Nature Climate Change 8 (10), 914-920.

Grassi, G., Schwingshackl, C., Gasser, T., Houghton, R.A., Sitch, S., Canadell, J.G., Cescatti, A., Ciais, P., Federici, S., Friedlingstein, P., Kurz, W.A., Sanz Sanchez, M.J., Abad Viñas, R., Alkama, R., Bultan, S., Ceccherini, G., Falk, S., Kato, E., Kennedy, D., Knauer, J., Korosuo, A., Melo, J., McGrath, M.J., Nabel, J.E.M.S., Poulter, B., Romanovskaya, A.A., Rossi, S., Tian, H., Walker, A.P., Yuan, W., Yue, X., Pongratz, J., 2023. Harmonising the land-use flux estimates of global models and national inventories for 2000–2020. Earth Syst. Sci. Data 15 (3), 1093-1114.

Grassi, G., Stehfest, E., Rogelj, J., van Vuuren, D., Cescatti, A., House, J., Nabuurs, G.-J., Rossi, S., Alkama, R., Viñas, R.A., Calvin, K., Ceccherini, G., Federici, S., Fujimori, S., Gusti, M., Hasegawa, T., Havlik, P., Humpenöder, F., Korosuo, A., Perugini, L., Tubiello, F.N., Popp, A., 2021. Critical adjustment of land mitigation pathways for assessing countries' climate progress. Nature Climate Change 11 (5), 425-434.

Gütschow, J., Pflüger, M., 2022. The PRIMAP-hist national historical emissions time series (1750-2021) v2.4 [Data set], Zenodo. Available at: https://zenodo.org/record/7179775 (accessed 17 October 2022).

Hansis, E., Davis, S.J., Pongratz, J., 2015. Relevance of methodological choices for accounting of land use change carbon fluxes. Global Biogeochemical Cycles, 2014GB004997.

Houghton, R.A., Castanho, A., 2023. Annual emissions of carbon from land use, land-use change, and forestry from 1850 to 2020. Earth Syst. Sci. Data 15 (5), 2025-2054.

IPCC, 2006. 2006 IPCC Guidelines for National Greenhouse Gas Inventories, Prepared by the National Greenhouse Gas Inventories Programme, Eggleston H.S., Buendia L., Miwa K., Ngara T. and Tanabe K. (eds). IGES, Japan. Available at: https://www.ipcc-nggip.iges.or.jp/public/2006gl/ (accessed 8 April 2019).

Konovalov, I.B., Lvova, D.A., 2018. Estimation of CO_2 emissions from fossil fuel burning in Europe. Federal Research Center Institute of Applied Physics of the Russian Academy of Sciences, Nizhny Novgorod Russia.

Kurokawa, J., Ohara, T., 2020. Long-term historical trends in air pollutant emissions in Asia: Regional Emission inventory in ASia (REAS) version 3. Atmos. Chem. Phys. 20 (21), 12761-12793.

Maksyutov, S., Brunner, D., Manning, A., Fraser, P., Tarasova, O., Volosciuk, C., 2019. From Atmospheric Observations and Analysis of Greenhouse Gases to Emission Estimates: a Scientific Adventure. WMO Bulletin 68 (2).

McGrath, M.J., Petrescu, A.M.R., Peylin, P., Andrew, R.M., Matthews, B., Dentener, F., Balkovič, J., Bastrikov, V., Becker, M., Broquet, G., Ciais, P., Fortems-Cheiney, A., Ganzenmüller, R., Grassi, G., Harris, I., Jones, M., Knauer, J., Kuhnert, M., Monteil, G., Munassar, S., Palmer, P.I., Peters, G.P., Qiu, C., Schelhaas, M.J., Tarasova, O., Vizzarri, M., Winkler, K., Balsamo, G., Berchet, A., Briggs, P., Brockmann, P., Chevallier, F., Conchedda, G., Crippa, M., Dellaert, S.N.C., Denier van der Gon, H.A.C., Filipek, S., Friedlingstein, P., Fuchs, R., Gauss, M., Gerbig, C., Guizzardi, D., Günther, D., Houghton, R.A., Janssens-Maenhout, G., Lauerwald, R., Lerink, B., Luijkx, I.T., Moulas, G., Muntean, M., Nabuurs, G.J., Paquirissamy, A., Perugini, L., Peters, W., Pilli, R., Pongratz, J., Regnier, P., Scholze, M., Serengil, Y., Smith, P., Solazzo, E., Thompson, R.L., Tubiello, F.N., Vesala, T., Walther, S., 2023. The consolidated European synthesis of CO2 emissions and removals for the European Union and United Kingdom: 1990–2020. Earth Syst. Sci. Data 15 (10), 4295-4370.

Menut, L., Bessagnet, B., Khvorostyanov, D., Beekmann, M., Blond, N., Colette, A., Coll, I., Curci, G., Foret, G., Hodzic, A., Mailler, S., Meleux, F., Monge, J.L., Pison, I., Siour, G., Turquety, S., Valari, M., Vautard, R., Vivanco, M.G., 2013. CHIMERE 2013: a model for regional atmospheric composition modelling. Geosci. Model Dev. 6 (4), 981-1028.

Minx, J.C., Lamb, W.F., Andrew, R.M., Canadell, J.G., Crippa, M., Döbbeling, N., Forster, P.M., Guizzardi, D., Olivier, J., Peters, G.P., Pongratz, J., Reisinger, A., Rigby, M.,

Saunois, M., Smith, S.J., Solazzo, E., Tian, H., 2021. A comprehensive dataset for global, regional and national greenhouse gas emissions by sector 1970-2019. Earth Systems Science Data 13, 5213–5252.

O'Rourke, P.R., Smith, S.J., Mott, A., Ahsan, H., McDuffie, E.E., Crippa, M., Klimont, Z., McDonald, B., Wang, S., Nicholson, M.B., Feng, L., Hoesly, R.M., 2021. CEDS v_2021_04_21 Release Emission Data (v_2021_02_05) [Data set], Zenodo. Available at: https://doi.org/10.5281/zenodo.4741285 (accessed 10 May 2021).

Petrescu, A.M.R., McGrath, M.J., Andrew, R.M., Peylin, P., Petres, G.P., Ciais, P., Broquet, G., Tubiello, F.N., Gerbig, C., Pongratz, J., Janssens-Maenhout, G., Grassi, G., Nabuurs, G.-J., Regnier, P., Lauerwald, R., Kuhnert, M., Balcovič, J., Schelhaas, M.-J., Denier van der Gon, H.A.C., Solazzo, E., Qiu, C., Pilli, R., Konovalov, I.B., Houghton, R., Günther, D., Perugini, L., Crippa, M., Ganzenmüller, R., Luijkx, I., Smith, P., Munassar, S., Thompson, R.L., Conchedda, G., Monteil, G., Scholze, M., Karstens, U., Brokmann, P., Dolman, H., 2021a. The consolidated European synthesis of CO_2 emissions and removals for EU27 and UK: 1990-2018. Earth System Science Data 13, 2363–2406.

Petrescu, A.M.R., Peters, G.P., Engelen, R., Houweling, S., Brunner, D., Tsuruta, A., Matthews, B., Patra, P.K., Belikov, D., Thompson, R.L., Höglund-Isaksson, L., Zhang, W., Segers, A.J., Etiope, G., Ciotoli, G., Peylin, P., Chevallier, F., Aalto, T., Andrew, R.M., Bastviken, D., Berchet, A., Broquet, G., Conchedda, G., Gütschow, J., Haussaire, J.-M., Lauerwald, R., Markkanen, T., van Peet, J.C.A., Pison, I., Regnier, P., Solum, E., Scholze, M., Tenkanen, M., Tubiello, F.N., van der Werf, G.R., Worden, J.R., 2023a. Reconciliation of observation- and inventory- based CH4 emissions for eight large global emitters. Earth System Science Data Submitted.

Petrescu, A.M.R., Peters, G.P., Janssens-Maenhout, G., Ciais, P., Tubiello, F.N., Grassi, G., Nabuurs, G.J., Leip, A., Carmona-Garcia, G., Winiwarter, W., Höglund-Isaksson, L., Günther, D., Solazzo, E., Kiesow, A., Bastos, A., Pongratz, J., Nabel, J.E.M.S., Conchedda, G., Pilli, R., Andrew, R.M., Schelhaas, M.J., Dolman, H., 2020. European anthropogenic AFOLU emissions and their uncertainties: a review and benchmark data. Earth Syst. Sci. Data 12, 961-1001.

Petrescu, A.M.R., Qiu, C., Ciais, P., Thompson, R.L., Peylin, P., McGrath, M.J., Solazzo, E., Janssens-Maenhout, G., Tubiello, F.N., Bergamaschi, P., Brunner, D., Peters, G.P., Höglund-Isaksson, L., Regnier, P., Lauerwald, R., Bastviken, D., Tsuruta, A., Winiwarter, W., Patra, P.K., Kuhnert, M., Oreggioni, G.D., Crippa, M., Saunois, M., Perugini, L., Markkanen, T., Aalto, T., Groot Zwaaftink, C.D., Tian, H., Yao, Y., Wilson, C., Conchedda, G., Günther, D., Leip, A., Smith, P., Haussaire, J.M., Leppänen, A., Manning, A.J., McNorton, J., Brockmann, P., Dolman, A.J., 2021b. The consolidated European synthesis of CH4 and N2O emissions for the European Union and United Kingdom: 1990–2017. Earth Syst. Sci. Data 13 (5), 2307-2362.

Petrescu, A.M.R., Qiu, C., McGrath, M.J., Peylin, P., Peters, G.P., Ciais, P., Thompson, R.L., Tsuruta, A., Brunner, D., Kuhnert, M., Matthews, B., Palmer, P.I., Tarasova, O., Regnier, P., Lauerwald, R., Bastviken, D., Höglund-Isaksson, L., Winiwarter, W., Etiope, G., Aalto, T., Balsamo, G., Bastrikov, V., Berchet, A., Brockmann, P., Ciotoli, G., Conchedda, G., Crippa, M., Dentener, F., Groot Zwaaftink, C.D., Guizzardi, D., Günther, D., Haussaire, J.M., Houweling, S., Janssens-Maenhout, G., Kouyate, M., Leip, A., Leppänen, A., Lugato, E., Maisonnier, M., Manning, A.J., Markkanen, T., McNorton, J., Muntean, M., Oreggioni, G.D., Patra, P.K., Perugini, L., Pison, I., Raivonen, M.T., Saunois, M., Segers, A.J., Smith, P., Solazzo, E., Tian, H., Tubiello, F.N., Vesala, T., van der Werf, G.R., Wilson, C., Zaehle, S., 2023b. The consolidated European synthesis of CH4 and N2O emissions for the European Union and United Kingdom: 1990–2019. Earth Syst. Sci. Data 15 (3), 1197-1268.

Pinty, B., Ciais, P., Dee, D., Dolman, H., Dowell, M., Engelen, R., Holmlund, K., Janssens-Maenhout, G., Meijer, Y., Palmer, P., Scholze, M., Gon, H.D.v.d., Heimann, M., Juvyns, O., Kentarchos, A., Zunker, H., 2019. An Operational Anthropogenic CO_2 Emissions Monitoring & Verification Support Capacity – Needs and high level

requirements for in situ measurements. European Commission Joint Research Centre EUR 29817 EN. Available at: https://ec.europa.eu/jrc/en/science-update/measuring-man-made-carbon-dioxide-co-emissions-support-paris-agreement (accessed 29 January 2021).

Rodgers, C.D., 2000. Inverse Methods for Atmospheric Sounding: Theory and Practice. World Scientific.

Rosan, T.M., Klein Goldewijk, K., Ganzenmüller, R., O'Sullivan, M., Pongratz, J., Mercado, L.M., Aragao, L.E.O.C., Heinrich, V., Von Randow, C., Wiltshire, A., Tubiello, F.N., Bastos, A., Friedlingstein, P., Sitch, S., 2021. A multi-data assessment of land use and land cover emissions from Brazil during 2000–2019. Environmental Research Letters 16 (7), 074004.

Saunois, M., Stavert, A.R., Poulter, B., Bousquet, P., Canadell, J.G., Jackson, R.B., Raymond, P.A., Dlugokencky, E.J., Houweling, S., Patra, P.K., Ciais, P., Arora, V.K., Bastviken, D., Bergamaschi, P., Blake, D.R., Brailsford, G., Bruhwiler, L., Carlson, K.M., Carrol, M., Castaldi, S., Chandra, N., Crevoisier, C., Crill, P.M., Covey, K., Curry, C.L., Etiope, G., Frankenberg, C., Gedney, N., Hegglin, M.I., Höglund-Isaksson, L., Hugelius, G., Ishizawa, M., Ito, A., Janssens-Maenhout, G., Jensen, K.M., Joos, F., Kleinen, T., Krummel, P.B., Langenfelds, R.L., Laruelle, G.G., Liu, L., Machida, T., Maksyutov, S., McDonald, K.C., McNorton, J., Miller, P.A., Melton, J.R., Morino, I., Müller, J., Murguia-Flores, F., Naik, V., Niwa, Y., Noce, S., O'Doherty, S., Parker, R.J., Peng, C., Peng, S., Peters, G.P., Prigent, C., Prinn, R., Ramonet, M., Regnier, P., Riley, W.J., Rosentreter, J.A., Segers, A., Simpson, I.J., Shi, H., Smith, S.J., Steele, L.P., Thornton, B.F., Tian, H., Tohjima, Y., Tubiello, F.N., Tsuruta, A., Viovy, N., Voulgarakis, A., Weber, T.S., van Weele, M., van der Werf, G.R., Weiss, R.F., Worthy, D., Wunch, D., Yin, Y., Yoshida, Y., Zhang, W., Zhang, Z., Zhao, Y., Zheng, B., Zhu, Q., Zhu, Q., Zhuang, Q., 2020. The Global Methane Budget 2000–2017. Earth System Science Data 12 (3), 1561-1623.

Schwingshackl, C., Obermeier, W.A., Bultan, S., Grassi, G., Canadell, J.G., Friedlingstein, P., Gasser, T., Houghton, R.A., Kurz, W.A., Sitch, S., Pongratz, J., 2022. Differences in land-based mitigation estimates reconciled by separating natural and land-use CO2 fluxes at the country level. One Earth 5 (12), 1367-1376.

Thompson, R.L., Chevallier, F., Maksyutov, S., Patra, P.K., Bowman, K., 2022. Chapter 4 - Top-down approaches, in: Poulter, B., Canadell, J.G., Hayes, D.J., Thompson, R.L. (Eds.), Balancing Greenhouse Gas Budgets. Elsevier, pp. 87-155. Available at: https://www.sciencedirect.com/science/article/pii/B9780128149522000083.

Tsuruta, A., Aalto, T., Backman, L., Hakkarainen, J., van der Laan-Luijkx, I.T., Krol, M.C., Spahni, R., Houweling, S., Laine, M., Dlugokencky, E., Gomez-Pelaez, A.J., van der Schoot, M., Langenfelds, R., Ellul, R., Arduini, J., Apadula, F., Gerbig, C., Feist, D.G., Kivi, R., Yoshida, Y., Peters, W., 2017. Global methane emission estimates for 2000–2012 from CarbonTracker Europe-CH4 v1.0. Geosci. Model Dev. 10 (3), 1261-1289.

Tubiello, F.N., Conchedda, G., Wanner, N., Federici, S., Rossi, S., Grassi, G., 2021. Carbon emissions and removals from forests: new estimates, 1990–2020. Earth Syst. Sci. Data 13 (4), 1681-1691.

UNFCCC, 2022. National Inventory Submissions 2022. United Nations Framework Convention on Climate Change. Available at: https://unfccc.int/ghg-inventories-annex-i-parties/2022 (accessed 14 June 2022).

Document History

Version	Author(s)	Date	Changes
V0.1	VU Amsterdam, CICERO	15/12/2023	First full draft
V0.2	VU Amsterdam, CICERO	21/12/2023	Incorporating comments from co-authors

Internal Review History

Internal Reviewers	Date	Comments
Internal review waived		

Estimated Effort Contribution per Partner

Partner	Effort
VU Amsterdam	2
CICERO	2
LSCE	2
Total	**6**